PHYSICAL REVIEW D **94,** 054025 (2016)

B and B_s meson spectroscopy

Stephen Godfrey,[1,*] Kenneth Moats,[1,†] and Eric S. Swanson[2,‡]

[1]*Ottawa-Carleton Institute for Physics, Department of Physics, Carleton University, Ottawa K1S 5B6, Canada*

[2]*Department of Physics and Astronomy, University of Pittsburgh, Pittsburgh, Pennsylvania 15260, USA*

(Received 18 July 2016; published 20 September 2016)

Properties of bottom and bottom-strange mesons are computed in two relativized quark models. Model masses and wave functions are used to predict radiative transition rates, and the $^3P_0$ quark pair creation model is used to compute strong decay widths. A comparison to recently observed bottom and bottom-strange states is made. We find that there are numerous excited B and B_s mesons that have relatively narrow widths and significant branching ratios to simple final states such as $B\pi$, $B^*\pi$, BK, and B^*K that could be observed in the near future.

DOI: 10.1103/PhysRevD.94.054025

I. INTRODUCTION

Meson spectroscopy has undergone a renaissance in recent years with the discovery of many new hadronic states, not only those that are well described by quark models but also many poorly understood states such as the enigmatic XYZ charmonium and bottomoniumlike states [1–3]. In the bottom meson sector, the CDF and D0 Collaborations at Fermilab, and more recently the LHCb experiment at CERN [4], have observed P-wave B and B_s states. In parallel to these advancements in experiment, lattice QCD is also making strides in calculating hadron masses and other properties [5]. Progress in both experiment and theory go hand in hand in advancing our understanding of hadron physics and QCD in the soft regime. Understanding the properties of the B mesons can play an important role in this enterprise as, in the heavy quark limit, B mesons can be viewed as the hydrogen "atoms" of QCD with a light quark interacting with a heavy static quark. Understanding the B mesons will give a more complete understanding of excited mesons and will also help put the newly discovered excited charmed mesons into the larger context. The significantly higher statistics expected at the LHC increases the likelihood of observing many new excited B mesons which will give us the opportunity to study $B_{(s)}$ meson spectroscopy in greater detail than previously possible. In anticipation of these experimental developments it will be useful to predict the properties of these states, as guidance both to help experimental searches and to test our theoretical understanding against experimental measurements once they have been observed.

In this paper we study B meson spectroscopy using the constituent quark model to calculate masses and wave functions. For unequal mass quarks and antiquarks C-parity is not a good quantum number so that states with the same parity and spin can mix (such as the $^3P_1$ and $^1P_1$ states). The relevant mixing angle is also calculated using the quark model. The wave functions are used to calculate radiative transition widths and as input to calculate strong decays using the $^3P_0$ quark pair creation model. We use two different relativistic quark models to gauge variations in predictions from details of the models. The quark models are based on a relativistic kinetic energy term with a short distance one-gluon-exchange potential with a strong coupling constant that runs and a linear confining potential [6–9]. We make predictions of properties which will be useful for both finding and understanding these states which are the mass predictions, E1 and M1 radiative transitions, and strong partial and total decay widths obtained using the $^3P_0$ pair creation model for states above threshold. We put these results together to help identify recently observed excited B mesons and to discuss the most likely means of observing excited B and B_s mesons and strategies for searching for them.

II. SPECTROSCOPY

We consider two relativized quark models. The first is the model of Godfrey and Isgur [6] which has been a useful guide to mesons, from the lightest isovector mesons to the heaviest bottomonium states. The second, alternate relativized model, which we refer to as the AR model or ARM, is due to Swanson and collaborators [10–12] which incorporates recent developments in effective field theory and lattice gauge theory. By considering two models we may be able to better gauge the predictive limitations of our results.

A. The relativized quark model

The relativized quark model incorporates a relativistic dispersion relation for the quark kinetic energy and an instantaneous interaction comprised of a short distance one-gluon-exchange Lorentz vector potential and a Lorentz scalar linear confining potential,

*godfrey@physics.carleton.ca
†kmoats@physics.carleton.ca
‡swanson@pitt.edu

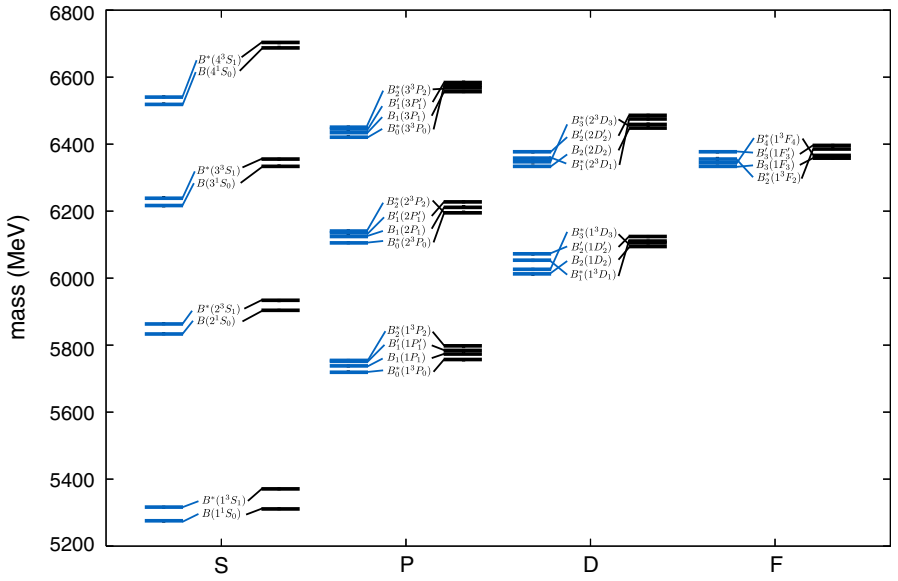

FIG. 1. Bottom mass predictions for the AR model (blue and left sets of lines) and Godfrey-Isgur model (black and right sets of lines).

$$H = H_0 + V_{q\bar{q}}(\vec{p}, \vec{r}), \tag{1}$$

where the relativistic kinetic term is given by

$$H_0 = \sqrt{\vec{p}_q^2 + m_q^2} + \sqrt{\vec{p}_{\bar{q}}^2 + m_{\bar{q}}^2}. \tag{2}$$

Just as in the nonrelativistic model, the quark-antiquark potential $V_{q\bar{q}}(\vec{p}, \vec{r})$ assumed here incorporates spin-dependent interactions that arise from the nonrelativistic reduction of the full interaction. The color Coulomb potential and the spin dependent potentials arising from one-gluon exchange include a QCD-motivated running coupling $\alpha_s(r)$, all terms in the potential are modified by a flavor-dependent potential smearing parameter σ, and quark masses in the spin-dependent interactions are replaced with quark kinetic energies. To first order in $(v_q/c)^2$, $V_{q\bar{q}}(\vec{p}, \vec{r})$ reduces to the standard nonrelativistic result. Details of the model and the method of solution can be found in Ref. [6].

For the case of a quark and antiquark of unequal mass charge conjugation parity is no longer a good quantum number so that states with different total spins but with the same total angular momentum, such as the $^3P_1 - ^1P_1$ and

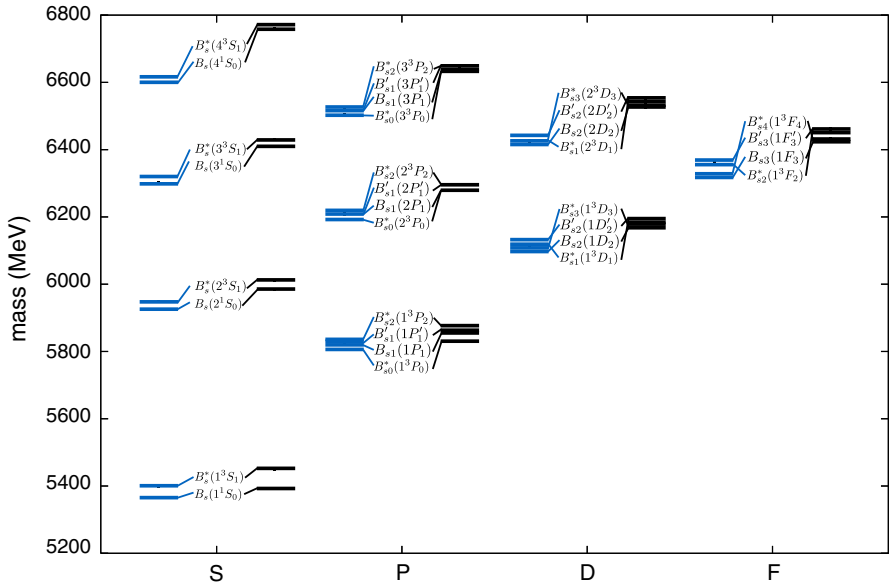

FIG. 2. Strange bottom mass predictions for the AR model (blue and left sets of lines) and Godfrey-Isgur model (black and right sets of lines).

$^3D_2 - ^1D_2$ pairs, can mix via the spin orbit interaction or some other mechanism. Consequently, the physical $j = 1$, P-wave states are linear combinations of $^3P_1$ and $^1P_1$ which we describe by

$$P = {}^1P_1 \cos\theta_{nP} + {}^3P_1 \sin\theta_{nP},$$
$$P' = -{}^1P_1 \sin\theta_{nP} + {}^3P_1 \cos\theta_{nP} \quad (3)$$

with analogous notation for the corresponding $L = D$, F, etc., pairs. In Eq. (3), $P \equiv L = 1$ designates the relative angular momentum of the $q\bar{q}$ pair and the subscript $J = 1$ is the total angular momentum of the $q\bar{q}$ pair which is equal to L. Our notation implicitly implies $L - S$ coupling between the quark spins and the relative orbital angular momentum. In the heavy quark limit in which the heavy quark mass $m_Q \to \infty$, the states can be described by the total angular momentum of the light quark, j, which couples to the spin

TABLE I. Predicted masses (in MeV), spin-orbit mixing angles, and effective harmonic oscillator parameters, $\beta_{\rm eff}$ (in GeV). Columns 2–5 show the results using the Godfrey-Isgur (GI) relativized quark model described in Sec. II A, and columns 6–9 show the results using the alternate relativized model (ARM) described in Sec. II B. The $P_1 - P_1'$, $D_2 - D_2'$, $F_3 - F_3'$, and $G_4 - G_4'$ states and mixing angles are defined using the convention of Eq. (3). Where two values of $\beta_{\rm eff}$ are listed, the first (second) refers to the singlet (triplet) state.

	GI $b\bar{q}$		GI $b\bar{s}$		ARM $b\bar{q}$		ARM $b\bar{s}$	
State	Mass	$\beta_{\rm eff}$	Mass	$\beta_{\rm eff}$	Mass	$\beta_{\rm eff}$	Mass	$\beta_{\rm eff}$
1^3S_1	5371	0.542	5450	0.595	5316	0.586	5400	0.616
1^1S_0	5312	0.580	5394	0.636	5275	0.628	5366	0.651
1^3P_2	5797	0.472	5876	0.504	5754	0.465	5836	0.487
$1P_1$	5777	0.499, 0.511	5857	0.528, 0.538	5738	0.481, 0.492	5822	0.500, 0.507
$1P_1'$	5784		5861		5753		5830	
1^3P_0	5756	0.536	5831	0.563	5720	0.525	5805	0.531
θ_{1P}	30.28°		39.12°		43.6°		37.9°	
2^3S_1	5933	0.468	6012	0.497	5864	0.460	5948	0.477
2^1S_0	5904	0.477	5984	0.508	5834	0.476	5925	0.489
1^3D_3	6106	0.444	6179	0.467	6026	0.428	6109	0.443
$1D_2$	6095	0.469, 0.463	6169	0.482, 0.487	6012	0.434, 0.436	6098	0.449, 0.450
$1D_2'$	6124		6196		6072		6133	
1^3D_1	6110	0.488	6182	0.504	6053	0.447	6119	0.459
θ_{1D}	39.69°		40.00°		48.7°		48.0°	
2^3P_2	6213	0.440	6295	0.462	6141	0.413	6220	0.428
$2P_1$	6197	0.452, 0.456	6279	0.472, 0.474	6126	0.423, 0.426	6208	0.435, 0.438
$2P_1'$	6228		6296		6132		6211	
2^3P_0	6213	0.466	6279	0.483	6106	0.439	6191	0.447
θ_{2P}	32.28°		33.05°		39.35°		32.1°	
3^3S_1	6355	0.437	6429	0.456	6240	0.412	6319	0.424
3^1S_0	6335	0.442	6410	0.462	6216	0.421	6301	0.431
1^3F_4	6364	0.429	6432	0.446	6244	0.408	6328	0.419
$1F_3$	6358	0.442, 0.446	6425	0.457, 0.460	6231	0.408, 0.408	6318	0.421, 0.421
$1F_3'$	6396		6462		6316		6369	
1^3F_2	6387	0.460	6454	0.472	6302	0.409	6358	0.423
θ_{1F}	41.13°		41.14°		48.05°		47.7°	
2^3D_3	6460	0.424	6535	0.442	6347	0.394	6428	0.405
$2D_2$	6450	0.438, 0.434	6526	0.449, 0.452	6334	0.399, 0.401	6417	0.410, 0.411
$2D_2'$	6486		6553		6377		6442	
2^3D_1	6475	0.448	6542	0.460	6357	0.410	6427	0.418
θ_{2D}	38.96°		39.46°		48.2°		47.3°	
3^3P_2	6570	0.422	6648	0.439	6451	0.388	6527	0.399
$3P_1$	6557	0.430, 0.432	6635	0.445, 0.445	6438	0.394, 0.395	6516	0.403, 0.404
$3P_1'$	6585		6650		6443		6519	
3^3P_0	6576	0.437	6639	0.451	6422	0.401	6504	0.409
θ_{3P}	31.57°		31.59°		41.9°		39.2°	
1^3G_5	6592	0.419	6654	0.433	6433	0.395	6517	0.403
$1G_4$	6588	0.429, 0.431	6650	0.441, 0.443	6420	0.392, 0.391	6507	0.403, 0.402
$1G_4'$	6628		6690		6521		6568	
1^3G_3	6622	0.442	6685	0.452	6508	0.389	6558	0.402
θ_{1G}	41.90°		41.87°		47.5°		47.3°	

of the heavy quark and corresponds to $j-j$ coupling. This limit gives rise to two doublets which for $L=1$ have $j=1/2$ and $j=3/2$ and corresponds to two physically independent mixing angles $\theta_{1P}=-\tan^{-1}(\sqrt{2})\simeq -54.7°$ and $\theta_{1P}=\tan^{-1}(1/\sqrt{2})\simeq 35.3°$ [13]. Some authors prefer to use the $j-j$ basis [14] but since we solve our Hamiltonian equations assuming $L-S$ eigenstates and then include the LS mixing, we use the notation of Eq. (3). It is straightforward to transform between the $L-S$ basis and the $j-j$ basis. It will turn out that radiative transitions are particularly sensitive to the ${}^3L_L-{}^1L_L$ mixing angle with predictions from different models in some cases giving radically different results. We also note that the definition of the mixing angles are fraught with ambiguities. For example, charge conjugating $q\bar{b}$ into $b\bar{q}$ flips the sign of the angle, and the phase convention depends on the order of coupling $\vec{L}$, $\vec{S}_q$, and $\vec{S}_{\bar{q}}$ [13].

The Hamiltonian problem was solved using the following parameters: the slope of the linear confining potential is 0.18 GeV^2, $m_q=0.220$ GeV, $m_s=0.419$ GeV, and $m_b=4.977$ GeV. Other parameters can be found in Ref. [6]. Predicted masses and mixing angles are given in Figs. 1 and 2 as well as in Tables I and II.

B. Alternate relativized model

The second relativized model has been developed in response to recent results from effective field theory and lattice gauge theory. The starting point is the general expression for the spin-dependent interactions in QCD as obtained from potential nonrelativistic quantum chromodynamics [15]. This interaction is described in terms of factorized scale-dependent Wilson coefficients and scale-dependent matrix elements of chromomagnetic and chromoelectric operators. The quark-antiquark interaction is modeled as the sum of a central confining term and the spin-dependent interaction (spin-independent corrections of order mv^2 also exist, but these are assumed to be subsumed into the central potential),

$$V_{q\bar{q}}=V_{\rm conf}+V_{SD}, \tag{4}$$

where $V_{\rm conf}$ is the standard Coulomb + linear scalar form

$$V_{\rm conf}(r)=-C_F\frac{\alpha(r)}{r}+br. \tag{5}$$

At lowest order in α_s the form of the spin-dependent interactions is given below [16]:

TABLE II. Predicted masses (in MeV), spin-orbit mixing angles, and effective harmonic oscillator parameters, $\beta_{\rm eff}$ (in GeV). Columns 2–5 show the results using the Godfrey-Isgur relativized quark model described in Sec. II A, and columns 6–9 show the results using the alternate relativized model described in Sec. II B. The P_1-P_1', D_2-D_2', F_3-F_3', and G_4-G_4' states and mixing angles are defined using the convention of Eq. (3). Where two values of $\beta_{\rm eff}$ are listed, the first (second) refers to the singlet (triplet) state.

	GI $b\bar{q}$		GI $b\bar{s}$		ARM $b\bar{q}$		ARM $b\bar{s}$	
State	Mass	$\beta_{\rm eff}$	Mass	$\beta_{\rm eff}$	Mass	$\beta_{\rm eff}$	Mass	$\beta_{\rm eff}$
2^3F_4	6679	0.414	6748	0.428	6524	0.383	6605	0.392
$2F_3$	6673	0.423, 0.425	6742	0.435, 0.436	6511	0.384, 0.384	6595	0.394, 0.392
$2F_3'$	6711		6775		6583		6638	
2^3F_2	6704	0.434	6768	0.443	6568	0.387	6627	0.397
θ_{2F}	40.86°		40.97°		47.9°		47.5°	
4^3S_1	6703	0.421	6773	0.436	6541	0.387	6617	0.397
4^1S_0	6689	0.424	6759	0.440	6520	0.393	6601	0.402
3^3D_3	6775	0.418	6849	0.426	6623	0.375	6699	0.384
$3D_2$	6767	0.419, 0.421	6841	0.431, 0.432	6610	0.379, 0.381	6689	0.388, 0.389
$3D_2'$	6800		6864		6642		6708	
3^3D_1	6792	0.427	6855	0.438	6622	0.388	6693	0.394
θ_{3D}	38.56°		39.14°		47.7°		46.8°	
4^3P_2	6883	0.411	6956	0.424	6717	0.372	6790	0.381
$4P_1$	6872	0.416, 0.417	6946	0.429, 0.429	6705	0.376, 0.376	6780	0.384, 0.384
$4P_1'$	6897		6959		6710		6783	
4^3P_0	6890	0.420	6950	0.432	6693	0.380	6770	0.387
θ_{4P}	31.00°		30.39°		48.6°		47.4°	
2^3G_5	6879	0.407	6942	0.419	6685	0.375	6766	0.383
$2G_4$	6875	0.415, 0.416	6938	0.425, 0.426	6672	0.374, 0.374	6756	0.383, 0.382
$2G_4'$	6914		6975		6764		6812	
2^3G_3	6909	0.424	6970	0.432	6750	0.373	6801	0.383
θ_{2G}	41.76°		41.78°		47.4°		47.2°	
5^3S_1	7008	0.411	7076	0.428	6800	0.372	6873	0.380
5^1S_0	6997	0.416	7063	0.426	6781	0.376	6858	0.383

$$V_{SD}(r) = \left(\frac{\boldsymbol{\sigma}_q}{4m_q^2} + \frac{\boldsymbol{\sigma}_{\bar{q}}}{4m_{\bar{q}}^2}\right) \cdot \mathbf{L}\left(\frac{1}{r}\frac{dV_{\rm conf}}{dr} + \frac{2}{r}\frac{dV_1}{dr}\right) + \left(\frac{\boldsymbol{\sigma}_{\bar{q}} + \boldsymbol{\sigma}_q}{2m_q m_{\bar{q}}}\right) \cdot \mathbf{L}\left(\frac{1}{r}\frac{dV_2}{dr}\right) + \frac{1}{12m_q m_{\bar{q}}}(3\boldsymbol{\sigma}_q \cdot \hat{\mathbf{r}}\boldsymbol{\sigma}_{\bar{q}} \cdot \hat{\mathbf{r}} - \boldsymbol{\sigma}_q \cdot \boldsymbol{\sigma}_{\bar{q}})V_3 + \frac{1}{12m_q m_{\bar{q}}}\boldsymbol{\sigma}_q \cdot \boldsymbol{\sigma}_{\bar{q}} V_4 + \frac{1}{2}\left[\left(\frac{\boldsymbol{\sigma}_q}{m_q^2} - \frac{\boldsymbol{\sigma}_{\bar{q}}}{m_{\bar{q}}^2}\right) \cdot \mathbf{L} + \left(\frac{\boldsymbol{\sigma}_q - \boldsymbol{\sigma}_{\bar{q}}}{m_q m_{\bar{q}}}\right) \cdot \mathbf{L}\right] V_5. \quad (6)$$

Here $\mathbf{L} = \mathbf{L}_q = -\mathbf{L}_{\bar{\mathbf{q}}}$, $r = |\mathbf{r}| = |\mathbf{r}_q - \mathbf{r}_{\bar{q}}|$ is the quark separation, and the $V_i = V_i(m_q, m_{\bar{q}}; r)$ are the QCD matrix elements mentioned above. The first four V_i are order α_s in perturbation theory, while V_5 is order α_s^2.

The alternate relativized model (ARM) assumes relativistic quark kinetic energies and a running coupling in the Coulombic interaction. The running coupling is motivated by the persistent overestimation of heavy meson decay constants [10], and by fits to different flavor sectors of the meson spectrum. The form used is related to the Fourier transform of

$$\alpha(k) = \frac{4\pi}{\beta_0 \log\left(\exp(\frac{4\pi}{\beta_0\alpha_0}) + \frac{k^2}{\Lambda^2}\right)}, \quad (7)$$

which has the expected ultraviolet behavior along with a postulated infrared fixed point. The leading coefficient of the QCD beta function is taken to be $\beta_0 = 9$, and α_0 and Λ are free parameters to be fit to the spectrum and heavy meson decay constants.

Traditionally the forms for the potentials V_i have been obtained by making nonrelativistic reductions of interaction kernels of the type

$$\frac{1}{2}\int d^3x d^3y \bar{\psi}(x)\Gamma\psi(x)V(x-y)\bar{\psi}(y)\Gamma\psi(y), \quad (8)$$

where the Dirac matrices are typically chosen to be unity or γ_0 (these correspond to "scalar" or "vector" interaction models, respectively). However, QCD need not be so simple, and we have therefore chosen to refer to lattice computations to model the interaction matrix elements. Direct measurement of the gluonic matrix elements reveal that V_3 and V_4 are short ranged (as expected for vector interactions), while V_1 and V_2 contain long-ranged components [17]. However, the latter do not follow the expectations of "scalar confinement" [18]; rather the string tension appearing in V_1 is reduced with respect to $V_{\rm conf}$, and there should be no long range interaction in V_2. We thus model the gluonic matrix elements as follows:

$$V_1 = (1-\epsilon)br, \quad (9)$$

$$V_2 = \epsilon br - C_F\alpha_S r, \quad (10)$$

$$V_3 = 3C_F\frac{\alpha_h}{r}, \quad (11)$$

$$V_4 = C_F\alpha_h\frac{b_h^2 e^{-b_h r}}{r}, \quad (12)$$

$$V_5 = 0. \quad (13)$$

Lattice results indicate [17] that $\epsilon \approx \frac{1}{4}$, which is fixed in the following. The form of V_4 is based on the running coupling employed, and V_5 has been taken to be zero (it was not measured in the lattice computation). The latter point is nontrivial since the perturbative expression for V_5 contains logarithms of ratios of quark masses, and therefore can be important in open flavor mesons. This point is discussed more in Ref. [11]. More details on the model construction are in Ref. [12].

A fit to 60 meson masses yields quark masses of $m_u = 0.4585$ GeV, $m_s = 0.5919$ GeV, $m_c = 1.772$ GeV, and $m_b = 5.145$ GeV. Potential parameters are $b = 0.1213$ GeV^2, $\alpha_h = 0.1536$, and $b_h = 2.138$ GeV.

C. Comparison to previous work

There is a long history of studying open flavor mesons in constituent quark models. Here we review some of the recent literature, noting similarities and differences with the current approach.

A notable early contribution was due to Di Pierro and Eichten, who examined the D, D_s, B, and B_s spectra with a constituent quark model based on the Dirac equation for the light quark in the potential generated by the heavy quark [19]. Strong decays of these states by pseudoscalar meson emission were then computed with the chiral quark model of Manohar and Georgi [20].

The unusual mass of the $D_s(2317)$ generated a series of papers on open flavor meson spectroscopy. Here we mention that of Close and Swanson, who computed the D and D_s spectra using a simple nonrelativistic quark model with a central Cornell potential and a smeared hyperfine interaction [21]. Strong decays were computed with the $^3P_0$ model with simple harmonic oscillator (SHO) mesonic wave functions and effective meson widths (as is done here). Radiative transitions, including those from molecular states, were also presented.

The $D_s(2317)$ also motivated the analysis of Ref. [11]. The novel feature of this investigation was the use of $O(\alpha_s^2)$ spin-dependent corrections to the static interquark potential—in particular flavor dependence is introduced via logarithmic dependence on quark mass. This can have strong effects on the open-flavor spectrum and can shift the nominal scalar meson mass down by roughly 100 MeV.

This paper also examined relativistic effects (due to light quark spinors) on radiative transitions and found large shifts.

Alternative relativistic (or "relativized") models also appeared in the late 2000s. For example, Matsuki *et al.* used scalar and vector interaction kernels in a Dirac equation with a Foldy-Wouthuysen reduction of the heavy quark portion of the interaction [22]. Related work by Ebert *et al.* appeared at about this time as well [23]. These authors used relativistic kinetic energies and vector, chromomagnetic, and scalar Dirac structures in the interaction kernels to obtain the D, D_s, B, and B_s spectra. Finally, Devlani and Rai made an $O(p^6)$ reduction of the quark kinetic energy and supplemented this with a Cornell central potential and the Breit spin-dependent interaction [24]. Unfortunately, the authors appeared to have employed an unregulated delta function in the latter interaction, which is not acceptable in quantum mechanical problems (evidently this problem was not discovered because the spectrum was obtained with a simple variational calculation). The first two of these papers did not examine radiative or strong transitions; radiative transitions were computed in the latter.

More recently, the chiral quark model has been revisited for the strong decays of open flavor mesons [25]. This work employed SHO mesonic wave functions with a fixed Gaussian width. Two additional papers have computed B and D meson spectra with the Godfrey-Isgur model [26,27]. They have also calculated strong decays using a very similar method to that presented here; the main difference is that the latter group incorporated a quark form factor in the $^3P_0$ vertex to suppress high energy decay modes and used SHO mesonic wave functions with a single Gaussian width. A similar computation of the B and D spectra was made with a model with relativistic quark kinetic energy and an interaction with a running coupling and smeared delta functions [28]. Decays were not considered. Finally, Liu *et al.* have made a Foldy-Wouthuysen reduction of the instantaneous approximation to the Bethe-Salpeter equation and obtained the D, D_s, B, and B_s spectra [29].

Shortly after this work appeared, a computation that used the model of Ref. [11] was submitted to the arXiv [30]. The authors computed B and B_s spectra and strong decays with the $^3P_0$ model using full mesonic wave functions. A factor of m_u/m_s was applied to the $^3P_0$ coupling to suppress strange quark production. This factor can be justified by considering the quark pair production interaction to be proportional to $\int \bar{\psi}\psi$ [31]; however, this is a model assumption, and we must resort to experiment to decide the issue.

III. RADIATIVE TRANSITIONS

A. E1 transitions

Radiative transitions could play an important role in the discovery and identification of B and B_s states. They are sensitive to the internal structure of states, in particular to $^3L_L - {}^1L_L$ mixing for states with $J = L$. In this section we calculate the electric dipole (E1) and magnetic dipole (M1) radiative widths. The partial width for an E1 radiative transition between states in the nonrelativistic quark model is given by [32]

$$\Gamma(n^{2S+1}L_J \to n'^{2S'+1}L'_{J'} + \gamma) = \frac{4}{3}\langle e_Q\rangle^2 \alpha k^3 C_{fi}\delta_{SS'}\delta_{LL'\pm 1}|\langle n'^{2S'+1}L'_{J'}|r|n^{2S+1}L_J\rangle|^2, \tag{14}$$

where

$$\langle e_Q\rangle = \frac{m_b e_q - m_q e_{\bar{b}}}{m_q + m_b}, \tag{15}$$

where $q = u,\ d,\ s$, we use the quark masses $m_u = m_d = 0.220$ GeV, $m_s = 0.419$ GeV and $m_b = 4.977$ GeV, $e_u = +2/3$, $e_d = e_s = e_b = -1/3$ are the quark charges in units of $|e|$, α is the fine-structure constant, k is the photon's energy, and C_{fi} is given by

$$C_{fi} = \max(L, L')(2J'+1)\begin{Bmatrix} L' & J' & S \\ J & L & 1 \end{Bmatrix}^2, \tag{16}$$

where $\{\cdots\}$ is a 6-j symbol. The matrix elements $\langle n'^{2S'+1}L'_{J'}|r|n^{2S+1}L_J\rangle$ are given in Tables IV–XXXV where applicable and were evaluated using the wave functions given by the relativized quark model [6]. Relativistic corrections are implicitly included in these E1 transitions through Siegert's theorem [33–35] by including spin-dependent interactions in the Hamiltonian used to calculate the meson masses and wave functions. The E1 radiative widths are given in Tables IV–XXXV where applicable.

B. M1 transitions

Radiative transitions which flip spin are described by M1 transitions. The rates for magnetic dipole transitions between S-wave heavy-light bound states are given in the nonrelativistic approximation by [36,37]

$$\Gamma(n^{2S+1}L_J \to n'^{2S'+1}L_{J'} + \gamma) = \frac{\alpha}{3}k^3(2J'+1)\delta_{S,S'\pm 1}\left|\frac{e_q}{m_q}\langle f|j_0\left(\frac{m_b}{m_q+m_b}kr\right)|i\rangle + \frac{e_b}{m_b}\langle f|j_0\left(\frac{m_q}{m_q+m_b}kr\right)|i\rangle\right|^2, \tag{17}$$

where e_q, the quark charges, and m_q, the quark masses, were given above, $L = 0$ for S waves, and $j_0(x)$ is the spherical Bessel function.

The M1 widths and overlap integrals are given in Tables IV–XXXV where applicable. Transitions in which the principle quantum number changes are referred to as hindered transitions, which are not allowed in the nonrelativistic limit due to the orthogonality of the wave

TABLE III. Light meson masses and effective harmonic oscillator parameters, $\beta_{\rm eff}$, used in the calculation of strong decay widths. The experimental values of the masses are taken from the Particle Data Group (PDG) [46]. The input value of the π mass is the weighted average of the experimental values of the π^0 and $\pi^\pm$ masses, and similarly for the input values of the K and K^* masses. All $\beta_{\rm eff}$ values are taken to be 0.4 GeV for the light mesons.

Meson	State	$M_{\rm input}$ [MeV]	$M_{\rm exp}$ [46] [MeV]	$\beta_{\rm eff}$ [GeV]
π	1^1S_0	138.8877	$134.8766\pm0.0006(\pi^0)$, $139.57018\pm0.00035(\pi^\pm)$	0.4
η	1^1S_0	547.862	547.862 ± 0.018	0.4
η'	1^1S_0	957.78	957.78 ± 0.06	0.4
ρ	1^3S_1	775.26	775.26 ± 0.25	0.4
ω	1^3S_1	782.65	782.65 ± 0.12	0.4
ϕ	1^3S_1	1019.461	1019.461 ± 0.019	0.4
K	1^1S_0	494.888	$497.614\pm0.024(K^0)$, $493.677\pm0.016(K^\pm)$	0.4
K^*	1^3S_1	894.36	$895.81\pm0.19(K^{*0})$, $891.66\pm0.26(K^{*\pm})$	0.4

functions. M1 transitions, especially hindered transitions, are notorious for their sensitivity to relativistic corrections [38]. In our calculations the wave function orthogonality is broken by including a smeared hyperfine interaction directly in the Hamiltonian so that the $^3S_1$ and $^1S_0$ states have slightly different wave functions. Ebert *et al.* are more rigorous in how they include relativistic corrections [39], but to improve the $J/\psi\to\eta_c\gamma$ result they modify the confining potential by making it a linear combination of Lorentz vector and Lorentz scalar pieces.

The E1 and M1 radiative widths are given in Tables IV–XXXV when they are large enough that they might be observed. The predicted masses given in Tables I and II are used for all states under the assumption that predicted masses are expected to be shifted by comparable amounts from their measured masses leaving the phase space to remain approximately correct.

Measuring radiative widths can help identify newly observed states, and in addition, given the sensitivity of radiative transitions to details of the models, precise measurements of electromagnetic transition rates would provide stringent tests of the various calculations.

TABLE IV. Partial widths and branching ratios for strong and electromagnetic decays of the $1S$ and $2S$ B mesons. The initial state's mass is given in MeV and is listed below the state's name in column 1. Column 4 gives the matrix element, $\mathcal{M}$, or a strong amplitude appropriate to the particular decay. For radiative transitions the E1 or M1 matrix elements are $\langle f|r|i\rangle$ (GeV^{-1}) and $\langle f|j_0(kr\frac{m_{b,q}}{m_q+m_b})|i\rangle$, respectively; these matrix elements were obtained using the wave functions of the GI model [6]. For strong decays, the nonzero partial wave amplitudes are given in units of GeV$^{-1/2}$. We only show radiative transitions that are likely to be observed and likewise generally do not show strong decay modes which have BR $< 0.1\%$, although they are included in calculating the total width. Details of the calculations are given in the text.

Initial state	Final state	M_f [MeV]	$\mathcal{M}$	Width (ub, db) [MeV]	BR (ub, db) [%]
B^*	$B\gamma$	5312	$\langle 1^1S_0\|j_0(kr\frac{m_{b,q}}{m_q+m_b})\|1^3S_1\rangle = 0.9946, 0.9971$	0.00431, 0.00123	100
5371	Total			0.00431, 0.00123	100
$B(2^3S_1)$	$B\gamma$	5312	$\langle 1^1S_0\|j_0(kr\frac{m_{b,q}}{m_q+m_b})\|2^3S_1\rangle = 0.2404, 0.06506$	0.260, 0.0674	0.24, 0.063
5933	$B(1^3P_2)\gamma$	5797	$\langle 1^3P_2\|r\|2^3S_1\rangle = -2.445$	0.0308, 0.00878	0.029, 0.0082
	$B(1P_1)\gamma$	5777	$\langle 1^3P_1\|r\|2^3S_1\rangle = -2.126$	0.00532, 0.00152	0.0049, 0.0014
	$B(1P_1')\gamma$	5784	$\langle 1^3P_1\|r\|2^3S_1\rangle = -2.126$	0.0137, 0.00390	0.013, 0.0036
	$B(1^3P_0)\gamma$	5756	$\langle 1^3P_0\|r\|2^3S_1\rangle = -1.927$	0.00825, 0.00235	0.0076, 0.0022
	$B\pi$		$^1P_1 = 0.136$	35.6	33.0
	$B\eta$		$^1P_1 = 0.0431$	1.78	1.6
	$B^*\pi$		$^3P_1 = -0.206$	67.6	62.8
	$B^*\eta$		$^3P_1 = -0.0312$	0.367	0.3
	B_sK		$^1P_1 = 0.0597$	2.23	2.1
	Total			107.8, 107.6	100
$B(2^1S_0)$	$B^*\gamma$	5371	$\langle 1^3S_1\|j_0(kr\frac{m_{b,q}}{m_q+m_b})\|2^1S_0\rangle = 0.1093, -0.6636$	0.108, 0.0250	0.11, 0.026
5904	$B(1P_1)\gamma$	5777	$\langle 1^1P_1\|r\|2^1S_0\rangle = -2.346$	0.0311, 0.00887	0.033, 0.0094
	$B(1P_1')\gamma$	5784	$\langle 1^1P_1\|r\|2^1S_0\rangle = -2.346$	0.00901, 0.00257	0.0095, 0.0027
	$B^*\pi$		$^3P_0 = -0.256$	94.6	$\sim$100
	Total			94.7, 94.6	100

IV. STRONG DECAYS

We use the $^3P_0$ model [31,40–43] to calculate all kinematically allowed strong decay widths for the B and B_s meson states listed in Tables I and II. The masses shown are the theoretical values calculated using the Godfrey-Isgur relativized quark model [6]. We use harmonic oscillator wave functions with the effective oscillator parameter, $\beta_{\rm eff}$, obtained by equating the rms radius of the harmonic oscillator wave function for the specified (n,l) quantum numbers to the rms radius of the wave

TABLE V. Partial widths and branching ratios for strong and electromagnetic decays of the $3S$ B mesons. See the caption to Table IV for further explanations.

Initial state	Final state	M_f [MeV]	$\mathcal{M}$	Width (ub, db) [MeV]	BR (ub, db) [%]
$B(3^3S_1)$	$B\gamma$	5312	$\langle 1^1S_0\|j_0(kr\frac{m_{b,q}}{m_q+m_b})\|3^3S_1\rangle = 0.1282, 0.02989$	0.319, 0.0822	0.23, 0.058
6355	$B(2^1S_0)\gamma$	5904	$\langle 2^1S_0\|j_0(kr\frac{m_{b,q}}{m_q+m_b})\|3^3S_1\rangle = 0.2666, 0.05527$	0.129, 0.0333	0.092, 0.024
	$B(1^3P_2)\gamma$	5797	$\langle 1^3P_2\|r\|3^3S_1\rangle = 0.3747$	0.0450, 0.0128	0.032, 0.0091
	$B(2^3P_2)\gamma$	6213	$\langle 2^3P_2\|r\|3^3S_1\rangle = -3.603$	0.0757, 0.0216	0.054, 0.015
	$B(2P_1)\gamma$	6197	$\langle 2^3P_1\|r\|3^3S_1\rangle = -3.202$	0.0140, 0.00398	0.0099, 0.0028
	$B(2P_1')\gamma$	6228	$\langle 2^3P_1\|r\|3^3S_1\rangle = -3.202$	0.0186, 0.00531	0.013, 0.0038
	$B(2^3P_0)\gamma$	6213	$\langle 2^3P_0\|r\|3^3S_1\rangle = -2.932$	0.0100, 0.00286	0.0071, 0.0020
	$B\pi$		$^1P_1 = 0.0252$	3.09	2.2
	$B\rho$		$^3P_1 = -0.0316$	3.38	2.4
	$B\eta'$		$^1P_1 = -0.0195$	0.775	0.6
	$B\omega$		$^3P_1 = -0.0192$	1.24	0.9
	$B^*\pi$		$^3P_1 = -0.0314$	4.33	3.1
	$B^*\rho$		$^1P_1 = -0.0223$, $^5P_1 = 0.0998$	29.7	21.2
	$B^*\eta'$		$^3P_1 = 0.0245$	0.646	0.4
	$B^*\omega$		$^1P_1 = -0.0133$, $^5P_1 = 0.0596$	10.5	7.4
	$B(2^1S_0)\pi$		$^1P_1 = 0.0888$	8.32	5.9
	$B(2^3S_1)\pi$		$^3P_1 = -0.132$	16.3	11.6
	$B(1P_1)\pi$		$^3S_1 = -0.00141i$, $^3D_1 = 0.119i$	24.0	17.0
	$B(1P_1')\pi$		$^3S_1 = 0.00757i$, $^3D_1 = 0.00797i$	0.201	0.1
	$B(1P_1')\eta$		$^3S_1 = -0.0516i$, $^3D_1 = 0.000519i$	1.35	1.0
	$B(1^3P_2)\pi$		$^5D_1 = -0.132i$	27.6	19.6
	B_sK		$^1P_1 = -0.0151$	0.850	0.6
	B_sK^*		$^3P_1 = -0.0430$	3.05	2.2
	B_s^*K		$^3P_1 = 0.0313$	3.22	2.3
	$B_s^*K^*$		$^1P_1 = -0.0101$, $^5P_1 = 0.0453$	1.35	1.0
	Total			140.8, 140.4	100
$B(3^1S_0)$	$B^*\gamma$	5371	$\langle 1^3S_1\|j_0(kr\frac{m_{b,q}}{m_q+m_b})\|3^1S_0\rangle = 0.04799, -0.02837$	0.112, 0.0258	0.074, 0.017
6335	$B(2^3S_1)\gamma$	5933	$\langle 2^3S_1\|j_0(kr\frac{m_{b,q}}{m_q+m_b})\|3^1S_0\rangle = 0.1608, -0.5684$	0.104, 0.0247	0.069, 0.016
	$B(1P_1)\gamma$	5777	$\langle 1^1P_1\|r\|3^1S_0\rangle = 0.2489$	0.0266, 0.00758	0.018, 0.0050
	$B(1P_1')\gamma$	5784	$\langle 1^1P_1\|r\|3^1S_0\rangle = 0.2489$	0.00876, 0.00250	0.0058, 0.0017
	$B(2P_1)\gamma$	6197	$\langle 2^1P_1\|r\|3^1S_0\rangle = -3.473$	0.0823, 0.0234	0.055, 0.016
	$B(2P_1')\gamma$	6228	$\langle 2^1P_1\|r\|3^1S_0\rangle = -3.473$	0.0157, 0.00448	0.010, 0.0030
	$B\rho$		$^3P_0 = 0.0512$	8.40	5.6
	$B\omega$		$^3P_0 = 0.0308$	3.00	2.0
	$B^*\pi$		$^3P_0 = -0.0314$	4.19	2.8
	$B^*\rho$		$^3P_0 = -0.113$	33.7	22.4
	$B^*\eta$		$^3P_0 = 0.00647$	0.151	0.1
	$B^*\omega$		$^3P_0 = -0.0669$	11.7	7.8
	$B(2^3S_1)\pi$		$^3P_0 = -0.166$	23.2	15.4
	$B(1^3P_0)\eta$		$^1S_0 = -0.0467i$	1.27	0.8
	$B(1^3P_2)\pi$		$^5D_0 = -0.187i$	51.7	34.3
	B_sK^*		$^3P_0 = 0.0499$	3.37	2.2
	B_s^*K		$^3P_0 = 0.0462$	6.67	4.4
	$B_s(1^3P_0)K$		$^1S_0 = -0.103i$	2.80	1.9
	Total			150.8, 150.6	100

functions calculated using the relativized quark model of Ref. [6]. The effective harmonic oscillator wave function parameters, $\beta_{\rm eff}$, that we use in our calculations are listed in Tables I and II. For the light mesons, we use a common value of $\beta_{\rm eff} = 0.4$ GeV (see below) and the experimental masses as input, given in Table III. For the constituent quark masses in our calculations both of the meson masses and of the strong decay widths, we use $m_b = 4.977$ GeV, $m_s = 0.419$ GeV, and $m_q = 0.220$ GeV. Finally, we use "relativistic phase space" as described in Refs. [42,44]. We use the calculated bottom and bottom-strange meson masses listed in Tables I and II. For the light mesons we used the measured masses listed in Table III. Details regarding the notation and conventions used in the $^3P_0$ model calculations are given in the appendix of [45].

Typical values of the parameters $\beta_{\rm eff}$ and γ are found from fits to light meson decays [21,42,47]. The predicted widths are fairly insensitive to the precise values used for $\beta_{\rm eff}$ provided γ is appropriately rescaled. However, γ can vary as much as 30% and still give reasonable overall fits of light meson decay widths [21,47]. This can result in factor of 2 changes to predicted widths, both smaller or larger. In our calculations of D and D_s meson strong decay widths from [48,49], we used a value of $\gamma = 0.4$, which has also

TABLE VI. Partial widths and branching ratios for strong and electromagnetic decays of the 4^3S_1 B meson. See the caption to Table IV for further explanations.

Initial state	Final state	M_f [MeV]	$\mathcal{M}$	Width (ub, db) [MeV]	BR (ub, db) [%]
$B(4^3S_1)$	$B\gamma$	5312	$\langle 1^1S_0\vert j_0(kr\frac{m_{b,q}}{m_q+m_b})\vert 4^3S_1\rangle = 0.08966, 0.01881$	0.345, 0.0886	0.24, 0.062
6703	$B(2^1S_0)\gamma$	5904	$\langle 2^1S_0\vert j_0(kr\frac{m_{b,q}}{m_q+m_b})\vert 4^3S_1\rangle = 0.1566, 0.02310$	0.231, 0.0588	0.16, 0.041
	$B(3^1S_0)\gamma$	6335	$\langle 3^1S_0\vert j_0(kr\frac{m_{b,q}}{m_q+m_b})\vert 4^3S_1\rangle = 0.2751, 0.05201$	0.0770, 0.0197	0.054, 0.014
	$B\pi$		$^1P_1 = 0.00820$	0.532	0.4
	$B^*\pi$		$^3P_1 = -0.00949$	0.665	0.5
	$B^*\rho$		$^1P_1 = -0.00356$, $^5P_1 = 0.0159$	1.65	1.2
	$B^*\eta'$		$^3P_1 = 0.00522$	0.146	0.1
	$B^*\omega$		$^1P_1 = -0.00212$, $^5P_1 = 0.00950$	0.584	0.4
	$B(2^1S_0)\pi$		$^1P_1 = 0.0238$	1.77	1.2
	$B(2^1S_0)\rho$		$^3P_1 = -0.0724$	4.18	2.9
	$B(2^1S_0)\omega$		$^3P_1 = -0.0368$	0.901	0.6
	$B(2^3S_1)\pi$		$^3P_1 = -0.0316$	2.90	2.0
	$B(2^3S_1)\eta$		$^3P_1 = 0.0129$	0.354	0.2
	$B(3^1S_0)\pi$		$^1P_1 = 0.0662$	3.11	2.2
	$B(3^3S_1)\pi$		$^3P_1 = -0.0984$	6.11	4.3
	$B(1^3P_0)\rho$		$^3S_1 = -0.0111i$	0.310	0.2
	$B(1P_1)\pi$		$^3S_1 = -1.40\times10^{-5}i$, $^3D_1 = 0.0132i$	0.699	0.5
	$B(1P_1)\rho$		$^3S_1 = 0.00152i$, $^3D_1 = 0.0313i$, $^5D_1 = -0.0543i$	9.11	6.4
	$B(1P_1)\eta$		$^3S_1 = 0.000742i$, $^3D_1 = -0.00764i$	0.198	0.1
	$B(1P_1)\omega$		$^3S_1 = 0.000723i$, $^3D_1 = 0.0181i$, $^5D_1 = -0.0313i$	2.97	2.1
	$B(1P_1')\rho$		$^3S_1 = -0.00950i$, $^3D_1 = 0.00166i$, $^5D_1 = -0.00288i$	0.228	0.2
	$B(1P_1')\eta$		$^3S_1 = -0.00721i$, $^3D_1 = -0.000505i$	0.172	0.1
	$B(1^3P_2)\pi$		$^5D_1 = -0.0128i$	0.639	0.4
	$B(1^3P_2)\rho$		$^3D_1 = -0.0170i$, $^5D_1 = -0.0219i$, $^7D_1 = 0.104i$	24.4	17.1
	$B(1^3P_2)\eta$		$^5D_1 = 0.0109i$	0.382	0.3
	$B(1^3P_2)\omega$		$^3D_1 = -0.00972i$, $^5D_1 = -0.0125i$, $^7D_1 = 0.0594i$	7.79	5.4
	$B(2P_1)\pi$		$^3S_1 = -0.00162i$, $^3D_1 = 0.110i$	16.0	11.2
	$B(2P_1')\pi$		$^3S_1 = 0.0192i$, $^3D_1 = 0.00504i$	0.465	0.3
	$B(2^3P_2)\pi$		$^5D_1 = -0.116i$	16.9	11.8
	$B(1D_2)\pi$		$^5P_1 = -0.000264$, $^5F_1 = -0.0820$	12.7	8.9
	$B(1D_2')\eta$		$^5P_1 = 0.0161$, $^5F_1 = -0.0000409$	0.153	0.1
	$B(1^3D_3)\pi$		$^7F_1 = 0.0836$	12.7	8.9
	$B(2D_2)\pi$		$^5P_1 = 0.00109$, $^5F_1 = 0.0225$	0.158	0.1
	B_s^*K		$^3P_1 = 0.00658$	0.271	0.2
	$B_s(2^1S_0)K$		$^1P_1 = -0.0276$	1.48	1.0
	$B_s(2^3S_1)K$		$^3P_1 = 0.0481$	4.02	2.8
	$B_s(1P_1)K$		$^3S_1 = -0.000496i$, $^3D_1 = -0.0282i$	2.29	1.6
	$B_s(1P_1')K$		$^3S_1 = -0.0122i$, $^3D_1 = 0.00265i$	0.446	0.3
	$B_s(1^3P_2)K$		$^5D_1 = 0.0344i$	3.23	2.3
	Total			142.9, 142.4	100

TABLE VII. Partial widths and branching ratios for strong and electromagnetic decays of the 4^1S_0 B meson. See the caption to Table IV for further explanations.

Initial state	Final state	M_f [MeV]	$\mathcal{M}$	Width (ub, db) [MeV]	BR (ub, db) [%]
$B(4^1S_0)$	$B^*\gamma$	5371	$\langle 1^3S_1\|j_0(kr\frac{m_{b,q}}{m_q+m_b})\|4^1S_0\rangle = 0.03513, -0.01534$	0.141, 0.0333	0.10, 0.024
6689	$B(2^3S_1)\gamma$	5933	$\langle 2^3S_1\|j_0(kr\frac{m_{b,q}}{m_q+m_b})\|4^1S_0\rangle = 0.09121, -0.02470$	0.204, 0.0493	0.15, 0.035
	$B(3^3S_1)\gamma$	6355	$\langle 3^3S_1\|j_0(kr\frac{m_{b,q}}{m_q+m_b})\|4^1S_0\rangle = 0.1852, -0.04902$	0.0801, 0.0193	0.057, 0.014
	$B\rho$		${}^3P_0 = 0.00728$	0.351	0.2
	$B^*\pi$		${}^3P_0 = -0.00899$	0.586	0.4
	$B^*\rho$		${}^3P_0 = -0.0186$	2.09	1.5
	$B^*\eta'$		${}^3P_0 = 0.00651$	0.221	0.2
	$B^*\omega$		${}^3P_0 = -0.0110$	0.726	0.5
	$B(2^1S_0)\rho$		${}^3P_0 = 0.0635$	1.99	1.4
	$B(2^3S_1)\pi$		${}^3P_0 = -0.0353$	3.50	2.5
	$B(2^3S_1)\eta$		${}^3P_0 = 0.0205$	0.848	0.6
	$B(3^3S_1)\pi$		${}^3P_0 = -0.123$	8.77	6.3
	$B(1^3P_0)\eta$		${}^1S_0 = -0.00649i$	0.143	0.1
	$B(1P_1)\rho$		${}^1S_0 = -0.000986i$, ${}^5D_0 = 0.0798i$	13.8	9.8
	$B(1P_1)\omega$		${}^1S_0 = -0.000330i$, ${}^5D_0 = 0.0457i$	4.43	3.2
	$B(1^3P_2)\pi$		${}^5D_0 = -0.0117i$	0.517	0.4
	$B(1^3P_2)\rho$		${}^5D_0 = -0.0942i$	17.5	12.5
	$B(1^3P_2)\eta$		${}^5D_0 = 0.0192i$	1.13	0.8
	$B(1^3P_2)\omega$		${}^5D_0 = -0.0534i$	5.44	3.9
	$B(2^3P_0)\pi$		${}^1S_0 = 0.0174i$	0.356	0.2
	$B(2^3P_2)\pi$		${}^5D_0 = -0.167i$	33.0	23.6
	$B(1^3D_1)\eta$		${}^3P_0 = 0.0163$	0.156	0.1
	$B(1^3D_3)\pi$		${}^7F_0 = 0.126$	27.6	19.8
	$B(1^3F_4)\pi$		${}^9G_0 = -0.0166i$	0.150	0.1
	B_s^*K		${}^3P_0 = 0.00876$	0.470	0.3
	$B_s(2^3S_1)K$		${}^3P_0 = 0.0658$	7.07	5.0
	$B_s(1^3P_0)K$		${}^1S_0 = -0.0110i$	0.360	0.2
	$B_s(1^3P_2)K$		${}^5D_0 = 0.0531i$	7.38	5.3
	Total			140.0, 139.7	100

been found to give a good description of strong decays of charmonium [21,43]. We adopt the same value of $\gamma = 0.4$ in our calculations of B and B_s meson strong decays. The resulting partial widths are listed in Tables IV–XXXV. We include more complete sets of decays in a Supplemental Material [50] that includes decays not included in the paper because we felt that their BRs were too small to likely be observed. To make our results as comprehensive as possible the Supplemental Material [50] also includes tables of strong decays for the $5S$, $4P$, $3D$, $2F$, and $2G$ states.

V. MODEL SENSITIVITY

The results of Tables IV–XXXV are presented in terms of Godfrey-Isgur model masses and wave functions. Rather than double the number of tables by giving the analogous ARM results, we have chosen to represent model sensitivity graphically. For example, Fig. 3 is a scatter plot of Godfrey-Isgur versus ARM masses. A close correspondence is evident, although ARM masses tend to be lower than GI masses higher in the spectrum due to the different string tensions employed in the models.

The similarity of the mass predictions is also reflected in the high correlation of the predicted strong decay widths of the two models, shown in Fig. 4. An alternate measure of the model sensitivity is to calculate the relative difference of the predicted strong decay widths which we take to be the difference between the GI predictions and the "alternate model" divided by the GI prediction. For the predictions of the alternate model, data were generated under a variety of conditions: specifically (i) full ARM predictions, (ii) ARM wave functions, (iii) ARM wave functions and quark masses, (iv) ARM wave functions and meson masses. For the purposes of illustration a representative set of decays was used to construct the frequency histogram of the relative difference of predicted strong decay widths shown in Fig. 5. One observes that the distribution is peaked at zero deviation, while the average deviation is 14%.

Radiative transitions can be very sensitive to model details. For example, the size of hindered M1 transitions depends crucially on assumed wave functions. Similarly, radiative transition rates for heavy-light mesons involve differences of light and heavy quark amplitudes, and these differences depend strongly on whether the light quark

TABLE VIII. Partial widths and branching ratios for strong and electromagnetic decays of the $1P$ and $2P$ B mesons. See the caption to Table IV for further explanations.

Initial state	Final state	M_f [MeV]	$\mathcal{M}$	Width (ub, db) [MeV]	BR (ub, db) [%]
$B(1^3P_0)$	$B^*\gamma$	5371	$\langle 1^3S_1\|r\|1^3P_0\rangle = 2.234$	0.325, 0.0927	0.21, 0.060
5756	$B\pi$		${}^1S_0 = -0.390i$	154	∼100
	Total			154	100
$B(1P_1)$	$B\gamma$	5312	$\langle 1^1S_0\|r\|1^1P_1\rangle = 2.110$	0.373, 0.106	5.1, 1.5
5777	$B^*\gamma$	5371	$\langle 1^3S_1\|r\|1^3P_1\rangle = 2.249$	0.0975, 0.0278	1.3, 0.40
	$B^*\pi$		${}^3S_1 = 0.0419i$, ${}^3D_1 = 0.0792i$	6.80	93.6, 98.1
	Total			7.27, 6.93	100
$B(1P_1')$	$B\gamma$	5312	$\langle 1^1S_0\|r\|1^1P_1\rangle = 2.110$	0.132, 0.0378	0.081, 0.023
5784	$B^*\gamma$	5371	$\langle 1^3S_1\|r\|1^3P_1\rangle = 2.249$	0.300, 0.0855	0.18, 0.053
	$B^*\pi$		${}^3S_1 = -0.431i$, ${}^3D_1 = 0.00588i$	163	∼100
	Total			163	100
$B(1^3P_2)$	$B^*\gamma$	5371	$\langle 1^3S_1\|r\|1^3P_2\rangle = 2.258$	0.444, 0.126	3.8, 1.1
5797	$B\pi$		${}^1D_2 = -0.0721i$	6.23	53.2, 54.7
	$B^*\pi$		${}^3D_2 = 0.0736i$	5.04	43.0, 44.2
	Total			11.71, 11.40	100
$B(2^3P_0)$	$B^*\gamma$	5371	$\langle 1^3S_1\|r\|2^3P_0\rangle = -0.3303$	0.0667, 0.0190	0.036, 0.010
6213	$B(2^3S_1)\gamma$	5933	$\langle 2^3S_1\|r\|2^3P_0\rangle = 3.453$	0.309, 0.0881	0.17, 0.047
	$B(1^3D_1)\gamma$	6110	$\langle 1^3D_1\|r\|2^3P_0\rangle = -2.441$	0.0161, 0.00459	0.0086, 0.0025
	$B\pi$		${}^1S_0 = -0.0720i$	19.5	10.5
	$B^*\rho$		${}^1S_0 = 0.138i$, ${}^5D_0 = -0.0867i$	36.8	19.8
	$B^*\omega$		${}^1S_0 = 0.0832i$, ${}^5D_0 = -0.0455i$	11.8	6.3
	$B(2^1S_0)\pi$		${}^1S_0 = -0.181i$	16.0	8.6
	$B(1P_1)\pi$		${}^3P_0 = 0.307$	93.2	50.0
	$B(1P_1')\pi$		${}^3P_0 = -0.0179$	0.308	0.2
	B_sK		${}^1S_0 = 0.0572i$	8.61	4.6
	Total			186.6, 186.3	100
$B(2P_1)$	$B^*\gamma$	5371	$\langle 1^3S_1\|r\|2^3P_1\rangle = -0.2030$	0.00681, 0.00194	0.0036, 0.0010
6197	$B(2^1S_0)\gamma$	5904	$\langle 2^1S_0\|r\|2^1P_1\rangle = 3.134$	0.208, 0.0594	0.11, 0.032
	$B(2^3S_1)\gamma$	5933	$\langle 2^3S_1\|r\|2^3P_1\rangle = 3.361$	0.0705, 0.0201	0.038, 0.011
	$B(1D_2)\gamma$	6095	$\langle 1^3D_2\|r\|2^3P_1\rangle = -2.507$, $\langle 1^1D_2\|r\|2^1P_1\rangle = -2.506$	0.0148, 0.00422	0.0079, 0.0022
	$B\rho$		${}^3S_1 = -0.138i$, ${}^3D_1 = -0.0269i$	36.9	19.7
	$B\omega$		${}^3S_1 = -0.0842i$, ${}^3D_1 = -0.0148i$	13.2	7.0
	$B^*\pi$		${}^3S_1 = 0.00459i$, ${}^3D_1 = -0.131i$	55.7	29.7
	$B^*\rho$		${}^3S_1 = 0.169i$, ${}^3D_1 = 0.0401i$, ${}^5D_1 = -0.0311i$	37.2	19.8
	$B^*\eta$		${}^3S_1 = 0.000206i$, ${}^3D_1 = -0.0499i$	6.25	3.3
	$B^*\omega$		${}^3S_1 = 0.102i$, ${}^3D_1 = 0.0202i$, ${}^5D_1 = -0.0157i$	12.3	6.6
	$B(2^3S_1)\pi$		${}^3S_1 = 0.0144i$, ${}^3D_1 = 0.0420i$	0.681	0.4
	$B(1^3P_0)\pi$		${}^1P_1 = -0.0484$	2.36	1.3
	$B(1P_1)\pi$		${}^3P_1 = -0.0807$	5.98	3.2
	$B(1P_1')\pi$		${}^3P_1 = -0.0356$	1.12	0.6
	$B(1^3P_2)\pi$		${}^5P_1 = -0.0574$, ${}^5F_1 = -0.0499$	4.82	2.6
	B_s^*K		${}^3S_1 = -0.00258i$, ${}^3D_1 = -0.0717i$	10.9	5.8
	Total			187.6, 187.4	100

amplitude is considered in the nonrelativistic limit [11]. It is therefore perhaps not surprising that the GI and AR models deviate somewhat in their predicted E1 transition rates, as shown in Fig. 6. Figure 7 shows the related frequency histogram, calculated as described above, and indicates that the GI E1 predictions tend to be approximately 50% larger than those of the AR model.

We find these results reasonably reassuring. It appears that constituent quark models that have been tuned to a wide range of hadrons provide similar predictions for hadronic properties. Perhaps the most interesting deviation seen here is the systematically lighter predictions of excited B and B_s states by the AR model with respect to the GI model. This is almost certainly due to the differing string tensions employed in the two models. Certainly, the "stiff" string tension of the GI model is preferred by lattice Wilson loop computations and bottomonium spectroscopy. However, the smaller string tension of the ARM fits lighter mesons better. It will be interesting to see which is preferred in the description of heavy-light mesons.

TABLE IX. Partial widths and branching ratios for strong and electromagnetic decays of the $2P$ B mesons. See the caption to Table IV for further explanations.

Initial state	Final state	M_f [MeV]	$\mathcal{M}$	Width (ub, db) [MeV]	BR (ub, db) [%]
$B(2P_1')$	$B^*\gamma$	5371	$\langle 1^3S_1\|r\|2^3P_1\rangle = -0.2030$	0.0189, 0.00538	0.0094, 0.0027
6228	$B(2^1S_0)\gamma$	5904	$\langle 2^1S_0\|r\|2^1P_1\rangle = 3.134$	0.111, 0.0316	0.055, 0.016
	$B(2^3S_1)\gamma$	5933	$\langle 2^3S_1\|r\|2^3P_1\rangle = 3.361$	0.243, 0.0692	0.12, 0.034
	$B(1^3D_1)\gamma$	6110	$\langle 1^3D_1\|r\|2^3P_1\rangle = -2.270$	0.00368, 0.00105	0.0018, 0.00052
	$B(1D_2')\gamma$	6124	$\langle 1^3D_2\|r\|2^3P_1\rangle = -2.507$, $\langle 1^1D_2\|r\|2^1P_1\rangle = -2.506$	0.0139, 0.00396	0.0069, 0.0020
	$B\rho$		${}^3S_1 = -0.0461i$, ${}^3D_1 = 0.0788i$	18.1	9.0
	$B\omega$		${}^3S_1 = -0.0283i$, ${}^3D_1 = 0.0440i$	5.79	2.9
	$B^*\pi$		${}^3S_1 = -0.0729i$, ${}^3D_1 = -0.00813i$	18.5	9.2
	$B^*\rho$		${}^3S_1 = -0.0865i$, ${}^3D_1 = -0.0381i$, ${}^5D_1 = -0.0741i$	22.4	11.1
	$B^*\omega$		${}^3S_1 = -0.0525i$, ${}^3D_1 = -0.0204i$, ${}^5D_1 = -0.0397i$	7.06	3.5
	$B(2^3S_1)\pi$		${}^3S_1 = -0.199i$, ${}^3D_1 = 0.0023i$	17.4	8.6
	$B(1^3P_0)\pi$		${}^1P_1 = 0.0257$	0.760	0.4
	$B(1P_1)\pi$		${}^3P_1 = -0.125$	16.4	8.1
	$B(1P_1')\pi$		${}^3P_1 = -0.0483$	2.38	1.2
	$B(1^3P_2)\pi$		${}^5P_1 = 0.292$, ${}^5F_1 = -0.00294$	82.0	40.6
	B_s^*K		${}^3S_1 = 0.0684i$, ${}^3D_1 = -0.00456i$	10.9	5.4
	Total			202.1, 201.8	100
$B(2^3P_2)$	$B(2^3S_1)\gamma$	5933	$\langle 2^3S_1\|r\|2^3P_2\rangle = 3.156$	0.258, 0.0736	0.13, 0.037
6213	$B(1^3D_3)\gamma$	6106	$\langle 1^3D_3\|r\|2^3P_2\rangle = -2.544$	0.0165, 0.00472	0.0083, 0.0024
	$B\pi$		${}^1D_2 = 0.0667i$	16.7	8.4
	$B\rho$		${}^3D_2 = 0.0591i$	7.06	3.6
	$B\eta$		${}^1D_2 = 0.0296i$	2.71	1.4
	$B\omega$		${}^3D_2 = 0.0328i$	2.12	1.1
	$B^*\pi$		${}^3D_2 = -0.0932i$	29.0	14.6
	$B^*\rho$		${}^1D_2 = 0.0187i$, ${}^5S_2 = -0.234i$, ${}^5D_2 = -0.0496i$	79.8	40.1
	$B^*\eta$		${}^3D_2 = -0.0379i$	3.78	1.9
	$B^*\omega$		${}^1D_2 = 0.00983i$, ${}^5S_2 = -0.143i$, ${}^5D_2 = -0.0260i$	27.6	13.9
	$B(2^1S_0)\pi$		${}^1D_2 = -0.0393i$	0.751	0.4
	$B(2^3S_1)\pi$		${}^3D_2 = 0.0394i$	0.611	0.3
	$B(1P_1)\pi$		${}^3P_2 = 0.0352$, ${}^3F_2 = 0.0445$	3.18	1.6
	$B(1P_1')\pi$		${}^3P_2 = -0.0602$, ${}^3F_2 = 0.00287$	3.47	1.7
	$B(1^3P_2)\pi$		${}^5P_2 = -0.0981$, ${}^5F_2 = -0.0361$	9.83	4.9
	B_sK		${}^1D_2 = 0.0452i$	5.36	2.7
	B_s^*K		${}^3D_2 = -0.0554i$	6.81	3.4
	Total			199.2, 199.0	100

VI. CLASSIFICATION OF THE OBSERVED BOTTOM MESONS

The experimental knowledge of excited B mesons is rather limited. However, recent measurements by the LHCb Collaboration [4] have demonstrated the potential to extend our knowledge of these states considerably. In the following section we will discuss the excited B mesons we believe are most likely to be observed in the near future and how they might be observed. In this section we will summarize the existing situation, comment on spectroscopic assignments, and suggest measurements that would improve our understanding of these states. A summary of the experimental status of the excited B mesons is presented in Table XXXVI.

Starting with the B mesons, four members of the $1P$ multiplet are expected to be seen around 5750 MeV, comprised of a doublet of two relatively narrow states and a doublet of two relatively broad states. The $B_1(5727)$ and $B_2^*(5739)$ with widths of 30 MeV and 24 MeV, respectively (we quote recent results from LHCb [4] which have smaller errors than listed in the PDG [46]), have measured properties that are in qualitative agreement with our predictions. The GI model overestimates the B_1 and B_2^* masses by approximately 50 MeV. However, the GI model also overestimates the B and B^* masses by a similar amount so it is reasonable to assume that the GI model in general overestimates B masses by ~50 MeV. In contrast, the ARM mass predictions agree with experiment within approximately 10 MeV. However, while the model predicts a doublet of two relatively narrow states, the predicted widths are quite a bit smaller than the measured widths: 7 MeV vs 30 MeV for the B_1 and 12 MeV vs 24 MeV for the B_2^*. In general we would not be surprised if our width predictions were off by a factor of 2 so we would consider

TABLE X. Partial widths and branching ratios for strong decays of the 3^3P_0 B meson. See the caption to Table IV for further explanations.

Initial state	Final state	$\mathcal{M}$	Width [MeV]	BR [%]
$B(3^3P_0)$	$B\pi$	$^1S_0 = -0.0192i$	2.49	1.5
6576	$B\eta'$	$^1S_0 = 0.0124i$	0.707	0.4
	$B^*\rho$	$^1S_0 = 0.0164i$, $^5D_0 = 0.0234i$	4.04	2.4
	$B^*\omega$	$^1S_0 = 0.00966i$, $^5D_0 = 0.0145i$	1.50	0.9
	$B(2^1S_0)\pi$	$^1S_0 = -0.0667i$	10.1	6.0
	$B(2^1S_0)\eta$	$^1S_0 = 0.0279i$	1.07	0.6
	$B(3^1S_0)\pi$	$^1S_0 = -0.130i$	4.70	2.8
	$B(1^3P_0)\rho$	$^3P_0 = 0.0473$	2.50	1.5
	$B(1^3P_0)\omega$	$^3P_0 = 0.0262$	0.702	0.4
	$B(1P_1)\pi$	$^3P_0 = 0.0248$	1.90	1.1
	$B(1P_1)\rho$	$^3P_0 = 0.0752$	4.55	2.7
	$B(1P_1)\eta$	$^3P_0 = -0.0335$	2.63	1.6
	$B(1P_1)\omega$	$^3P_0 = 0.0378$	0.960	0.6
	$B(1P_1')\pi$	$^3P_0 = -0.00824$	0.207	0.1
	$B(1P_1')\rho$	$^3P_0 = 0.0576$	2.25	1.4
	$B(1P_1')\eta$	$^3P_0 = 0.00857$	0.168	0.1
	$B(1P_1')\omega$	$^3P_0 = 0.0264$	0.359	0.2
	$B(2P_1)\pi$	$^3P_0 = 0.231$	40.2	24.1
	$B(2P_1')\pi$	$^3P_0 = -0.0257$	0.416	0.2
	$B(1D_2)\pi$	$^5D_0 = 0.189i$	43.0	25.8
	$B(1D_2')\pi$	$^5D_0 = -0.0260i$	0.722	0.4
	B_sK	$^1S_0 = 0.0151i$	1.28	0.8
	$B_s^*K^*$	$^1S_0 = 0.00336i$, $^5D_0 = 0.0479i$	8.23	4.9
	$B_s(2^1S_0)K$	$^1S_0 = 0.108i$	12.2	7.3
	$B_s(1P_1)K$	$^3P_0 = -0.0938$	17.0	10.2
	$B_s(1P_1')K$	$^3P_0 = 0.0383$	2.79	1.7
	Total		166.8	100

the B_2^* width prediction to be acceptable, also taking into account experimental error. However, the discrepancy of the B_1 width prediction is most likely due to the sensitivity of the prediction to the $^3P_1 - {}^1P_1$ mixing angle (θ_{1P}). Even a small change in the mixing angle would have a dramatic effect on the width prediction, and in fact we could use this information to constrain θ_{1P}.

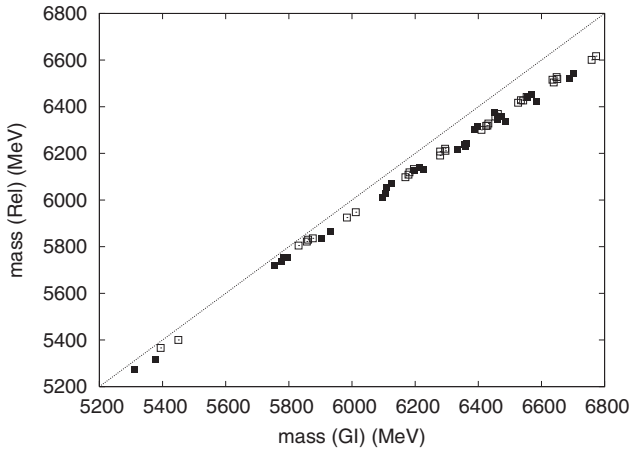

FIG. 3. Mass predictions for Godfrey-Isgur (GI) and ARM (Rel) models. Solid symbols are B states; open symbols are B_s states.

The $B(5970)$ has been seen in the $B\pi$ final state by the CDF Collaboration with a mass of 5961 ± 13 MeV for the $B(5970)^+$ and 5977 ± 13 MeV for the $B(5970)^0$ with widths of 60 ± 50 MeV and 70 ± 42 MeV, respectively [46]. The only B mesons that are close in mass to the $B(5970)$ are the $B^*(2^3S_1)$ and $B(2^1S_0)$ states. However, the $B(2^1S_0)$ cannot decay to a $B\pi$ final state, leaving only the $B^*(2^3S_1)$ as a possible candidate. The GI model predicts the mass of the $B^*(2^3S_1)$ to be 5933 MeV although as previously noted we believe that the GI model overestimates B masses by approximately 50 MeV. The AR model predicts the mass of this state to be 5864 MeV. Thus the observed mass appears to be too large to be identified with the $B^*(2^3S_1)$ state. However, the predicted width for the $B^*(2^3S_1)$ is 108 MeV which, given both the large experimental errors and theoretical uncertainties, is consistent with the measured widths. So while the $B(5970)$ might be identified with the $B^*(2^3S_1)$, given the large discrepancy between the predicted and observed mass we wait for further measurements of this state before making a conclusion.

Recently LHCb [4] reported the observation of new states, the $B_J(5840)$ and the $B_J(5960)$ with masses and widths of $M(B_J(5840)) = 5857$ MeV, $\Gamma(B_J(5840)) = 175.9$ MeV and $M(B_J(5960)) = 5967$ MeV, $\Gamma(B_J(5960)) = 73$ MeV where we have averaged the masses and widths for the two observed charge states and do not quote experimental errors as they are quite large and the extracted values are very model dependent. LHCb suggests these may be the $B(2^1S_0)$ and $B^*(2^3S_1)$ states. This can be compared to the predicted masses (from ARM) and widths for the two states of $M = 5834$ MeV and $\Gamma = 95$ MeV for the $B(2^1S_0)$ and $M = 5864$ MeV and $\Gamma = 108$ MeV for the $B^*(2^3S_1)$. The predicted properties of the $B(2^1S_0)$ are consistent with those of $B_J(5840)$ within experimental and theoretical uncertainties, and while the predicted $B^*(2^3S_1)$ width is consistent with that of the $B_J(5960)$, the predicted mass is about 100 MeV too low. All things considered, these new states can be identified with the $2S$ B mesons but ideally more measurements are needed to support this conclusion. A final comment is that the properties of the $B(5970)$ seen by CDF are consistent with the properties of the $B_J(5960)$ seen by LHCb.

The two remaining excited bottom mesons that have been observed are the bottom-strange states: the $B_{s1}(5830)^0$ with $M = 5828.78 \pm 0.35$ MeV and $\Gamma = 0.5 \pm 0.4$ MeV and the $B_{s2}^*(5840)^0$ with $M = 5839.83 \pm 0.19$ MeV and $\Gamma = 1.47 \pm 0.33$ MeV [46]. Further, for the B_{s2}^*, $\Gamma(B^{*+}K^-)/\Gamma(B^+K^-) = 0.093 \pm 0.018$. We compare these to the properties of the $B_{s1}(1P)$ with $M = 5822$ MeV and $\Gamma = 0.11$ MeV and the $B_{s2}^*(1^3P_2)$ with $M = 5836$ MeV

TABLE XI. Partial widths and branching ratios for strong decays of the $3P_1$ B meson. See the caption to Table IV for further explanations.

Initial state	Final state	$\mathcal{M}$	Width [MeV]	BR [%]
$B(3P_1)$	$B\rho$	${}^3S_1 = -0.0154i$, ${}^3D_1 = 0.000314i$	1.26	1.4
6557	$B\omega$	${}^3S_1 = -0.00924i$, ${}^3D_1 = 0.000372i$	0.453	0.5
	$B^*\pi$	${}^3S_1 = 0.00147i$, ${}^3D_1 = -0.0287i$	5.01	5.4
	$B^*\rho$	${}^3S_1 = 0.0185i$, ${}^3D_1 = -0.013i$, ${}^5D_1 = 0.0107i$	2.99	3.2
	$B^*\eta$	${}^3S_1 = 8.17 \times 10^{-5}i$, ${}^3D_1 = -0.00482i$	0.128	0.1
	$B^*\eta'$	${}^3S_1 = -0.000739i$, ${}^3D_1 = 0.0153i$	0.886	1.0
	$B^*\omega$	${}^3S_1 = 0.0109i$, ${}^3D_1 = -0.00807i$, ${}^5D_1 = 0.00663i$	1.09	1.2
	$B(2^3S_1)\pi$	${}^3S_1 = 0.00403i$, ${}^3D_1 = -0.0959i$	18.2	19.5
	$B(2^3S_1)\eta$	${}^3S_1 = -0.00350i$, ${}^3D_1 = -0.0276i$	0.777	0.8
	$B(3^3S_1)\pi$	${}^3S_1 = 0.0125i$, ${}^3D_1 = 0.0227i$	0.119	0.1
	$B(1^3P_0)\pi$	${}^1P_1 = -0.00789$	0.193	0.2
	$B(1^3P_0)\rho$	${}^3P_1 = 0.0210$	0.365	0.4
	$B(1^3P_0)\eta$	${}^1P_1 = 0.00817$	0.157	0.2
	$B(1P_1)\rho$	${}^1P_1 = 0.00336$, ${}^3P_1 = -0.0120$, ${}^5P_1 = 0.0619$, ${}^5F_1 = 0.000266$	1.46	1.6
	$B(1P_1)\eta$	${}^3P_1 = 0.00863$	0.164	0.2
	$B(1P_1')\eta$	${}^3P_1 = 0.00742$	0.118	0.1
	$B(1^3P_2)\pi$	${}^5P_1 = -0.00406$, ${}^5F_1 = 0.105$	31.4	33.6
	$B(1^3P_2)\eta$	${}^5P_1 = 0.00789$, ${}^5F_1 = 0.0305$	2.03	2.2
	$B(2^3P_0)\pi$	${}^1P_1 = -0.0451$	1.25	1.3
	$B(2P_1)\pi$	${}^3P_1 = -0.0633$	2.70	2.9
	$B(2P_1')\pi$	${}^3P_1 = -0.0294$	0.486	0.5
	$B(2^3P_2)\pi$	${}^5P_1 = -0.0468$, ${}^5F_1 = -0.0512$	2.96	3.2
	$B(1^3D_1)\pi$	${}^3S_1 = -0.00109i$, ${}^3D_1 = -0.0179i$	0.335	0.4
	$B(1D_2)\pi$	${}^5D_1 = -0.0558i$	3.47	3.7
	$B(1D_2')\pi$	${}^5D_1 = -0.0149i$	0.218	0.2
	$B(1^3D_3)\pi$	${}^7D_1 = -0.0465i$, ${}^7G_1 = -0.0365i$	3.72	4.0
	B_sK^*	${}^3S_1 = -0.00885i$, ${}^3D_1 = 0.00829i$	0.581	0.6
	B_s^*K	${}^3S_1 = -0.000882i$, ${}^3D_1 = 0.0137i$	0.935	1.0
	$B_s^*K^*$	${}^3S_1 = 0.00276i$, ${}^3D_1 = -0.0257i$, ${}^5D_1 = 0.0199i$	3.57	3.8
	$B_s(2^3S_1)K$	${}^3S_1 = -0.00994i$, ${}^3D_1 = -0.0298i$	0.670	0.7
	$B_s(1^3P_0)K$	${}^1P_1 = 0.0237$	1.12	1.2
	$B_s(1P_1)K$	${}^3P_1 = 0.0267$	1.28	1.4
	$B_s(1P_1')K$	${}^3P_1 = 0.0156$	0.434	0.5
	$B_s(1^3P_2)K$	${}^5P_1 = 0.0202$, ${}^5F_1 = 0.0352$	2.74	2.9
	Total		93.4	100

and $\Gamma = 0.78$ MeV where we quote the mass predictions of the AR model. The predicted masses are in good agreement with the measured masses, and the predicted width of the $B_{s2}^*(1^3P_2)$ is in acceptable agreement with the $B_{s2}^*(5840)^0$ measured width. However, as in the case of the $B_1(5727)$ we again surmise that the discrepancy is due to the sensitivity of the $B_{s1}(1P)$ width to the ${}^3P_1 - {}^1P_1$ mixing angle. The $B_{s1}(1P)$ is also close to the B^*K threshold so is very sensitive to phase space. As shown in Table XXVII, there are no kinematically allowed strong decay modes for the $B_s(1P_1)$ and $B_s(1P_1')$ when using their predicted Godfrey-Isgur masses as input. However, using the measured mass for the $B_{s1}(1P)$ state as input to the ${}^3P_0$ model calculations opens up the $B_s(1P_1) \to B^*K$ decay mode with a partial width of 0.331 MeV.

To summarize, the information on excited bottom mesons is limited. For both the bottom and bottom-strange mesons, two narrow states have been seen and their properties are consistent with those of the 1^3P_2 and $1P_1$ quark model states. Two more states have been observed, most recently by the LHCb Collaboration [4], but the experimental uncertainties are quite large. Although these states may be the $B(2^1S_0)$ and $B^*(2^3S_1)$ states, more data are needed to confirm these identifications. However, the recent LHCb results show the promise that LHCb holds in opening up new frontiers in bottom meson spectroscopy. In the next section we examine the B meson landscape and suggest promising avenues for finding new excited bottom mesons.

VII. EXPERIMENTAL SIGNATURES AND SEARCH STRATEGIES

We expect that the excited B mesons most likely to be observed in the near future are those that are relatively

TABLE XII. Partial widths and branching ratios for strong decays of the $3P_1'$ B meson. See the caption to Table IV for further explanations.

Initial state	Final state	$\mathcal{M}$	Width [MeV]	BR [%]
$B(3P_1')$	$B\rho$	${}^3S_1 = -0.00553i$, ${}^3D_1 = 0.00242i$	0.204	0.1
6585	$B^*\pi$	${}^3S_1 = -0.0187i$, ${}^3D_1 = -0.00187i$	2.23	1.3
	$B^*\rho$	${}^3S_1 = -0.00976i$, ${}^3D_1 = 0.00456i$, ${}^5D_1 = 0.0106i$	1.15	0.7
	$B^*\eta'$	${}^3S_1 = 0.0131i$, ${}^3D_1 = 0.00114i$	0.707	0.4
	$B^*\omega$	${}^3S_1 = -0.00582i$, ${}^3D_1 = 0.00299i$, ${}^5D_1 = 0.00682i$	0.447	0.2
	$B(2^3S_1)\pi$	${}^3S_1 = -0.0659i$, ${}^3D_1 = -0.00616i$	9.40	5.4
	$B(2^3S_1)\eta$	${}^3S_1 = 0.0383i$, ${}^3D_1 = -0.00224i$	1.81	1.0
	$B(3^3S_1)\pi$	${}^3S_1 = -0.142i$, ${}^3D_1 = 0.00193i$	5.05	2.9
	$B(1^3P_0)\rho$	${}^3P_1 = 0.0400$	1.99	1.1
	$B(1^3P_0)\omega$	${}^3P_1 = 0.0226$	0.589	0.3
	$B(1P_1)\pi$	${}^3P_1 = -0.0120$	0.458	0.3
	$B(1P_1)\rho$	${}^1P_1 = -0.00515$, ${}^3P_1 = -0.0429$, ${}^5P_1 = 0.0369$, ${}^5F_1 = -0.00939$	3.17	1.8
	$B(1P_1)\eta$	${}^3P_1 = 0.0109$	0.286	0.2
	$B(1P_1)\omega$	${}^1P_1 = -0.00276$, ${}^3P_1 = -0.0229$, ${}^5P_1 = 0.0197$, ${}^5F_1 = -0.00384$	0.790	0.4
	$B(1P_1')\pi$	${}^3P_1 = -0.00982$	0.300	0.2
	$B(1P_1')\rho$	${}^1P_1 = 0.0396$, ${}^3P_1 = 0.0509$, ${}^5P_1 = 0.00286$, ${}^5F_1 = -0.000376$	3.53	2.0
	$B(1P_1')\eta$	${}^3P_1 = 0.00905$	0.193	0.1
	$B(1P_1')\omega$	${}^1P_1 = 0.0204$, ${}^3P_1 = 0.0262$, ${}^5P_1 = 0.00146$, ${}^5F_1 = -0.000137$	0.797	0.4
	$B(1^3P_2)\pi$	${}^5P_1 = 0.0273$, ${}^5F_1 = 0.00756$	2.43	1.4
	$B(1^3P_2)\rho$	${}^3P_1 = 0.0145$, ${}^5P_1 = 0.0658$, ${}^5F_1 = 0.000873$, ${}^7F_1 = 0.00309$	2.69	1.5
	$B(1^3P_2)\eta$	${}^5P_1 = -0.0323$, ${}^5F_1 = 0.00235$	2.37	1.4
	$B(1^3P_2)\omega$	${}^3P_1 = 0.00589$, ${}^5P_1 = 0.0267$, ${}^5F_1 = 0.000157$, ${}^7F_1 = 0.000556$	0.298	0.2
	$B(2^3P_0)\pi$	${}^1P_1 = 0.0229$	0.379	0.2
	$B(2P_1)\pi$	${}^3P_1 = -0.0960$	7.26	4.2
	$B(2P_1')\pi$	${}^3P_1 = -0.0399$	1.06	0.6
	$B(2^3P_2)\pi$	${}^5P_1 = 0.212$, ${}^5F_1 = -0.00392$	32.6	18.6
	$B(1^3D_1)\pi$	${}^3S_1 = 0.000422i$, ${}^3D_1 = 0.0204i$	0.492	0.3
	$B(1D_2)\pi$	${}^5D_1 = -0.0918i$	10.5	6.0
	$B(1D_2')\pi$	${}^5D_1 = -0.0222i$	0.549	0.3
	$B(1^3D_3)\pi$	${}^7D_1 = 0.178i$, ${}^7G_1 = -0.00288i$	37.9	21.7
	B_sK^*	${}^3S_1 = -0.00477i$, ${}^3D_1 = -0.0198i$	1.75	1.0
	B_s^*K	${}^3S_1 = 0.0168i$, ${}^3D_1 = 0.00116i$	1.47	0.8
	$B_s^*K^*$	${}^3S_1 = -0.00367i$, ${}^3D_1 = 0.0159i$, ${}^5D_1 = 0.0326i$	4.87	2.8
	$B_s(2^3S_1)K$	${}^3S_1 = 0.128i$, ${}^3D_1 = -0.00291i$	14.8	8.5
	$B_s(1^3P_0)K$	${}^1P_1 = -0.0118$	0.302	0.2
	$B_s(1P_1)K$	${}^3P_1 = 0.0384$	2.96	1.7
	$B_s(1P_1')K$	${}^3P_1 = 0.0208$	0.854	0.5
	$B_s(1^3P_2)K$	${}^5P_1 = -0.0923$, ${}^5F_1 = 0.00290$	15.9	9.1
	Total		174.8	100

narrow and that have a large branching ratio (BR) to a simple final state such as $B\pi$, $B^*\pi$, BK, or B^*K. There has been great recent progress in finding excited charm mesons in the analogous $D\pi$ final states [49]. In this section we examine Tables IV–XXXV to identify states that meet these criteria.

Starting with the B and B_s $1P$ multiplets the $1P_1$ and 1^3P_2 states have already been seen. Their predicted properties are in reasonable agreement with the measured properties within the theoretical uncertainties. The hallmark of these states is that they have relatively small total widths with large BRs to simple final states. We expect the total widths for the $j_q = 1/2$ doublet to be considerably larger but still not so large that an observable signal in a simple final state should be seen. Specifically, we calculate the total width for the $B(1^3P_0)$ to be 154 MeV decaying almost 100% of the time to $B\pi$ (with a small BR to $B^*\gamma$), and $\Gamma(B(1P_1')) = 163$ MeV decaying almost 100% of the time to $B^*\pi$. Similarly we calculate $\Gamma(B_s(1^3P_0)) = 138$ MeV decaying predominantly to BK, and the $B_s(1P_1')$ is below B^*K threshold so is expected to be quite narrow with its dominant BRs to $B_s\gamma$ and $B_s^*\gamma$. The ratio of these two BRs would determine the ${}^3P_1 - {}^1P_1$ mixing angle. For these predicted total widths it should be possible to observe the missing B and B_s $1P$ states in the near future. The challenge will be disentangling overlapping states, but this should be possible with sufficient statistics.

Next highest in mass are the $2S$ states. The $B(2^3S_1)$ is predicted to have a mass of 5864 MeV, and $\Gamma = 108$ MeV

TABLE XIII. Partial widths and branching ratios for strong decays of the 3^3P_2 B meson. See the caption to Table IV for further explanations.

Initial state	Final state	$\mathcal{M}$	Width [MeV]	BR [%]
$B(3^3P_2)$	$B\pi$	$^1D_2 = 0.0194i$	2.52	2.9
6570	$B\eta$	$^1D_2 = 0.00563i$	0.194	0.2
	$B\eta'$	$^1D_2 = -0.00459i$	0.0961	0.1
	$B^*\pi$	$^3D_2 = -0.0241i$	3.60	4.1
	$B^*\rho$	$^1D_2 = -0.00218i$, $^5S_2 = -0.0239i$, $^5D_2 = 0.00576i$	2.99	3.4
	$B^*\eta$	$^3D_2 = -0.00548i$	0.169	0.2
	$B^*\eta'$	$^3D_2 = 0.00974i$	0.371	0.4
	$B^*\omega$	$^1D_2 = -0.00146i$, $^5S_2 = -0.0143i$, $^5D_2 = 0.00387i$	1.08	1.2
	$B(2^1S_0)\pi$	$^1D_2 = 0.0515i$	5.89	6.7
	$B(2^1S_0)\eta$	$^1D_2 = 0.0223i$	0.662	0.8
	$B(2^3S_1)\pi$	$^3D_2 = -0.0696i$	9.92	11.3
	$B(2^3S_1)\eta$	$^3D_2 = -0.0238i$	0.625	0.7
	$B(3^1S_0)\pi$	$^1D_2 = -0.0238i$	0.148	0.2
	$B(3^3S_1)\pi$	$^3D_2 = 0.0226i$	0.107	0.1
	$B(1^3P_0)\rho$	$^3P_2 = 0.0417$	1.79	2.0
	$B(1^3P_0)\omega$	$^3P_2 = 0.0227$	0.481	0.5
	$B(1P_1)\pi$	$^3P_2 = 0.00463$, $^3F_2 = -0.0650$	13.0	14.8
	$B(1P_1)\rho$	$^3P_2 = 0.000502$, $^3F_2 = 0.00184$, $^5P_2 = -0.0339$, $^5F_2 = -0.00260$	0.800	0.9
	$B(1P_1)\eta$	$^3P_2 = -0.00362$, $^3F_2 = -0.0218$	1.12	1.3
	$B(1P_1)\omega$	$^3P_2 = 0.000221$, $^3F_2 = 0.000497$, $^5P_2 = -0.0158$, $^5F_2 = -0.000703$	0.133	0.2
	$B(1P_1')\pi$	$^3P_2 = -0.0104$, $^3F_2 = -0.00408$	0.376	0.4
	$B(1P_1')\rho$	$^3P_2 = 0.0432$, $^3F_2 = 4.97 \times 10^{-5}$, $^5P_2 = -0.000832$, $^5F_2 = -7.03 \times 10^{-5}$	1.01	1.2
	$B(1P_1')\eta$	$^3P_2 = 0.0104$, $^3F_2 = -0.00123$	0.248	0.3
	$B(1^3P_2)\pi$	$^5P_2 = -0.00928$, $^5F_2 = 0.0620$	11.5	13.1
	$B(1^3P_2)\eta$	$^5P_2 = 0.0108$, $^5F_2 = 0.0197$	1.08	1.2
	$B(2P_1)\pi$	$^3P_2 = 0.0258$, $^3F_2 = 0.0479$	2.15	2.4
	$B(2P_1')\pi$	$^3P_2 = -0.0534$, $^3F_2 = 0.00170$	1.74	2.0
	$B(2^3P_2)\pi$	$^5P_2 = -0.0745$, $^5F_2 = -0.0366$	4.58	5.2
	$B(1^3D_1)\pi$	$^3D_2 = 0.0135i$	0.202	0.2
	$B(1D_2)\pi$	$^5S_2 = 0.000404i$, $^5D_2 = 0.0303i$, $^5G_2 = 0.0308i$	2.19	2.5
	$B(1D_2')\pi$	$^5S_2 = -0.000462i$, $^5D_2 = -0.0204i$, $^5G_2 = 0.000290i$	0.433	0.5
	$B(1^3D_3)\pi$	$^7D_2 = -0.0672i$, $^7G_2 = -0.0233i$	5.70	6.5
	B_sK^*	$^3D_2 = -0.0143i$	0.835	1.0
	B_s^*K	$^3D_2 = 0.00704i$	0.251	0.3
	$B_s^*K^*$	$^1D_2 = -0.00850i$, $^5S_2 = -0.00852i$, $^5D_2 = 0.0225i$	2.28	2.6
	$B_s(2^1S_0)K$	$^1D_2 = 0.0292i$	0.849	1.0
	$B_s(2^3S_1)K$	$^3D_2 = -0.0277i$	0.601	0.7
	$B_s(1P_1)K$	$^3P_2 = -0.00675$, $^3F_2 = -0.0267$	1.43	1.6
	$B_s(1P_1')K$	$^3P_2 = 0.0313$, $^3F_2 = 0.00250$	1.83	2.1
	$B_s(1^3P_2)K$	$^5P_2 = 0.0302$, $^5F_2 = 0.0232$	2.54	2.9
	Total		87.7	100

with $\mathrm{BR}(B\pi) = 33\%$ and $\mathrm{BR}(B^*\pi) = 63\%$. The properties of the $B(2^1S_0)$ are $M = 5834$ MeV, $\Gamma = 95$ MeV with $\mathrm{BR}(B^*\pi) \simeq 100\%$. In both cases we quote the ARM mass prediction. There is evidence that LHCb has seen these states, but as discussed above more data are needed to confirm this. For the analogous bottom-strange states we find for the $B_s(2^3S_1)$ $M = 5948$ MeV, $\Gamma = 114$ MeV with $\mathrm{BR}(BK) = 38.3\%$ and $\mathrm{BR}(B^*K) = 58.4\%$, and for the $B_s(2^1S_0)$ $M = 5925$ MeV, $\Gamma = 76$ MeV with $\mathrm{BR}(B^*K) \simeq 100\%$. These states are relatively narrow with large BRs to simple final states so it should be possible to observe them in the near future.

As we move to higher mass states the situation becomes more complicated. In general the mass multiplets are closer together with relatively small splittings within multiplets [$\mathcal{O}(10$ MeV)], and many of the states become broader due to the increased phase space resulting in many overlapping resonances. To disentangle this will require higher statistics to measure the spins. LHCb has demonstrated their ability to accomplish this with spin measurements in the charm meson sector. However, not all states are broad due to angular momentum suppression in decays, so it should still be possible to find some of these excited states. In what follows we will focus on the states most likely to be found first.

TABLE XIV. Partial widths and branching ratios for strong and electromagnetic decays of the $1D$ B mesons. See the caption to Table IV for further explanations.

Initial state	Final state	M_f [MeV]	$\mathcal{M}$	Width (ub, db) [MeV]	BR (ub, db) [%]
$B(1^3D_1)$	$B(1^3P_0)\gamma$	5756	$\langle 1^3P_0\|r\|1^3D_1\rangle = 2.951$	0.297, 0.0847	0.15, 0.043
6110	$B(1P_1)\gamma$	5777	$\langle 1^3P_1\|r\|1^3D_1\rangle = 3.089$	0.0522, 0.0149	0.026, 0.0076
	$B(1P_1')\gamma$	5784	$\langle 1^3P_1\|r\|1^3D_1\rangle = 3.089$	0.144, 0.0411	0.073, 0.021
	$B(1^3P_2)\gamma$	5797	$\langle 1^3P_2\|r\|1^3D_1\rangle = 3.295$	0.0130, 0.00371	0.0066, 0.0019
	$B\pi$		${}^1P_1 = 0.140$	59.5	30.3
	$B\rho$		${}^3P_1 = -0.0548$	2.30	1.2
	$B\eta$		${}^1P_1 = 0.0647$	9.59	4.9
	$B\omega$		${}^3P_1 = -0.0264$	0.440	0.2
	$B^*\pi$		${}^3P_1 = 0.107$	30.2	15.4
	$B^*\eta$		${}^3P_1 = 0.0463$	3.96	2.0
	$B(2^1S_0)\pi$		${}^1P_1 = -0.0341$	0.215	0.1
	$B(1P_1)\pi$		${}^3S_1 = -0.330i$, ${}^3D_1 = -0.0381i$	63.0	32.0
	$B(1P_1')\pi$		${}^3S_1 = -0.0278i$, ${}^3D_1 = 0.00191i$	0.425	0.2
	$B(1^3P_2)\pi$		${}^5D_1 = -0.0355i$	0.632	0.3
	B_sK		${}^1P_1 = 0.0997$	18.7	9.5
	B_s^*K		${}^3P_1 = 0.0695$	7.21	3.7
	Total			196.7, 196.3	100
$B(1D_2)$	$B(1P_1)\gamma$	5777	$\langle 1^3P_1\|r\|1^3D_2\rangle = 3.095$, $\langle 1^1P_1\|r\|1^1D_2\rangle = 3.163$	0.397, 0.113	1.7, 0.49
6095	$B(1P_1')\gamma$	5784	$\langle 1^3P_1\|r\|1^3D_2\rangle = 3.095$, $\langle 1^1P_1\|r\|1^1D_2\rangle = 3.163$	0.00267, 0.000761	0.012, 0.0033
	$B(1^3P_2)\gamma$	5797	$\langle 1^3P_2\|r\|1^3D_2\rangle = 3.324$	0.0422, 0.0120	0.18, 0.052
	$B\rho$		${}^3P_2 = -0.0597$, ${}^3F_2 = -8.03 \times 10^{-5}$	1.57	6.8
	$B^*\pi$		${}^3P_2 = 0.00228$, ${}^3F_2 = -0.0889$	20.1	86.5, 87.7
	$B^*\eta$		${}^3P_2 = 0.00118$, ${}^3F_2 = -0.0134$	0.316	1.4
	$B(1^3P_0)\pi$		${}^1D_2 = 0.00838i$	0.0415	0.2
	$B(1P_1)\pi$		${}^3D_2 = 0.0254i$	0.333	1.4
	$B(1P_1')\pi$		${}^3D_2 = 0.00778i$	0.0300	0.1
	$B(1^3P_2)\pi$		${}^5S_2 = -0.00612i$, ${}^5D_2 = 0.0146i$, ${}^5G_2 = 0.00237i$	0.115	0.5
	B_s^*K		${}^3P_2 = 0.00179$, ${}^3F_2 = -0.0129$	0.237	1.0
	Total			23.2, 22.9	100
$B(1D_2')$	$B(1P_1)\gamma$	5777	$\langle 1^3P_1\|r\|1^3D_2\rangle = 3.095$, $\langle 1^1P_1\|r\|1^1D_2\rangle = 3.163$	0.0290, 0.00827	0.014, 0.0039
6124	$B(1P_1')\gamma$	5784	$\langle 1^3P_1\|r\|1^3D_2\rangle = 3.095$, $\langle 1^1P_1\|r\|1^1D_2\rangle = 3.163$	0.433, 0.123	0.20, 0.058
	$B(1^3P_2)\gamma$	5797	$\langle 1^3P_2\|r\|1^3D_2\rangle = 3.324$	0.0805, 0.0230	0.038, 0.011
	$B\rho$		${}^3P_2 = -0.0250$, ${}^3F_2 = 0.00442$	0.640	0.3
	$B^*\pi$		${}^3P_2 = 0.188$, ${}^3F_2 = -4.40 \times 10^{-5}$	96.3	45.2
	$B^*\eta$		${}^3P_2 = 0.0848$, ${}^3F_2 = -3.24 \times 10^{-5}$	14.1	6.6
	$B(2^3S_1)\pi$		${}^3P_2 = -0.0417$, ${}^3F_2 = 1.45 \times 10^{-5}$	0.260	0.1
	$B(1P_1)\pi$		${}^3D_2 = 0.0348i$	0.757	0.4
	$B(1^3P_2)\pi$		${}^5S_2 = -0.362i$, ${}^5D_2 = -0.0507i$, ${}^5G_2 = 2.94 \times 10^{-5}i$	73.8	34.6
	B_s^*K		${}^3P_2 = 0.130$, ${}^3F_2 = -1.66 \times 10^{-5}$	26.8	12.6
	Total			213.4, 213.0	100
$B(1^3D_3)$	$B(1^3P_2)\gamma$	5797	$\langle 1^3P_2\|r\|1^3D_3\rangle = 3.346$	0.464, 0.132	1.5, 0.43
6106	$B\pi$		${}^1F_3 = 0.0694$	14.4	46.4, 46.9
	$B\eta$		${}^1F_3 = 0.0140$	0.441	1.4
	$B^*\pi$		${}^3F_3 = -0.0737$	14.2	45.8, 46.3
	$B^*\eta$		${}^3F_3 = -0.0119$	0.257	0.8
	$B(1P_1)\pi$		${}^3D_3 = -0.0142i$, ${}^3G_3 = -0.00302i$	0.117	0.4
	$B(1P_1')\pi$		${}^3D_3 = 0.0108i$, ${}^3G_3 = -0.000187i$	0.0615	0.2
	$B(1^3P_2)\pi$		${}^5D_3 = 0.0307i$, ${}^5G_3 = 0.00189i$	0.460	1.5
	B_sK		${}^1F_3 = 0.0140$	0.366	1.2
	B_s^*K		${}^3F_3 = -0.0116$	0.197	0.6
	Total			31.0, 30.7	100

The $1D$ multiplets are next highest in mass. They consist of a narrow doublet and a broad doublet. The narrow B doublet consists of the $1D_2$ with total width 23 MeV with $\mathrm{BR}(B^*\pi) = 87\%$ and the 1^3D_3 with total width 31 MeV with $\mathrm{BR}(B\pi) = 46\%$ and $\mathrm{BR}(B^*\pi) = 46\%$. These two states should have strong signals in their dominant decay modes. However, because these two states are close in mass it will likely require an angular distribution analysis to

TABLE XV. Partial widths and branching ratios for strong decays of the 2^3D_1 B meson. See the caption to Table IV for further explanations.

Initial state	Final state	$\mathcal{M}$	Width [MeV]	BR [%]
$B(2^3D_1)$	$B\pi$	${}^1P_1 = 0.0400$	9.35	4.1
6475	$B\eta$	${}^1P_1 = 0.00938$	0.465	0.2
	$B\eta'$	${}^1P_1 = -0.0205$	1.47	0.6
	$B^*\pi$	${}^3P_1 = 0.0266$	3.79	1.7
	$B^*\rho$	${}^1P_1 = -0.0149$, ${}^5P_1 = 0.00665$, ${}^5F_1 = 0.104$	44.2	19.5
	$B^*\eta'$	${}^3P_1 = -0.0207$	1.22	0.5
	$B^*\omega$	${}^1P_1 = -0.00917$, ${}^5P_1 = 0.00410$, ${}^5F_1 = 0.0594$	14.3	6.3
	$B(2^1S_0)\pi$	${}^1P_1 = 0.0685$	7.82	3.4
	$B(2^1S_0)\eta$	${}^1P_1 = 0.0316$	0.502	0.2
	$B(2^3S_1)\pi$	${}^3P_1 = 0.0542$	4.44	2.0
	$B(1P_1)\pi$	${}^3S_1 = -0.0507i$, ${}^3D_1 = 0.0822i$	22.6	10.0
	$B(1P_1)\eta$	${}^3S_1 = 0.0400i$, ${}^3D_1 = 0.0269i$	3.66	1.6
	$B(1P_1')\pi$	${}^3S_1 = -0.00302i$, ${}^3D_1 = -0.0296i$	2.10	0.9
	$B(1P_1')\eta$	${}^3S_1 = 0.00331i$, ${}^3D_1 = -0.0122i$	0.242	0.1
	$B(1^3P_2)\pi$	${}^5D_1 = 0.0875i$	17.6	7.8
	$B(1^3P_2)\eta$	${}^5D_1 = 0.0261i$	0.972	0.4
	$B(2P_1)\pi$	${}^3S_1 = -0.198i$, ${}^3D_1 = -0.0367i$	15.8	7.0
	$B(2^3P_2)\pi$	${}^5D_1 = -0.0323i$	0.354	0.2
	$B(1D_2)\pi$	${}^5P_1 = 0.242$, ${}^5F_1 = 0.0240$	44.4	19.6
	$B(1^3D_3)\pi$	${}^7F_1 = 0.0273$	0.529	0.2
	B_sK	${}^1P_1 = -0.0111$	0.582	0.2
	B_sK^*	${}^3P_1 = 0.0300$	2.78	1.2
	B_s^*K	${}^3P_1 = -0.0125$	0.663	0.3
	$B_s^*K^*$	${}^1P_1 = -0.0292$, ${}^5P_1 = 0.0131$, ${}^5F_1 = 0.0222$	3.73	1.6
	$B_s(1P_1)K$	${}^3S_1 = 0.128i$, ${}^3D_1 = 0.0319i$	21.2	9.4
	$B_s(1P_1')K$	${}^3S_1 = -0.0103i$, ${}^3D_1 = -0.0222i$	0.714	0.3
	$B_s(1^3P_2)K$	${}^5D_1 = 0.0322i$	1.12	0.5
	Total		226.8	100

distinguish the $1D_2$ from the 1^3D_3 in the $B^*\pi$ final state. Nevertheless, it should be possible to observe the two narrow $1D$ states. In contrast, for the two broad states, 1^3D_1 and $1D_2'$, despite the fact that the $1D_2'$ is expected to have a large BR of 45% to $B^*\pi$ and the 1^3D_1 of 30% to $B\pi$, because they are expected to have total widths of approximately 200 MeV it will likely be difficult to extract a strong signal. These observations equally apply to the $B_s(1D)$ states. The narrow $B_s(1D_2)$ and $B_s(1^3D_3)$ states have widths of 16 MeV and 26 MeV, respectively. The $B_s(1D_2)$ has a BR to B^*K of 97% while the $B_s(1^3D_3)$ has BRs to BK of 53% and to B^*K of 43%. In contrast, the broad $D_s(1^3D_1)$ has a width of 183 MeV with a BR to BK of 59% and to B^*K of 29% while the broad $B_s(1D_2')$ has a width of 194 MeV with BR to B^*K of 88%. We conclude that the narrow states will produce strong signals although sitting in broad backgrounds so that measuring their spins and parities will be helpful in identifying them.

Next in mass are the $2P$ multiplets. All members of the nonstrange bottom $2P$ multiplet are relatively broad with $\Gamma \sim 200$ MeV which is significantly greater than the intramultiplet mass splitting. The largest BRs are mainly to more complicated final states, for example, $\mathrm{BR}(B(2^3P_0) \to B(1P_1)\pi) = 50\%$ and $\mathrm{BR}(B(2P_1') \to B(1^3P_2)\pi) = 41\%$. The most promising possibility is to study the $B\pi$ final state which only the $B(2^3P_0)$ and $B(2^3P_2)$ can decay to with BRs of 10.5% and 8.4%, respectively. Because the expected widths are so much larger than the splitting, distinguishing the states will require an angular momentum analysis to identify the two states. The $B(2P_1)$ and $B(2P_1')$ both decay to $B^*\pi$ with BRs of 30% and 9%, respectively. But again, because they are overlapping resonances, more information would be needed to distinguish the two states, such as BRs to other final states such as $B\rho$ and $B^*\rho$, although this would be difficult because the $B(2^3P_0)$ and $B(2^3P_2)$ also decay to $B^*\rho$ with BRs of approximately 20% and 40%, respectively. We conclude that only the $B(2^3P_0)$ and $B(2^3P_2)$ might be observed in the foreseeable future.

In contrast, the $2P$ B_s mesons divide into two relatively narrow states, $B_s(2^3P_0)$ and $B_s(2P_1')$, and two relatively broad states, $B_s(2P_1)$ and $B_s(2^3P_2)$. The $B_s(2^3P_0)$ has a total width of 71 MeV and BR to BK of 44% and the $B_s(2P_1')$ has a total width of 79 MeV with a BR of 31% to B^*K and 28% to BK^*. In contrast, the $B_s(2P_1)$ has total width of 218 MeV, and the $B_s(2^3P_2)$ has a total width of 246 MeV. Although the $B_s(2P_1)$ and $B_s(2^3P_2)$ overlap with the $B_s(2^3P_0)$ and $B_s(2P_1')$, and the $B_s(2P_1)$ has significant BRs to B^*K of 40% and to BK^* of 33%, and the

TABLE XVI. Partial widths and branching ratios for strong decays of the $2D_2$ B meson. See the caption to Table IV for further explanations.

Initial state	Final state	$\mathcal{M}$	Width [MeV]	BR [%]
$B(2D_2)$	$B\rho$	${}^3P_2 = 0.00895$, ${}^3F_2 = 0.0127$	1.04	1.0
6450	$B\omega$	${}^3P_2 = 0.00618$, ${}^3F_2 = 0.00730$	0.390	0.4
	$B^*\pi$	${}^3P_2 = 0.000507$, ${}^3F_2 = 0.0628$	20.4	19.6
	$B^*\rho$	${}^3P_2 = -0.0228$, ${}^3F_2 = -0.0519$, ${}^5P_2 = 0.0119$, ${}^5F_2 = 0.0477$	21.1	20.3
	$B^*\eta$	${}^3P_2 = 0.000429$, ${}^3F_2 = 0.0287$	3.76	3.6
	$B^*\eta'$	${}^3P_2 = 0.000660$, ${}^3F_2 = 0.0114$	0.329	0.3
	$B^*\omega$	${}^3P_2 = -0.0141$, ${}^3F_2 = -0.0296$, ${}^5P_2 = 0.00738$, ${}^5F_2 = 0.0272$	6.92	6.7
	$B(2^3S_1)\pi$	${}^3P_2 = -0.000203$, ${}^3F_2 = -0.0666$	6.13	5.9
	$B(1^3P_0)\pi$	${}^1D_2 = -0.0323i$	2.50	2.4
	$B(1^3P_0)\eta$	${}^1D_2 = -0.0116i$	0.209	0.2
	$B(1P_1)\pi$	${}^3D_2 = -0.0477i$	5.14	5.0
	$B(1P_1)\eta$	${}^3D_2 = -0.0136i$	0.257	0.2
	$B(1P_1')\pi$	${}^3D_2 = -0.0314i$	2.19	2.1
	$B(1P_1')\eta$	${}^3D_2 = -0.00986i$	0.129	0.1
	$B(1^3P_2)\pi$	${}^5S_2 = -0.000724i$, ${}^5D_2 = -0.0381i$, ${}^5G_2 = -0.0644i$	12.0	11.5
	$B(1^3P_2)\eta$	${}^5S_2 = -0.00103i$, ${}^5D_2 = -0.00978i$, ${}^5G_2 = -0.00386i$	0.137	0.1
	$B(2P_1)\pi$	${}^3D_2 = 0.0209i$	0.137	0.1
	$B(1D_2)\pi$	${}^5P_2 = -0.0517$, ${}^5F_2 = -0.0162$	1.92	1.8
	$B(1^3D_3)\pi$	${}^7P_2 = -0.0163$, ${}^7F_2 = -0.0135$, ${}^7H_2 = -0.00239$	0.279	0.3
	B_sK^*	${}^3P_2 = 0.0473$, ${}^3F_2 = 0.00319$	6.30	6.1
	B_s^*K	${}^3P_2 = 0.000934$, ${}^3F_2 = 0.0409$	6.77	6.5
	$B_s^*K^*$	${}^3P_2 = -0.0399$, ${}^3F_2 = -0.00893$, ${}^5P_2 = 0.0222$, ${}^5F_2 = 0.00824$	4.83	4.6
	$B_s(1^3P_0)K$	${}^1D_2 = -0.0167i$	0.341	0.3
	$B_s(1P_1)K$	${}^3D_2 = -0.0186i$	0.359	0.3
	$B_s(1P_1')K$	${}^3D_2 = -0.0105i$	0.112	0.1
	$B_s(1^3P_2)K$	${}^5S_2 = -0.00227i$, ${}^5D_2 = -0.0113i$, ${}^5G_2 = -0.00240i$	0.126	0.1
	Total		103.9	100

$B_s(2^3P_2)$ to BK of 12% and to B^*K of 20%, it should be possible to extract a meaningful signal for the $B_s(2^3P_0)$ in the BK final state and for the $B_s(2P_1')$ in the B^*K final state.

The $3S$ and $1F$ multiplets are very close in mass, at approximately 6300 MeV, and overlap. The $B(3^3S_1)$ and $B(3^1S_0)$ have total widths of 140 and 151 MeV, respectively, with BRs of $\mathrm{BR}(3^3S_1 \to B\pi) = 2.2\%$, $\mathrm{BR}(3^3S_1 \to B^*\pi) = 3.1\%$, and $\mathrm{BR}(3^1S_0 \to B^*\pi) = 2.8\%$ so that the signals to observe these states are rather small. Both states have large BR to $B^*\rho$ of 21% and 22%, respectively, so these are potentially interesting but also more challenging; as the final state consists of three pions it would be necessary to perform a Dalitz plot analysis to reconstruct the intermediate ρ meson. The narrow $B(1F)$ states are the $B(1F_3)$ with total width 106 MeV and $\mathrm{BR}(B^*\pi) = 25\%$, and the $B(1^3F_4)$ with total width 110 MeV and $\mathrm{BR}(B^*\pi) = 15\%$ and $\mathrm{BR}(B\pi) = 14\%$. So, in fact, the narrow $1F$ states might be more likely to be observed than the $3S$ states although it will be challenging. We also note that these states also have reasonable BRs to $B^*\rho$ of 20% for the $B(1F_3)$ and 47% for the $B(1^3F_4)$.

The situation for the $B_s(3S)$ states is similar, although perhaps a bit more promising, with total widths of 130 MeV for the $B_s(3^3S_1)$ and 121 MeV for the $B_s(3^1S_0)$ with relatively small BRs to the simple final states; $\mathrm{BR}(B_s(3^3S_1) \to BK) = 5.5\%$, $\mathrm{BR}(B_s(3^3S_1) \to B^*K) = 6.9\%$, and $\mathrm{BR}(B_s(3^1S_0) \to B^*K) = 6.7\%$. The narrow $B_s(1F)$ states are the $B_s(1F_3)$ with total width 138 MeV and BR to B^*K of 28% and the $B_s(1^3F_4)$ with total width of 139 MeV and BR to BK of 18% and to B^*K of 17%. Another prominent decay mode for all these states is BK^*. So although there are numerous overlapping resonances, some of these states are narrow enough with a reasonable signal strength to a simple final state that if one can determine their spin it should be possible to observe them.

As we move higher in mass, more final states become kinematically allowed so that BRs to simple states become smaller with some exceptions, which we note in what follows. We refer the interested reader to Tables IV–XXXV for more details.

The $B(3P_1)$ and $B(3^3P_2)$ are relatively narrow with total widths of 93 MeV and 88 MeV, respectively, with the $B(3P_1)$ having $\mathrm{BR}(B^*\pi) = 5.4\%$ and the $B(^3P_2)$ having $\mathrm{BR}(B\pi) = 2.9\%$ and $\mathrm{BR}(B^*\pi) = 4\%$. The $B(2D_2)$ has a total width of 104 MeV with $\mathrm{BR}(B^*\pi) = 19.6\%$, and the $B(2^3D_3)$ has a total width of 94 MeV with $\mathrm{BR}(B\pi) = 4.3\%$ and $\mathrm{BR}(B^*\pi) = 8.6\%$.

TABLE XVII. Partial widths and branching ratios for strong decays of the $2D_2'$ B meson. See the caption to Table IV for further explanations.

Initial state	Final state	$\mathcal{M}$	Width [MeV]	BR [%]
$B(2D_2')$	$B\rho$	${}^3P_2 = -0.00175$, ${}^3F_2 = -0.0603$	16.9	7.2
6486	$B\omega$	${}^3P_2 = -0.000820$, ${}^3F_2 = -0.0347$	5.54	2.4
	$B^*\pi$	${}^3P_2 = 0.0523$, ${}^3F_2 = -0.00101$	15.0	6.4
	$B^*\rho$	${}^3P_2 = 0.0107$, ${}^3F_2 = 0.0450$, ${}^5P_2 = 0.00799$, ${}^5F_2 = 0.0632$	25.3	10.8
	$B^*\eta$	${}^3P_2 = 0.0115$, ${}^3F_2 = -0.000253$	0.645	0.3
	$B^*\eta'$	${}^3P_2 = -0.0307$, ${}^3F_2 = 1.74 \times 10^{-6}$	2.79	1.2
	$B^*\omega$	${}^3P_2 = 0.00686$, ${}^3F_2 = 0.0257$, ${}^5P_2 = 0.00520$, ${}^5F_2 = 0.0362$	8.28	3.5
	$B(2^3S_1)\pi$	${}^3P_2 = 0.0914$, ${}^3F_2 = -0.000691$	13.1	5.6
	$B(1^3P_0)\pi$	${}^1D_2 = 0.0220i$	1.27	0.5
	$B(1P_1)\pi$	${}^3D_2 = -0.0552i$	7.56	3.2
	$B(1P_1)\eta$	${}^3D_2 = -0.0191i$	0.605	0.2
	$B(1P_1')\pi$	${}^3D_2 = -0.0329i$	2.65	1.1
	$B(1P_1')\eta$	${}^3D_2 = -0.0131i$	0.274	0.1
	$B(1^3P_2)\pi$	${}^5S_2 = -0.0608i$, ${}^5D_2 = 0.0983i$, ${}^5G_2 = -0.000409i$	31.5	13.4
	$B(1^3P_2)\eta$	${}^5S_2 = 0.0424i$, ${}^5D_2 = 0.0322i$, ${}^5G_2 = -5.20 \times 10^{-5}i$	4.26	1.8
	$B(2P_1)\pi$	${}^3D_2 = 0.0327i$	0.451	0.2
	$B(2^3P_2)\pi$	${}^5S_2 = -0.206i$, ${}^5D_2 = -0.0443i$, ${}^5G_2 = 5.93 \times 10^{-5}i$	16.5	7.0
	$B(1D_2)\pi$	${}^5P_2 = -0.0612$, ${}^5F_2 = -0.0253$	3.49	1.5
	$B(1^3D_3)\pi$	${}^7P_2 = 0.248$, ${}^7F_2 = 0.0315$, ${}^7H_2 = -4.94 \times 10^{-5}$	46.9	19.9
	B_sK^*	${}^3P_2 = 0.00838$, ${}^3F_2 = -0.0187$	1.34	0.6
	B_s^*K	${}^3P_2 = -0.0139$, ${}^3F_2 = -0.000261$	0.838	0.4
	$B_s^*K^*$	${}^3P_2 = 0.0320$, ${}^3F_2 = 0.0105$, ${}^5P_2 = 0.0272$, ${}^5F_2 = 0.0148$	5.41	2.3
	$B_s(1^3P_0)K$	${}^1D_2 = 0.0140i$	0.291	0.1
	$B_s(1P_1)K$	${}^3D_2 = -0.0276i$	0.982	0.4
	$B_s(1P_1')K$	${}^3D_2 = -0.0142i$	0.255	0.1
	$B_s(1^3P_2)K$	${}^5S_2 = 0.134i$, ${}^5D_2 = 0.0406i$, ${}^5G_2 = -2.97 \times 10^{-5}i$	22.9	9.7
	Total		235.3	100

The $B_s(4^3S_1)$ has a total width of 104 MeV with BR to BK and B^*K of 2.9% and 4%, respectively, and the $B_s(4^1S_0)$ has a total width of 85 MeV with BR to B^*K of 5.3%. The $B_s(3P)$ multiplets are all relatively narrow with large BRs to simple final states. For example, most prominently, the $B_s(3^3P_0)$ has a total width of 51 MeV with BR to BK of 24%, and the $B_s(3P_1')$ has a total width of 48 MeV with BR to B^*K of 21%. The final state we note is the $B_s(2^3D_3)$ with total width of 107 MeV and BR to BK and B^*K of 6.4% and 13.8%, respectively.

Finally, we included the strong decay widths for the $1G$ multiplets as the $B(1G_4)$ and $B(1^3G_5)$ are relatively narrow, $\Gamma[B(1G_4)] = 96\,\text{MeV}$, and $\Gamma[B(1^3G_5)] = 102\,\text{MeV}$, with large BRs to simple final states; $\text{BR}[B(1G_4) \to B^*\pi] = 24.2\%$, $\text{BR}[B(1^3G_5) \to B\pi] = 12.1\%$, and $\text{BR}[B(1^3G_5) \to B^*\pi] = 13.2\%$. These states overlap with the $3P$ multiplet and are close in mass to the $2F$ states so that it will be necessary to determine their spins to identify them. It would be interesting to find these states as they are high L states analogous to Rydberg states of atomic physics. Their masses would give insights into the confining potential and their splittings on the nature of the spin dependent potentials. They would test our understanding of QCD in a region that has not been explored. In contrast, the $B_s(1G)$ states are broader, ~200–300 MeV, so are less likely to be easily found.

The important conclusion we wish to draw from these results is that there are numerous excited bottom mesons that are expected to be relatively narrow with significant BRs to simple final states. With sufficient statistics it should be possible to observe many of these states and improve our knowledge of bottom spectroscopy. The challenge is that there is significant overlapping of these states so it will be necessary to perform an angular distribution analysis to determine the spins of the underlying states to disentangle the observed final states.

TABLE XVIII. Partial widths and branching ratios for strong decays of the 2^3D_3 B meson. See the caption to Table IV for further explanations.

Initial state	Final state	$\mathcal{M}$	Width [MeV]	BR [%]
$B(2^3D_3)$	$B\pi$	${}^1F_3 = -0.0266$	4.05	4.3
6460	$B\rho$	${}^3F_3 = -0.0416$	7.57	8.1
	$B\eta$	${}^1F_3 = -0.0144$	1.06	1.1
	$B\eta'$	${}^1F_3 = -0.0100$	0.335	0.4
	$B\omega$	${}^3F_3 = -0.0239$	2.48	2.6
	$B^*\pi$	${}^3F_3 = 0.0392$	8.05	8.6
	$B^*\rho$	${}^1F_3 = -0.0218$, ${}^5P_3 = 0.0215$, ${}^5F_3 = 0.0479$	12.4	13.3
	$B^*\eta$	${}^3F_3 = 0.0194$	1.75	1.9
	$B^*\eta'$	${}^3F_3 = 0.00906$	0.217	0.2
	$B^*\omega$	${}^1F_3 = -0.0125$, ${}^5P_3 = 0.0139$, ${}^5F_3 = 0.0273$	4.17	4.5
	$B(2^1S_0)\pi$	${}^1F_3 = 0.0501$	3.97	4.2
	$B(2^3S_1)\pi$	${}^3F_3 = -0.0538$	4.14	4.4
	$B(1P_1)\pi$	${}^3D_3 = 0.0254i$, ${}^3G_3 = 0.0503i$	7.36	7.9
	$B(1P_1)\eta$	${}^3D_3 = 0.00838i$, ${}^3G_3 = 0.00428i$	0.129	0.1
	$B(1P_1')\pi$	${}^3D_3 = -0.0433i$, ${}^3G_3 = 0.00306i$	4.30	4.6
	$B(1P_1')\eta$	${}^3D_3 = -0.0149i$, ${}^3G_3 = 0.000229i$	0.311	0.3
	$B(1^3P_2)\pi$	${}^5D_3 = -0.0589i$, ${}^5G_3 = -0.0402i$	11.2	12.0
	$B(1^3P_2)\eta$	${}^5D_3 = -0.0170i$, ${}^5G_3 = -0.00277i$	0.388	0.4
	$B(2^3P_2)\pi$	${}^5D_3 = 0.0235i$, ${}^5G_3 = 0.00149i$	0.163	0.2
	$B(1D_2)\pi$	${}^5P_3 = 0.0124$, ${}^5F_3 = 0.0123$, ${}^5H_3 = 0.00252$	0.215	0.2
	$B(1D_2')\pi$	${}^5P_3 = -0.0156$, ${}^5F_3 = -0.0035$, ${}^5H_3 = 1.74 \times 10^{-5}$	0.148	0.2
	$B(1^3D_3)\pi$	${}^7P_3 = -0.0562$, ${}^7F_3 = -0.0200$, ${}^7H_3 = -0.00156$	2.32	2.5
	B_sK	${}^1F_3 = -0.0226$	2.35	2.5
	B_sK^*	${}^3F_3 = -0.0114$	0.380	0.4
	B_s^*K	${}^3F_3 = 0.0286$	3.38	3.6
	$B_s^*K^*$	${}^1F_3 = -0.00419$, ${}^5P_3 = 0.0644$, ${}^5F_3 = 0.00918$	9.65	10.3
	$B_s(1P_1')K$	${}^3D_3 = -0.0215i$, ${}^3G_3 = -0.000268i$	0.498	0.5
	$B_s(1^3P_2)K$	${}^5D_3 = -0.0202i$, ${}^5G_3 = -0.00180i$	0.400	0.4
	Total		93.5	100

TABLE XIX. Partial widths and branching ratios for strong and electromagnetic decays of the $1F$ B mesons. See the caption to Table IV for further explanations.

Initial state	Final state	M_f [MeV]	$\mathcal{M}$	Width (ub, db) [MeV]	BR (ub, db) [%]
$B(1^3F_2)$	$B(1^3D_1)\gamma$	6110	$\langle 1^3D_1\|r\|1^3F_2\rangle = 3.833$	0.399, 0.114	0.20, 0.056
6387	$B(1D_2)\gamma$	6095	$\langle 1^3D_2\|r\|1^3F_2\rangle = 3.978$	0.0378, 0.0108	0.019, 0.0053
	$B(1D_2')\gamma$	6124	$\langle 1^3D_2\|r\|1^3F_2\rangle = 3.978$	0.0402, 0.0115	0.020, 0.0057
	$B(1^3D_3)\gamma$	6106	$\langle 1^3D_3\|r\|1^3F_2\rangle = 4.153$	0.00259, 0.000738	0.0013, 0.00036
	$B\pi$		${}^1D_2 = 0.0732i$	27.4	13.6
	$B\rho$		${}^3D_2 = -0.0642i$	15.2	7.5
	$B\eta$		${}^1D_2 = 0.0335i$	5.07	2.5
	$B\eta'$		${}^1D_2 = 0.0202i$	1.00	0.5
	$B\omega$		${}^3D_2 = -0.0368i$	4.97	2.5
	$B^*\pi$		${}^3D_2 = 0.0647i$	19.5	9.6
	$B^*\rho$		${}^1D_2 = 0.0442i$, ${}^5D_2 = -0.0334i$, ${}^5G_2 = -0.0337i$	13.2	6.5
	$B^*\eta$		${}^3D_2 = 0.0289i$	3.35	1.7
	$B^*\omega$		${}^1D_2 = 0.0252i$, ${}^5D_2 = -0.0191i$, ${}^5G_2 = -0.0186i$	4.18	2.1
	$B(2^1S_0)\pi$		${}^1D_2 = -0.0474i$	2.72	1.4
	$B(2^3S_1)\pi$		${}^3D_2 = -0.0359i$	1.38	0.7
	$B(1P_1)\pi$		${}^3P_2 = 0.150$, ${}^3F_2 = 0.0364$	44.9	22.2
	$B(1P_1)\eta$		${}^3P_2 = 0.0558$, ${}^3F_2 = 0.00200$	2.73	1.4
	$B(1P_1')\pi$		${}^3P_2 = 0.0124$, ${}^3F_2 = -0.0123$	0.560	0.3
	$B(1^3P_2)\pi$		${}^5P_2 = 0.0533$, ${}^5F_2 = 0.0438$	8.41	4.2
	$B(1^3P_2)\eta$		${}^5P_2 = 0.0172$, ${}^5F_2 = 0.00147$	0.209	0.1
	$B(2P_1)\pi$		${}^3P_2 = -0.0489$, ${}^3F_2 = -0.000688$	0.348	0.2
	$B(1D_2)\pi$		${}^5S_2 = -0.260i$, ${}^5D_2 = -0.0410i$, ${}^5G_2 = -0.000956i$	29.9	14.8
	B_sK		${}^1D_2 = 0.0451i$	8.10	4.0
	B_sK^*		${}^3D_2 = -0.0163i$	0.547	0.3
	B_s^*K		${}^3D_2 = 0.0383i$	5.19	2.6
	$B_s(1P_1)K$		${}^3P_2 = 0.0672$, ${}^3F_2 = 0.000939$	2.48	1.2
	Total			202.4, 202.0	100
$B(1F_3)$	$B(1D_2)\gamma$	6095	$\langle 1^3D_2\|r\|1^3F_3\rangle = 3.989$, $\langle 1^1D_2\|r\|1^1F_3\rangle = 4.040$	0.427, 0.122	0.40, 0.12
6358	$B(1^3D_3)\gamma$	6106	$\langle 1^3D_3\|r\|1^3F_3\rangle = 4.184$	0.0207, 0.00590	0.020, 0.0056
	$B\rho$		${}^3D_3 = -0.0997i$, ${}^3G_3 = -0.00376i$	34.1	32.4
	$B\omega$		${}^3D_3 = -0.0571i$, ${}^3G_3 = -0.00209i$	11.0	10.4
	$B^*\pi$		${}^3D_3 = 0.000340i$, ${}^3G_3 = -0.0769i$	26.2	24.8
	$B^*\rho$		${}^3D_3 = 0.0672i$, ${}^3G_3 = 0.0152i$, ${}^5D_3 = -0.0475i$, ${}^5G_3 = -0.0146i$	20.7	19.6
	$B^*\eta$		${}^3D_3 = 8.06 \times 10^{-5}i$, ${}^3G_3 = -0.0196i$	1.46	1.4
	$B^*\omega$		${}^3D_3 = 0.0382i$, ${}^3G_3 = 0.00829i$, ${}^5D_3 = -0.0270i$, ${}^5G_3 = -0.00800i$	6.56	6.2
	$B(1^3P_0)\pi$		${}^1F_3 = -0.0157$	0.453	0.4
	$B(1P_1)\pi$		${}^3F_3 = -0.0284$	1.38	1.3
	$B(1P_1')\pi$		${}^3F_3 = -0.0148$	0.369	0.4
	$B(1^3P_2)\pi$		${}^5P_3 = 7.60 \times 10^{-5}$, ${}^5F_3 = -0.0226$, ${}^5H_3 = -0.0103$	0.994	0.9
	B_sK^*		${}^3D_3 = -0.0196i$, ${}^3G_3 = -0.000142i$	0.653	0.6
	B_s^*K		${}^3D_3 = 0.0000478i$, ${}^3G_3 = -0.0178i$	1.04	1.0
	Total			105.6, 105.2	100

TABLE XX. Partial widths and branching ratios for strong and electromagnetic decays of the $1F$ B mesons. See the caption to Table IV for further explanations.

Initial state	Final state	M_f [MeV]	$\mathcal{M}$	Width (ub, db) [MeV]	BR (ub, db) [%]
$B(1F_3')$	$B(1D_2)\gamma$	6095	$\langle 1^3D_2\|r\|1^3F_3\rangle = 3.989$, $\langle 1^1D_2\|r\|1^1F_3\rangle = 4.040$	0.00229, 0.000652	0.0010, 0.00029
6396	$B(1D_2')\gamma$	6124	$\langle 1^3D_2\|r\|1^3F_3\rangle = 3.989$, $\langle 1^1D_2\|r\|1^1F_3\rangle = 4.040$	0.457, 0.130	0.21, 0.059
	$B(1^3D_3)\gamma$	6106	$\langle 1^3D_3\|r\|1^3F_3\rangle = 4.184$	0.0408, 0.0116	0.018, 0.0052
	$B\rho$		${}^3D_3 = -0.0143i$, ${}^3G_3 = 0.0325i$	4.78	2.2
	$B\omega$		${}^3D_3 = -0.00823i$, ${}^3G_3 = 0.0182i$	1.49	0.7
	$B^*\pi$		${}^3D_3 = 0.102i$, ${}^3G_3 = 0.000694i$	49.2	22.2
	$B^*\rho$		${}^3D_3 = -0.0636i$, ${}^3G_3 = -0.0178i$, ${}^5D_3 = -0.0590i$, ${}^5G_3 = -0.0226i$	27.0	12.2
	$B^*\eta$		${}^3D_3 = 0.0466i$, ${}^3G_3 = 0.000207i$	8.89	4.0
	$B^*\eta'$		${}^3D_3 = 0.0189i$, ${}^3G_3 = 1.27 \times 10^{-5}i$	0.636	0.3
	$B^*\omega$		${}^3D_3 = -0.0363i$, ${}^3G_3 = -0.00987i$, ${}^5D_3 = -0.0337i$, ${}^5G_3 = -0.0125i$	8.65	3.9
	$B(2^3S_1)\pi$		${}^3D_3 = -0.0637i$, ${}^3G_3 = -0.000195i$	4.51	2.0
	$B(1^3P_0)\pi$		${}^1F_3 = 0.0119$	0.291	0.1
	$B(1P_1)\pi$		${}^3F_3 = -0.0349$	2.35	1.1
	$B(1P_1')\pi$		${}^3F_3 = -0.0150$	0.428	0.2
	$B(1^3P_2)\pi$		${}^5P_3 = 0.172$, ${}^5F_3 = 0.0501$, ${}^5H_3 = 0.000184$	58.1	26.2
	$B(1^3P_2)\eta$		${}^5P_3 = 0.0618$, ${}^5F_3 = 0.00218$, ${}^5H_3 = 1.32 \times 10^{-6}$	2.99	1.4
	$B(2^3P_2)\pi$		${}^5P_3 = -0.0507$, ${}^5F_3 = -0.000786$	0.332	0.2
	$B(1^3D_3)\pi$		${}^7S_3 = -0.283i$, ${}^7D_3 = -0.0481i$, ${}^7G_3 = -0.00142i$	35.0	15.8
	B_s^*K		${}^3D_3 = 0.0629i$, ${}^3G_3 = 0.000192i$	14.3	6.4
	$B_s^*K^*$		${}^3D_3 = -0.0104i$, ${}^3G_3 = -0.000452i$, ${}^5D_3 = -0.00960i$, ${}^5G_3 = -0.000572i$	0.286	0.1
	$B_s(1^3P_2)K$		${}^5P_3 = 0.0687$, ${}^5F_3 = 0.000880$	2.13	1.0
	Total			222.1, 221.8	100
$B(1^3F_4)$	$B(1^3D_3)\gamma$	6106	$\langle 1^3D_3\|r\|1^3F_4\rangle = 4.206$	0.468, 0.133	0.42, 0.12
6364	$B\pi$		${}^1G_4 = 0.056i$	15.5	14.0
	$B\rho$		${}^3G_4 = 0.0212i$	1.57	1.4
	$B\eta$		${}^1G_4 = 0.0156i$	1.06	1.0
	$B\omega$		${}^3G_4 = 0.0118i$	0.481	0.4
	$B^*\pi$		${}^3G_4 = -0.0604i$	16.3	14.8
	$B^*\rho$		${}^1G_4 = 0.00803i$, ${}^5D_4 = -0.132i$, ${}^5G_4 = -0.0159i$	51.9	47.1
	$B^*\eta$		${}^3G_4 = -0.0157i$	0.944	0.8
	$B^*\omega$		${}^1G_4 = 0.00441i$, ${}^5D_4 = -0.0750i$, ${}^5G_4 = -0.00873i$	16.5	15.0
	$B(1P_1)\pi$		${}^3F_4 = 0.0184$, ${}^3H_4 = 0.00973$	0.758	0.7
	$B(1P_1')\pi$		${}^3F_4 = -0.0208$, ${}^3H_4 = 0.000588$	0.740	0.7
	$B(1^3P_2)\pi$		${}^5F_4 = -0.0374$, ${}^5H_4 = -0.00679$	2.38	2.2
	B_sK		${}^1G_4 = 0.0141i$	0.752	0.7
	B_s^*K		${}^3G_4 = -0.0143i$	0.683	0.6
	Total			110.4, 110.0	100

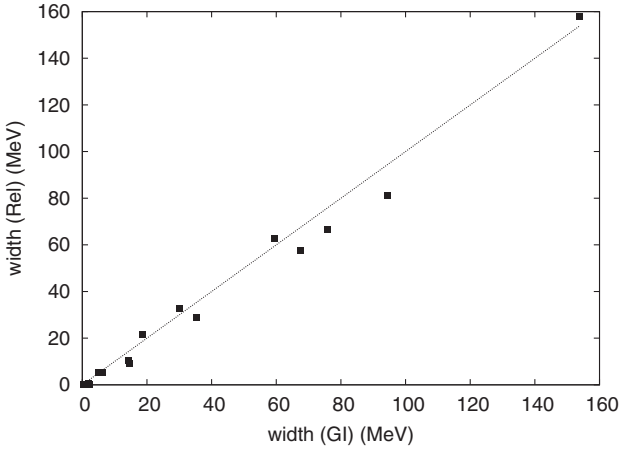

FIG. 4. Selected strong decay width predictions for Godfrey-Isgur (GI) and AR (Rel) models.

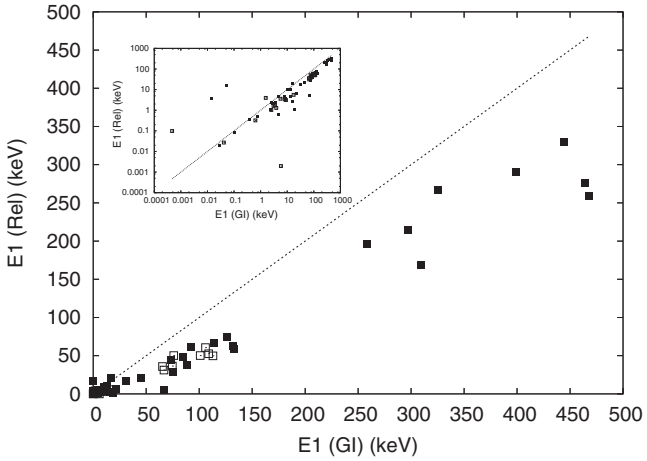

FIG. 6. E1 transition rate predictions for Godfrey-Isgur (GI) and AR (Rel) models. Solid symbols are B states; open symbols are B_s states. Inset: log-log scale.

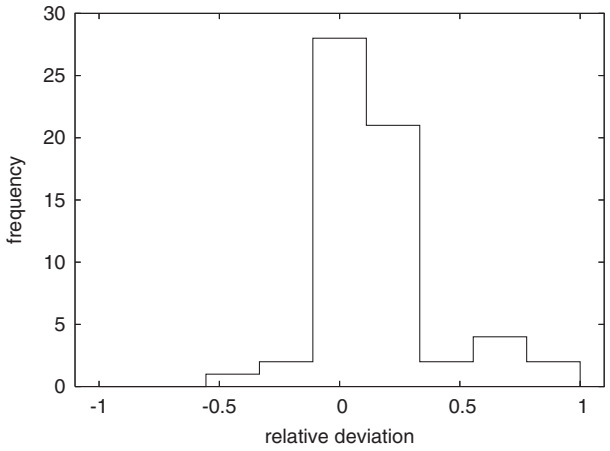

FIG. 5. Relative deviation of strong decay predictions.

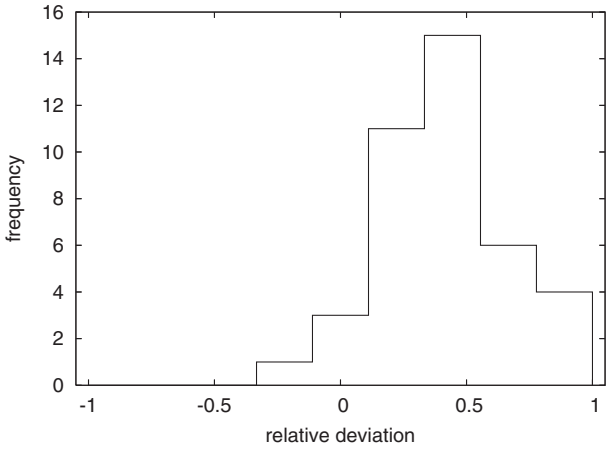

FIG. 7. Relative deviations of E1 radiative transition rates.

TABLE XXI. Partial widths and branching ratios for strong decays of the $1G$ B mesons. In this table, we do not show strong decay modes which have BR $< 0.5\%$, although they are included in calculating the total width. See the caption to Table IV for further explanations.

Initial state	Final state	$\mathcal{M}$	Width [MeV]	BR [%]
$B(1^3G_3)$	$B\pi$	${}^1F_3 = -0.0420$	12.7	6.9
6622	$B\rho$	${}^3F_3 = 0.0413$	10.2	5.6
	$B\eta$	${}^1F_3 = -0.0191$	2.42	1.3
	$B\eta'$	${}^1F_3 = -0.0171$	1.50	0.8
	$B\omega$	${}^3F_3 = 0.0238$	3.36	1.8
	$B^*\pi$	${}^3F_3 = -0.0396$	10.4	5.7
	$B^*\rho$	${}^1F_3 = -0.0286$, ${}^5F_3 = 0.0261$, ${}^5H_3 = 0.0453$	19.2	10.5
	$B^*\eta$	${}^3F_3 = -0.0178$	1.92	1.0
	$B^*\eta'$	${}^3F_3 = -0.0142$	0.908	0.5
	$B^*\omega$	${}^1F_3 = -0.0165$, ${}^5F_3 = 0.0150$, ${}^5H_3 = 0.0256$	6.19	3.4
	$B(2^1S_0)\pi$	${}^1F_3 = 0.0427$	4.66	2.6
	$B(2^3S_1)\pi$	${}^3F_3 = 0.0358$	3.05	1.7
	$B(1P_1)\pi$	${}^3D_3 = 0.0841i$, ${}^3G_3 = 0.0290i$	27.1	14.8
	$B(1P_1)\rho$	${}^3D_3 = -0.0332i$, ${}^3G_3 = -0.000956i$, ${}^5D_3 = -0.0235i$, ${}^5G_3 = -0.00253i$	2.40	1.3
	$B(1P_1)\eta$	${}^3D_3 = 0.0387i$, ${}^3G_3 = 0.00608i$	4.14	2.3
	$B(1P_1')\pi$	${}^3D_3 = 0.00685i$, ${}^3G_3 = -0.0158i$	1.00	0.5
	$B(1^3P_2)\pi$	${}^5D_3 = 0.0367i$, ${}^5G_3 = 0.0387i$	9.35	5.1
	$B(1^3P_2)\eta$	${}^5D_3 = 0.0168i$, ${}^5G_3 = 0.00761i$	0.866	0.5
	$B(2P_1)\pi$	${}^3D_3 = -0.0619i$, ${}^3G_3 = -0.00518i$	3.65	2.0
	$B(1D_2)\pi$	${}^5P_3 = 0.126$, ${}^5F_3 = 0.0410$, ${}^5H_3 = 0.00290$	25.2	13.8
	$B(1^3D_3)\pi$	${}^7P_3 = 0.0298$, ${}^7F_3 = 0.0268$, ${}^7H_3 = 0.00470$	2.25	1.2
	$B(1F_3)\pi$	${}^7S_3 = -0.202i$, ${}^7D_3 = -0.0341i$, ${}^7G_3 = -0.00108i$, ${}^7I_3 = -1.12 \times 10^{-5}i$	14.5	7.9
	B_sK	${}^1F_3 = -0.0224$	3.02	1.6
	B_sK^*	${}^3F_3 = 0.0139$	0.891	0.5
	B_s^*K	${}^3F_3 = -0.0207$	2.36	1.3
	$B_s(1P_1)K$	${}^3D_3 = 0.0505i$, ${}^3G_3 = 0.00467i$	5.82	3.2
	$B_s(1^3P_2)K$	${}^5D_3 = 0.0217i$, ${}^5G_3 = 0.00655i$	1.10	0.6
	Total		183.2	100
$B(1G_4)$	$B\rho$	${}^3F_4 = 0.0626$, ${}^3H_4 = 0.00345$	22.1	23.1
6588	$B\omega$	${}^3F_4 = 0.0360$, ${}^3H_4 = 0.00195$	7.28	7.6
	$B^*\pi$	${}^3F_4 = -0.000117$, ${}^3H_4 = 0.0605$	23.2	24.2
	$B^*\rho$	${}^3F_4 = -0.0456$, ${}^3H_4 = -0.0213$, ${}^5F_4 = 0.0353$, ${}^5H_4 = 0.0208$	21.4	22.3
	$B^*\eta$	${}^3F_4 = -2.55 \times 10^{-5}$, ${}^3H_4 = 0.0182$	1.91	2.0
	$B^*\omega$	${}^3F_4 = -0.0262$, ${}^3H_4 = -0.0120$, ${}^5F_4 = 0.0203$, ${}^5H_4 = 0.0118$	6.95	7.2
	$B(2^3S_1)\pi$	${}^3F_4 = -0.000228$, ${}^3H_4 = -0.0175$	0.660	0.7
	$B(1^3P_0)\pi$	${}^1G_4 = -0.0164i$	0.897	0.9
	$B(1P_1)\pi$	${}^3G_4 = -0.0249i$	1.97	2.1
	$B(1P_1)\rho$	${}^1G_4 = -4.31 \times 10^{-5}i$, ${}^3G_4 = 0.000319i$, ${}^5D_4 = -0.0363i$, ${}^5G_4 = -0.000758i$, ${}^5I_4 = -2.75 \times 10^{-6}i$	1.31	1.4
	$B(1P_1')\pi$	${}^3G_4 = -0.0163i$	0.835	0.9
	$B(1^3P_2)\pi$	${}^5G_4 = -0.0224i$, ${}^5I_4 = -0.0166i$	2.36	2.5
	B_sK^*	${}^3F_4 = 0.0195$, ${}^3H_4 = 0.000467$	1.62	1.7
	B_s^*K	${}^3F_4 = 5.85 \times 10^{-6}$, ${}^3H_4 = 0.0142$	1.06	1.1
	$B_s^*K^*$	${}^3F_4 = -0.0128$, ${}^3H_4 = -0.00245$, ${}^5F_4 = 0.00988$, ${}^5H_4 = 0.00239$	1.01	1.0
	Total		95.8	100

TABLE XXII. Partial widths and branching ratios for strong decays of the $1G$ B mesons. In this table, we do not show strong decay modes which have BR $< 0.5\%$, although they are included in calculating the total width. See the caption to Table IV for further explanations.

Initial state	Final state	$\mathcal{M}$	Width [MeV]	BR [%]
$B(1G_4')$	$B\rho$	${}^3F_4 = 0.00695$, ${}^3H_4 = -0.0355$	7.89	3.9
6628	$B\omega$	${}^3F_4 = 0.00401$, ${}^3H_4 = -0.0202$	2.53	1.2
	$B^*\pi$	${}^3F_4 = -0.0598$, ${}^3H_4 = -0.000236$	23.9	11.8
	$B^*\rho$	${}^3F_4 = 0.0422$, ${}^3H_4 = 0.0229$, ${}^5F_4 = 0.0406$, ${}^5H_4 = 0.0277$	25.7	12.7
	$B^*\eta$	${}^3F_4 = -0.0272$, ${}^3H_4 = -8.44 \times 10^{-5}$	4.56	2.2
	$B^*\eta'$	${}^3F_4 = -0.0226$, ${}^3H_4 = -3.42 \times 10^{-5}$	2.33	1.2
	$B^*\omega$	${}^3F_4 = 0.0243$, ${}^3H_4 = 0.0129$, ${}^5F_4 = 0.0234$, ${}^5H_4 = 0.0157$	8.40	4.1
	$B(2^3S_1)\pi$	${}^3F_4 = 0.0586$, ${}^3H_4 = 0.000181$	8.27	4.1
	$B(1P_1)\pi$	${}^3G_4 = -0.0288i$	2.87	1.4
	$B(1^3P_2)\pi$	${}^5D_4 = 0.0977i$, ${}^5G_4 = 0.0402i$, ${}^5I_4 = 0.000151i$	37.1	18.3
	$B(1^3P_2)\rho$	${}^3G_4 = -0.000475i$, ${}^5D_4 = -0.0381i$, ${}^5G_4 = -0.00168i$, ${}^5I_4 = -3.66 \times 10^{-5}i$, ${}^7D_4 = -0.0199i$, ${}^7G_4 = -0.00192i$, ${}^7I_4 = -6.67 \times 10^{-5}i$	2.35	1.2
	$B(1^3P_2)\eta$	${}^5D_4 = 0.0461i$, ${}^5G_4 = 0.00816i$, ${}^5I_4 = 1.75 \times 10^{-5}i$	5.68	2.8
	$B(2^3P_2)\pi$	${}^5D_4 = -0.0691i$, ${}^5G_4 = -0.00692i$, ${}^5I_4 = -1.16 \times 10^{-5}i$	4.35	2.1
	$B(1^3D_3)\pi$	${}^7P_4 = 0.139$, ${}^7F_4 = 0.0493$, ${}^7H_4 = 0.00444$, ${}^7J_4 = 8.90 \times 10^{-6}$	30.8	15.2
	$B(1^3F_4)\pi$	${}^9S_4 = -0.218i$, ${}^9D_4 = -0.0389i$, ${}^9G_4 = -0.00135i$, ${}^9I_4 = -1.79 \times 10^{-5}i$	16.9	8.3
	B_s^*K	${}^3F_4 = -0.0323$, ${}^3H_4 = -7.37 \times 10^{-5}$	5.82	2.9
	$B_s^*K^*$	${}^3F_4 = 0.0134$, ${}^3H_4 = 0.00313$, ${}^5F_4 = 0.0129$, ${}^5H_4 = 0.00380$	1.53	0.8
	$B_s(1^3P_2)K$	${}^5D_4 = 0.0604i$, ${}^5G_4 = 0.00706i$, ${}^5I_4 = 1.00 \times 10^{-5}i$	8.03	4.0
	Total		203.2	100
$B(1^3G_5)$	$B\pi$	${}^1H_5 = -0.0423$	12.3	12.1
6592	$B\rho$	${}^3H_5 = -0.0237$	3.19	3.1
	$B\eta$	${}^1H_5 = -0.0133$	1.12	1.1
	$B\omega$	${}^3H_5 = -0.0134$	1.02	1.0
	$B^*\pi$	${}^3H_5 = 0.0461$	13.5	13.2
	$B^*\rho$	${}^1H_5 = -0.0111$, ${}^5F_5 = 0.0881$, ${}^5H_5 = 0.0207$	42.5	41.7
	$B^*\eta$	${}^3H_5 = 0.0140$	1.13	1.1
	$B^*\omega$	${}^1H_5 = -0.00628$, ${}^5F_5 = 0.0506$, ${}^5H_5 = 0.0117$	13.9	13.6
	$B(2^1S_0)\pi$	${}^1H_5 = 0.0148$	0.515	0.5
	$B(1P_1)\pi$	${}^3G_5 = 0.0174i$, ${}^3I_5 = 0.0143i$	1.63	1.6
	$B(1P_1')\pi$	${}^3G_5 = -0.0224i$, ${}^3I_5 = 0.000823i$	1.58	1.6
	$B(1^3P_2)\pi$	${}^5G_5 = -0.0341i$, ${}^5I_5 = -0.0102i$	3.88	3.8
	$B(1^3P_2)\rho$	${}^3G_5 = 3.39 \times 10^{-5}i$, ${}^5G_5 = 6.78 \times 10^{-5}i$, ${}^7D_5 = -0.0271i$, ${}^7G_5 = -0.000376i$, ${}^7I_5 = -2.34 \times 10^{-6}i$	0.536	0.5
	$B(1^3D_3)\pi$	${}^7F_5 = -0.0217$, ${}^7H_5 = -0.00390$, ${}^7J_5 = -0.000293$	0.601	0.6
	B_sK	${}^1H_5 = -0.0103$	0.604	0.6
	B_s^*K	${}^3H_5 = 0.0110$	0.637	0.6
	$B_s^*K^*$	${}^1H_5 = -0.00131$, ${}^5F_5 = 0.0253$, ${}^5H_5 = 0.00243$	2.43	2.4
	Total		102.2	100

TABLE XXIII. Partial widths and branching ratios for strong and electromagnetic decays of the $1S$ and $2S$ B_s mesons. The initial state's mass is given in MeV and is listed below the state's name in column 1. Column 4 gives the matrix element, $\mathcal{M}$, or strong amplitude as appropriate to the particular decay. For radiative transitions the E1 or M1 matrix elements are $\langle f|r|i\rangle$ (GeV^{-1}) and $\langle f|j_0(kr\frac{m_{b,s}}{m_s+m_b})|i\rangle$, respectively; these matrix elements were obtained using the wave functions of the GI model [6]. For strong decays, the nonzero partial wave amplitudes are given in units of GeV$^{-1/2}$. We only show radiative transitions that are likely to be observed and likewise generally do not show strong decay modes which have BR $< 0.1\%$, although they are included in calculating the total width. Details of the calculations are given in the text.

Initial state	Final state	M_f [MeV]	$\mathcal{M}$	Width [MeV]	BR [%]
B_s^*	$B_s\gamma$	5394	$\langle 1^1S_0\|j_0(kr\frac{m_{b,s}}{m_s+m_b})\|1^3S_1\rangle = 0.9953, 0.9971$	0.000313	100
5450	Total			0.000313	100
$B_s(2^3S_1)$	$B_s\gamma$	5394	$\langle 1^1S_0\|j_0(kr\frac{m_{b,s}}{m_s+m_b})\|2^3S_1\rangle = 0.2079, 0.06476$	0.0142	0.012
6012	$B_s(1^3P_2)\gamma$	5876	$\langle 1^3P_2\|r\|2^3S_1\rangle = -2.344$	0.00808	0.0070
	$B_s(1P_1)\gamma$	5857	$\langle 1^3P_1\|r\|2^3S_1\rangle = -2.098$	0.00228	0.0020
	$B_s(1P_1')\gamma$	5861	$\langle 1^3P_1\|r\|2^3S_1\rangle = -2.098$	0.0032	0.0028
	$B_s(1^3P_0)\gamma$	5831	$\langle 1^3P_0\|r\|2^3S_1\rangle = -1.916$	0.00252	0.0022
	BK		${}^1P_1 = 0.157$	43.7	38.3
	B^*K		${}^3P_1 = -0.221$	66.6	58.4
	$B_s\eta$		${}^1P_1 = -0.056$	2.95	2.6
	$B_s^*\eta$		${}^3P_1 = 0.0414$	0.669	0.6
	Total			114.0	100
$B_s(2^1S_0)$	$B_s^*\gamma$	5450	$\langle 1^3S_1\|j_0(kr\frac{m_{b,s}}{m_s+m_b})\|2^1S_0\rangle = 0.07796, -0.06457$	0.00323	0.0043
5984	$B_s(1P_1)\gamma$	5857	$\langle 1^1P_1\|r\|2^1S_0\rangle = -2.282$	0.00673	0.0089
	$B_s(1P_1')\gamma$	5861	$\langle 1^1P_1\|r\|2^1S_0\rangle = -2.282$	0.00406	0.0054
	B^*K		${}^3P_0 = -0.255$	75.8	$\sim$100
	Total			75.8	100

TABLE XXIV. Partial widths and branching ratios for strong and electromagnetic decays of the $3S$ B_s mesons. See the caption to Table XXIII for further explanations.

Initial state	Final state	M_f [MeV]	$\mathcal{M}$	Width [MeV]	BR [%]
$B_s(3^3S_1)$	$B_s\gamma$	5394	$\langle 1^1S_0\|j_0(kr\frac{m_{b,s}}{m_s+m_b})\|3^3S_1\rangle = 0.1086, 0.02980$	0.0164	0.013
6429	$B_s(2^1S_0)\gamma$	5984	$\langle 2^1S_0\|j_0(kr\frac{m_{b,s}}{m_s+m_b})\|3^3S_1\rangle = 0.2359, 0.05756$	0.00710	0.0055
	$B_s(1^3P_2)\gamma$	5876	$\langle 1^3P_2\|r\|3^3S_1\rangle = 0.3170$	0.00896	0.0069
	$B_s(2^3P_2)\gamma$	6295	$\langle 2^3P_2\|r\|3^3S_1\rangle = -3.493$	0.0174	0.013
	$B_s(2P_1)\gamma$	6279	$\langle 2^3P_1\|r\|3^3S_1\rangle = -3.196$	0.00357	0.0028
	$B_s(2P_1')\gamma$	6296	$\langle 2^3P_1\|r\|3^3S_1\rangle = -3.196$	0.00598	0.0046
	$B_s(2^3P_0)\gamma$	6279	$\langle 2^3P_0\|r\|3^3S_1\rangle = -2.973$	0.00347	0.0027
	BK		$^1P_1 = 0.0379$	7.18	5.5
	BK^*		$^3P_1 = -0.0413$	5.89	4.5
	B^*K		$^3P_1 = -0.0444$	8.89	6.8
	B^*K^*		$^1P_1 = -0.0314$, $^5P_1 = 0.140$	58.2	44.8
	$B(2^1S_0)K$		$^1P_1 = 0.0794$	3.21	2.5
	$B(1P_1)K$		$^3S_1 = 0.00310i$, $^3D_1 = 0.114i$	19.0	14.6
	$B(1P_1')K$		$^3S_1 = -0.0425i$, $^3D_1 = 0.00757i$	2.62	2.0
	$B(1^3P_2)K$		$^5D_1 = -0.117i$	18.2	14.0
	$B_s\eta'$		$^1P_1 = -0.0276$	1.49	1.2
	$B_s\phi$		$^3P_1 = -0.0340$	1.06	0.8
	$B_s^*\eta$		$^3P_1 = -0.0124$	0.579	0.4
	$B_s^*\eta'$		$^3P_1 = 0.0305$	0.917	0.7
	$B_s(1P_1')\eta$		$^3S_1 = 0.0697i$, $^3D_1 = 0.000789i$	2.29	1.8
	Total			129.8	100
$B_s(3^1S_0)$	$B_s^*\gamma$	5450	$\langle 1^3S_1\|j_0(kr\frac{m_{b,s}}{m_s+m_b})\|3^1S_0\rangle = 0.03084, -0.2852$	0.00261	0.0022
6410	$B_s(2^3S_1)\gamma$	6012	$\langle 2^3S_1\|j_0(kr\frac{m_{b,s}}{m_s+m_b})\|3^1S_0\rangle = 0.1280, -0.05419$	0.00401	0.0033
	$B_s(1P_1)\gamma$	5857	$\langle 1^1P_1\|r\|3^1S_0\rangle = 0.2487$	0.00595	0.0049
	$B_s(1P_1')\gamma$	5861	$\langle 1^1P_1\|r\|3^1S_0\rangle = 0.2487$	0.00386	0.0032
	$B_s(2P_1)\gamma$	6279	$\langle 2^1P_1\|r\|3^1S_0\rangle = -3.418$	0.0190	0.016
	$B_s(2P_1')\gamma$	6296	$\langle 2^1P_1\|r\|3^1S_0\rangle = -3.418$	0.00538	0.0045
	BK^*		$^3P_0 = 0.069$	15.4	12.8
	B^*K		$^3P_0 = -0.0431$	8.07	6.7
	B^*K^*		$^3P_0 = -0.158$	64.6	53.5
	$B(1^3P_0)K$		$^1S_0 = -0.039i$	2.23	1.8
	$B(1^3P_2)K$		$^5D_0 = -0.15i$	26.4	21.9
	$B_s^*\eta$		$^3P_0 = -0.0222$	1.77	1.5
	$B_s(1^3P_0)\eta$		$^1S_0 = 0.0619i$	2.24	1.8
	Total			120.8	100

TABLE XXV. Partial widths and branching ratios for strong and electromagnetic decays of the 4^3S_1 B_s meson. See the caption to Table XXIII for further explanations.

Initial state	Final state	M_f [MeV]	$\mathcal{M}$	Width [MeV]	BR [%]
$B_s(4^3S_1)$	$B_s\gamma$	5394	$\langle 1^1S_0\|j_0(kr\frac{m_{b,s}}{m_s+m_b})\|4^3S_1\rangle = 0.07398, 0.01975$	0.0168	0.016
6773	$B_s(2^1S_0)\gamma$	5984	$\langle 2^1S_0\|j_0(kr\frac{m_{b,s}}{m_s+m_b})\|4^3S_1\rangle = 0.1338, 0.02237$	0.0116	0.011
	$B_s(3^1S_0)\gamma$	6410	$\langle 3^1S_0\|j_0(kr\frac{m_{b,s}}{m_s+m_b})\|4^3S_1\rangle = 0.2473, 0.04972$	0.00432	0.0042
	BK		${}^1P_1 = 0.019$	2.97	2.9
	B^*K		${}^3P_1 = -0.0234$	4.18	4.0
	B^*K^*		${}^1P_1 = -0.00333$, ${}^5P_1 = 0.0149$	1.50	1.4
	$B(2^1S_0)K$		${}^1P_1 = 0.0224$	1.53	1.5
	$B(2^3S_1)K$		${}^3P_1 = -0.0224$	1.43	1.4
	$B(1^3P_0)K^*$		${}^3S_1 = -0.00876i$	0.183	0.2
	$B(1P_1)K$		${}^3S_1 = 0.000650i$, ${}^3D_1 = 0.0147i$	0.878	0.8
	$B(1P_1)K^*$		${}^3S_1 = -2.25\times10^{-5}i$, ${}^3D_1 = 0.0405i$, ${}^5D_1 = -0.0702i$	14.1	13.6
	$B(1P_1')K$		${}^3S_1 = -0.00809i$, ${}^3D_1 = 0.000786i$	0.265	0.2
	$B(1P_1')K^*$		${}^3S_1 = 0.00618i$, ${}^3D_1 = 0.00223i$, ${}^5D_1 = -0.00387i$	0.120	0.1
	$B(1^3P_2)K$		${}^5D_1 = -0.0107i$	0.449	0.4
	$B(1^3P_2)K^*$		${}^3D_1 = -0.0203i$, ${}^5D_1 = -0.0262i$, ${}^7D_1 = 0.124i$	31.0	29.9
	$B(2P_1)K$		${}^3S_1 = 0.00228i$, ${}^3D_1 = 0.0936i$	8.10	7.8
	$B(2P_1')K$		${}^3S_1 = -0.0881i$, ${}^3D_1 = 0.00297i$	5.37	5.2
	$B(2^3P_2)K$		${}^5D_1 = -0.0842i$	5.71	5.5
	$B(1^3D_1)K$		${}^3P_1 = -0.0144$	0.319	0.3
	$B(1D_2)K$		${}^5P_1 = 0.000148$, ${}^5F_1 = -0.0736$	8.94	8.6
	$B(1D_2')K$		${}^5P_1 = 0.0360$, ${}^5F_1 = -0.000661$	1.87	1.8
	$B(1^3D_3)K$		${}^7F_1 = 0.0712$	8.00	7.7
	$B_s\eta'$		${}^1P_1 = -0.00428$	0.108	0.1
	$B_s\phi$		${}^3P_1 = -0.00760$	0.320	0.3
	$B_s^*\eta'$		${}^3P_1 = 0.00627$	0.209	0.2
	$B_s^*\phi$		${}^1P_1 = -0.00254$, ${}^5P_1 = 0.0114$	0.667	0.6
	$B_s(2^1S_0)\eta$		${}^1P_1 = 0.0139$	0.441	0.4
	$B_s(2^3S_1)\eta$		${}^3P_1 = -0.0274$	1.55	1.5
	$B_s(1P_1)\eta$		${}^3S_1 = 0.000559i$, ${}^3D_1 = 0.0176i$	1.02	1.0
	$B_s(1P_1')\eta$		${}^3S_1 = 0.0112i$, ${}^3D_1 = -0.00161i$	0.419	0.4
	$B_s(1^3P_2)\eta$		${}^5D_1 = -0.0223i$	1.56	1.5
	$B_s(1D_2')\eta$		${}^5P_1 = -0.0198$, ${}^5F_1 = -9.47\times10^{-5}$	0.226	0.2
	Total			103.7	100

TABLE XXVI. Partial widths and branching ratios for strong and electromagnetic decays of the 4^1S_0 B_s meson. See the caption to Table XXIII for further explanations.

Initial state	Final state	M_f [MeV]	$\mathcal{M}$	Width [MeV]	BR [%]
$B_s(4^1S_0)$	$B_s^*\gamma$	5450	$\langle 1^3S_1\|j_0(kr\frac{m_{b,s}}{m_s+m_b})\|4^1S_0\rangle = 0.02012, -0.01626$	0.00332	0.0039
6759	$B_s(2^3S_1)\gamma$	6012	$\langle 2^3S_1\|j_0(kr\frac{m_{b,s}}{m_s+m_b})\|4^1S_0\rangle = 0.06664, -0.02662$	0.00156	0.0018
	B^*K		$^3P_0 = -0.0244$	4.45	5.3
	B^*K^*		$^3P_0 = -0.0213$	2.85	3.4
	$B(2^3S_1)K$		$^3P_0 = -0.0177$	0.851	1.0
	$B(1^3P_0)K$		$^1S_0 = -0.00711i$	0.208	0.2
	$B(1P_1)K^*$		$^1S_0 = 0.00200i$, $^5D_0 = 0.0981i$	18.9	22.3
	$B(1P_1')K^*$		$^1S_0 = -0.0273i$, $^5D_0 = 0.00537i$	1.45	1.7
	$B(1^3P_2)K^*$		$^5D_0 = -0.104i$	18.3	21.6
	$B(2^3P_0)K$		$^1S_0 = -0.0890i$	5.45	6.4
	$B(2^3P_2)K$		$^5D_0 = -0.0978i$	6.62	7.8
	$B(1^3D_1)K$		$^3P_0 = 0.0385$	2.14	2.5
	$B(1^3D_3)K$		$^7F_0 = 0.0989$	14.4	17.0
	$B_s\phi$		$^3P_0 = 0.00874$	0.411	0.5
	$B_s^*\eta$		$^3P_0 = -0.00621$	0.257	0.3
	$B_s^*\eta'$		$^3P_0 = 0.00712$	0.261	0.3
	$B_s^*\phi$		$^3P_0 = -0.00831$	0.329	0.4
	$B_s(2^3S_1)\eta$		$^3P_0 = -0.0399$	3.10	3.7
	$B_s(1^3P_0)\eta$		$^1S_0 = 0.0102i$	0.352	0.4
	$B_s(1^3P_2)\eta$		$^5D_0 = -0.0363i$	3.97	4.7
	$B_s(1^3D_1)\eta$		$^3P_0 = -0.0204$	0.238	0.3
	Total			84.7	100

TABLE XXVII. Partial widths and branching ratios for strong and electromagnetic decays of the $1P$ B_s mesons. See the caption to Table XXIII for further explanations.

Initial state	Final state	M_f [MeV]	$\mathcal{M}$	Width [MeV]	BR [%]
$B_s(1^3P_0)$	$B_s^*\gamma$	5450	$\langle 1^3S_1\|r\|1^3P_0\rangle = 2.051$	0.0760	0.055
5831	BK		$^1S_0 = -0.558i$	138	~100
	Total			138	100
$B_s(1P_1)$	$B_s\gamma$	5394	$\langle 1^1S_0\|r\|1^1P_1\rangle = 1.922$	0.0706	65.7
5857	$B_s^*\gamma$	5450	$\langle 1^3S_1\|r\|1^3P_1\rangle = 2.058$	0.0369	34.3
	No strong decays				
	Total			0.1075	100
$B_s(1P_1')$	$B_s\gamma$	5394	$\langle 1^1S_0\|r\|1^1P_1\rangle = 1.922$	0.0478	45.5
5861	$B_s^*\gamma$	5450	$\langle 1^3S_1\|r\|1^3P_1\rangle = 2.058$	0.0573	54.5
	No strong decays				
	Total			0.1051	100
$B_s(1^3P_2)$	$B_s^*\gamma$	5450	$\langle 1^3S_1\|r\|1^3P_2\rangle = 2.056$	0.106	13.6
5876	BK		$^1D_2 = -0.0285i$	0.663	85.4
	B^*K		$^3D_2 = 0.00536i$	0.00799	1.0
	Total			0.777	100

TABLE XXVIII. Partial widths and branching ratios for strong and electromagnetic decays of the $2P$ B_s mesons. See the caption to Table XXIII for further explanations.

Initial state	Final state	M_f [MeV]	$\mathcal{M}$	Width [MeV]	BR [%]
$B_s(2^3P_0)$	$B_s^*\gamma$	5450	$\langle 1^3S_1\|r\|2^3P_0\rangle = -0.1862$	0.00581	0.0082
6279	$B_s(2^3S_1)\gamma$	6012	$\langle 2^3S_1\|r\|2^3P_0\rangle = 3.225$	0.0668	0.094
	$B_s(1^3D_1)\gamma$	6182	$\langle 1^3D_1\|r\|2^3P_0\rangle = -2.424$	0.00387	0.0054
	BK		$^1S_0 = -0.0908i$	31.0	43.6
	B^*K^*		$^1S_0 = 0.225i$, $^5D_0 = -0.0283i$	36.5	51.4
	$B(1P_1)K$		$^3P_0 = 0.108$	2.85	4.0
	$B_s\eta$		$^1S_0 = -0.0152i$	0.686	1.0
	Total			71.0	100
$B_s(2P_1)$	$B_s(2^1S_0)\gamma$	5984	$\langle 2^1S_0\|r\|2^1P_1\rangle = 2.889$	0.0507	0.023
6279	$B_s(2^3S_1)\gamma$	6012	$\langle 2^3S_1\|r\|2^3P_1\rangle = 3.120$	0.0186	0.0085
	$B_s(1D_2)\gamma$	6169	$\langle 1^3D_2\|r\|2^3P_1\rangle = -2.459$, $\langle 1^1D_2\|r\|2^1P_1\rangle = -2.454$	0.00514	0.0024
	BK^*		$^3S_1 = -0.203i$, $^3D_1 = -0.0270i$	72.4	33.1
	B^*K		$^3S_1 = 0.00394i$, $^3D_1 = -0.162i$	86.5	39.6
	B^*K^*		$^3S_1 = 0.257i$, $^3D_1 = 0.0170i$, $^5D_1 = -0.0135i$	47.5	21.7
	$B(1^3P_0)K$		$^1P_1 = -0.0308$	0.461	0.2
	$B(1P_1)K$		$^3P_1 = -0.0299$	0.219	0.1
	$B_s^*\eta$		$^3S_1 = 0.000557i$, $^3D_1 = 0.0666i$	11.3	5.2
	Total			218.4	100
$B_s(2P_1')$	$B_s\gamma$	5394	$\langle 1^1S_0\|r\|2^1P_1\rangle = 0.07821$	0.000385	0.00049
6296	$B_s(2^1S_0)\gamma$	5984	$\langle 2^1S_0\|r\|2^1P_1\rangle = 2.889$	0.0252	0.032
	$B_s(2^3S_1)\gamma$	6012	$\langle 2^3S_1\|r\|2^3P_1\rangle = 3.120$	0.0523	0.066
	$B_s(1^3D_1)\gamma$	6182	$\langle 1^3D_1\|r\|2^3P_1\rangle = -2.265$	0.000944	0.0012
	$B_s(1D_2')\gamma$	6196	$\langle 1^3D_2\|r\|2^3P_1\rangle = -2.459$, $\langle 1^1D_2\|r\|2^1P_1\rangle = -2.454$	0.00347	0.0044
	BK^*		$^3S_1 = -0.0706i$, $^3D_1 = 0.0800i$	22.1	28.1
	B^*K		$^3S_1 = -0.0840i$, $^3D_1 = -0.00687i$	24.3	30.9
	B^*K^*		$^3S_1 = -0.148i$, $^3D_1 = -0.0232i$, $^5D_1 = -0.0437i$	26.2	33.3
	$B(1^3P_0)K$		$^1P_1 = 0.0210$	0.279	0.4
	$B(1P_1)K$		$^3P_1 = -0.0763$	2.60	3.3
	$B(1P_1')K$		$^3P_1 = -0.0255$	0.243	0.3
	$B(1^3P_2)K$		$^5P_1 = 0.0798$, $^5F_1 = -1.14 \times 10^{-5}$	1.14	1.4
	$B_s^*\eta$		$^3S_1 = -0.0245i$, $^3D_1 = 0.00285i$	1.62	2.1
	Total			78.6	100
$B_s(2^3P_2)$	$B_s^*\gamma$	5450	$\langle 1^3S_1\|r\|2^3P_2\rangle = 0.09397$	0.00156	0.00063
6295	$B_s(2^3S_1)\gamma$	6012	$\langle 2^3S_1\|r\|2^3P_2\rangle = 2.940$	0.0654	0.027
	$B_s(1^3D_3)\gamma$	6179	$\langle 1^3D_3\|r\|2^3P_2\rangle = -2.476$	0.00561	0.0023
	BK		$^1D_2 = 0.0863i$	28.9	11.8
	BK^*		$^3D_2 = 0.0655i$	8.26	3.4
	B^*K		$^3D_2 = -0.120i$	49.0	19.9
	B^*K^*		$^1D_2 = 0.0130i$, $^5S_2 = -0.372i$, $^5D_2 = -0.0344i$	147	59.8
	$B(1P_1')K$		$^3P_2 = -0.0300$, $^3F_2 = 0.000124$	0.323	0.1
	$B_s\eta$		$^1D_2 = -0.0413i$	5.28	2.2
	$B_s^*\eta$		$^3D_2 = 0.0516i$	7.10	2.9
	Total			246	100

TABLE XXIX. Partial widths and branching ratios for strong decays of the $3P$ B_s mesons. See the caption to Table XXIII for further explanations.

Initial state	Final state	$\mathcal{M}$	Width [MeV]	BR [%]
$B_s(3^3P_0)$	BK	${}^1S_0 = -0.0424i$	12.4	24.3
6639	B^*K^*	${}^1S_0 = 0.0206i$, ${}^5D_0 = 0.0186i$	3.88	7.6
	$B(2^1S_0)K$	${}^1S_0 = -0.0426i$	3.72	7.3
	$B(1D_2)K$	${}^5D_0 = 0.0852i$	4.88	9.6
	$B_s\eta$	${}^1S_0 = -0.00629i$	0.239	0.5
	$B_s\eta'$	${}^1S_0 = 0.0156i$	1.08	2.1
	$B_s^*\phi$	${}^1S_0 = 0.00356i$, ${}^5D_0 = 0.0575i$	11.1	21.8
	$B_s(2^1S_0)\eta$	${}^1S_0 = -0.0616i$	4.72	9.3
	$B_s(1P_1)\eta$	${}^3P_0 = 0.0590$	7.70	15.1
	$B_s(1P_1')\eta$	${}^3P_0 = -0.0238$	1.23	2.4
	Total		51.0	100
$B_s(3P_1)$	BK^*	${}^3S_1 = -0.0116i$, ${}^3D_1 = -0.00437i$	0.858	0.8
6635	B^*K	${}^3S_1 = 0.00257i$, ${}^3D_1 = -0.0502i$	16.0	14.8
	B^*K^*	${}^3S_1 = 0.0222i$, ${}^3D_1 = -0.00758i$, ${}^5D_1 = 0.00613i$	2.93	2.7
	$B(2^3S_1)K$	${}^3S_1 = 0.00148i$, ${}^3D_1 = -0.125i$	28.3	26.1
	$B(1^3P_2)K$	${}^5P_1 = 0.00162$, ${}^5F_1 = 0.125$	43.9	40.6
	$B(1^3D_1)K$	${}^3S_1 = -0.0517i$, ${}^3D_1 = -0.00518i$	1.38	1.3
	$B(1D_2)K$	${}^5D_1 = -0.0246i$	0.389	0.4
	$B(1^3D_3)K$	${}^7D_1 = -0.0166i$, ${}^7G_1 = -0.00201i$	0.154	0.1
	$B_s\phi$	${}^3S_1 = -0.0150i$, ${}^3D_1 = 0.0106i$	1.34	1.2
	$B_s^*\eta'$	${}^3S_1 = -0.000851i$, ${}^3D_1 = 0.0228i$	1.96	1.8
	$B_s^*\phi$	${}^3S_1 = 0.00463i$, ${}^3D_1 = -0.0322i$, ${}^5D_1 = 0.0244i$	5.45	5.0
	$B_s(2^3S_1)\eta$	${}^3S_1 = 0.00558i$, ${}^3D_1 = 0.0346i$	1.21	1.1
	$B_s(1^3P_0)\eta$	${}^1P_1 = -0.0135$	0.431	0.4
	$B_s(1P_1)\eta$	${}^3P_1 = -0.0163$	0.583	0.5
	$B_s(1P_1')\eta$	${}^3P_1 = -0.00940$	0.190	0.2
	$B_s(1^3P_2)\eta$	${}^5P_1 = -0.0132$, ${}^5F_1 = -0.0373$	3.20	3.0
	Total		108.2	100

TABLE XXX. Partial widths and branching ratios for strong decays of the $3P$ B_s mesons. See the caption to Table XXIII for further explanations.

Initial state	Final state	$\mathcal{M}$	Width [MeV]	BR [%]
$B_s(3P_1')$	BK^*	$^3S_1 = -0.00356i$, $^3D_1 = 0.0135i$	1.12	2.4
6650	B^*K	$^3S_1 = -0.0394i$, $^3D_1 = -0.00329i$	10.1	21.2
	B^*K^*	$^3S_1 = -0.0119i$, $^3D_1 = 0.00163i$, $^5D_1 = 0.00391i$	0.818	1.7
	$B(2^3S_1)K$	$^3S_1 = -0.0333i$, $^3D_1 = -0.00806i$	2.25	4.7
	$B(1P_1)K$	$^3P_1 = -0.00599$	0.110	0.2
	$B(1^3P_2)K$	$^5P_1 = 0.00180$, $^5F_1 = 0.00833$	0.213	0.4
	$B(1^3D_1)K$	$^3S_1 = -0.0026i$, $^3D_1 = 0.00827i$	0.0483	0.1
	$B(1D_2)K$	$^5D_1 = -0.0500i$	1.91	4.0
	$B(1^3D_3)K$	$^7D_1 = 0.0834i$, $^7G_1 = -0.000258i$	4.71	9.9
	$B_s\phi$	$^3S_1 = -0.00716i$, $^3D_1 = -0.0246i$	2.72	5.7
	$B_s^*\eta$	$^3S_1 = -0.00835i$, $^3D_1 = -2.47 \times 10^{-5}i$	0.394	0.8
	$B_s^*\eta'$	$^3S_1 = 0.0146i$, $^3D_1 = 0.00154i$	0.856	1.8
	$B_s^*\phi$	$^3S_1 = -0.00460i$, $^3D_1 = 0.0199i$, $^5D_1 = 0.0401i$	7.03	14.7
	$B_s(2^3S_1)\eta$	$^3S_1 = -0.0749i$, $^3D_1 = 0.00256i$	6.24	13.1
	$B_s(1^3P_0)\eta$	$^1P_1 = 0.00672$	0.113	0.2
	$B_s(1P_1)\eta$	$^3P_1 = -0.0234$	1.26	2.6
	$B_s(1P_1')\eta$	$^3P_1 = -0.0125$	0.357	0.7
	$B_s(1^3P_2)\eta$	$^5P_1 = 0.0584$, $^5F_1 = -0.00263$	7.36	15.4
	Total		47.7	100
$B_s(3^3P_2)$	BK	$^1D_2 = 0.0323i$	7.29	6.8
6648	BK^*	$^3D_2 = 0.0138i$	1.10	1.0
	B^*K	$^3D_2 = -0.0406i$	10.6	9.9
	B^*K^*	$^1D_2 = 0.000413i$, $^5S_2 = -0.0270i$, $^5D_2 = -0.00109i$	3.74	3.5
	$B(2^1S_0)K$	$^1D_2 = 0.0752i$	12.0	11.2
	$B(2^3S_1)K$	$^3D_2 = -0.0961i$	17.6	16.5
	$B(1P_1)K$	$^3P_2 = 0.00261$, $^3F_2 = -0.0829$	21.1	19.8
	$B(1^3P_2)K$	$^5P_2 = -0.00256$, $^5F_2 = 0.0772$	17.4	16.3
	$B(1D_2)K$	$^5S_2 = 0.000314i$, $^5D_2 = 0.0168i$, $^5G_2 = 0.00404i$	0.223	0.2
	$B(1D_2')K$	$^5S_2 = -0.0541i$, $^5D_2 = -0.00562i$, $^5G_2 = 9.66 \times 10^{-6}i$	1.46	1.4
	$B(1^3D_3)K$	$^7D_2 = -0.0317i$, $^7G_2 = -0.00218i$	0.665	0.6
	$B_s\eta'$	$^1D_2 = -0.00906i$	0.372	0.3
	$B_s\phi$	$^3D_2 = -0.0186i$	1.42	1.3
	$B_s^*\eta'$	$^3D_2 = 0.0157i$	0.965	0.9
	$B_s^*\phi$	$^1D_2 = -0.0111i$, $^5S_2 = -0.0130i$, $^5D_2 = 0.0294i$	3.99	3.7
	$B_s(2^1S_0)\eta$	$^1D_2 = -0.0287i$	1.08	1.0
	$B_s(2^3S_1)\eta$	$^3D_2 = 0.0300i$	0.985	0.9
	$B_s(1P_1)\eta$	$^3P_2 = 0.00403$, $^3F_2 = 0.0283$	1.86	1.7
	$B_s(1P_1')\eta$	$^3P_2 = -0.0185$, $^3F_2 = -0.00253$	0.782	0.7
	$B_s(1^3P_2)\eta$	$^5P_2 = -0.0190$, $^5F_2 = -0.0245$	2.05	1.9
	Total		106.8	100

TABLE XXXI. Partial widths and branching ratios for strong and electromagnetic decays of the $1D$ B_s mesons. See the caption to Table XXIII for further explanations.

Initial state	Final state	M_f [MeV]	$\mathcal{M}$	Width [MeV]	BR [%]
$B_s(1^3D_1)$	$B_s(1^3P_0)\gamma$	5831	$\langle 1^3P_0\|r\|1^3D_1\rangle = 2.805$	0.0747	0.041
6182	$B_s(1P_1)\gamma$	5857	$\langle 1^3P_1\|r\|1^3D_1\rangle = 2.939$	0.0196	0.011
	$B_s(1P_1')\gamma$	5861	$\langle 1^3P_1\|r\|1^3D_1\rangle = 2.939$	0.0285	0.016
	$B_s(1^3P_2)\gamma$	5876	$\langle 1^3P_2\|r\|1^3D_1\rangle = 3.113$	0.00307	0.0017
	BK		${}^1P_1 = 0.19$	108	59.0
	B^*K		${}^3P_1 = 0.144$	52.8	28.9
	$B_s\eta$		${}^1P_1 = -0.0832$	15.4	8.4
	$B_s^*\eta$		${}^3P_1 = -0.0589$	6.26	3.4
	Total			183.0	100
$B_s(1D_2)$	$B_s(1P_1)\gamma$	5857	$\langle 1^3P_1\|r\|1^3D_2\rangle = 2.940$, $\langle 1^1P_1\|r\|1^1D_2\rangle = 2.994$	0.0959	0.58
6169	$B_s(1P_1')\gamma$	5861	$\langle 1^3P_1\|r\|1^3D_2\rangle = 2.940$, $\langle 1^1P_1\|r\|1^1D_2\rangle = 2.994$	0.000368	0.0022
	$B_s(1^3P_2)\gamma$	5876	$\langle 1^3P_2\|r\|1^3D_2\rangle = 3.127$	0.0102	0.062
	B^*K		${}^3P_2 = 0.00252$, ${}^3F_2 = -0.0803$	15.9	97.1
	$B_s^*\eta$		${}^3P_2 = -0.000861$, ${}^3F_2 = 0.0150$	0.387	2.4
	Total			16.4	100
$B_s(1D_2')$	$B_s(1P_1)\gamma$	5857	$\langle 1^3P_1\|r\|1^3D_2\rangle = 2.940$, $\langle 1^1P_1\|r\|1^1D_2\rangle = 2.994$	0.00107	0.00055
6196	$B_s(1P_1')\gamma$	5861	$\langle 1^3P_1\|r\|1^3D_2\rangle = 2.940$, $\langle 1^1P_1\|r\|1^1D_2\rangle = 2.994$	0.112	0.058
	$B_s(1^3P_2)\gamma$	5876	$\langle 1^3P_2\|r\|1^3D_2\rangle = 3.127$	0.0188	0.0097
	B^*K		${}^3P_2 = 0.254$, ${}^3F_2 = 0.00193$	171	88.3
	$B_s^*\eta$		${}^3P_2 = -0.108$, ${}^3F_2 = -0.000397$	22.3	11.5
	Total			194	100
$B_s(1^3D_3)$	$B_s(1^3P_2)\gamma$	5876	$\langle 1^3P_2\|r\|1^3D_3\rangle = 3.134$	0.109	0.41
6179	BK		${}^1F_3 = 0.0688$	14.0	53.0
	B^*K		${}^3F_3 = -0.0672$	11.4	43.1
	$B_s\eta$		${}^1F_3 = -0.0154$	0.522	2.0
	$B_s^*\eta$		${}^3F_3 = 0.0131$	0.305	1.1
	Total			26.4	100

TABLE XXXII. Partial widths and branching ratios for strong decays of the $2D$ B_s mesons. See the caption to Table XXIII for further explanations.

Initial state	Final state	$\mathcal{M}$	Width [MeV]	BR [%]
$B_s(2^3D_1)$	BK	${}^1P_1 = 0.0672$	27.1	12.7
6542	B^*K	${}^3P_1 = 0.0441$	10.7	5.0
	B^*K^*	${}^1P_1 = -0.0161$, ${}^5P_1 = 0.00719$, ${}^5F_1 = 0.133$	72.5	33.9
	$B(2^1S_0)K$	${}^1P_1 = 0.127$	21.8	10.2
	$B(2^3S_1)K$	${}^3P_1 = 0.0917$	9.72	4.6
	$B(1P_1)K$	${}^3S_1 = -0.0205i$, ${}^3D_1 = 0.0986i$	22.9	10.7
	$B(1P_1')K$	${}^3S_1 = -0.000732i$, ${}^3D_1 = -0.0370i$	3.03	1.4
	$B(1^3P_2)K$	${}^5D_1 = 0.103i$	22.2	10.4
	$B_s\eta'$	${}^1P_1 = -0.0318$	3.38	1.6
	$B_s\phi$	${}^3P_1 = 0.0368$	3.80	1.8
	$B_s^*\eta'$	${}^3P_1 = -0.0290$	2.26	1.1
	$B_s^*\phi$	${}^1P_1 = -0.0337$, ${}^5P_1 = 0.0151$, ${}^5F_1 = 0.0161$	3.29	1.5
	$B_s(2^1S_0)\eta$	${}^1P_1 = -0.0279$	0.251	0.1
	$B_s(1P_1)\eta$	${}^3S_1 = -0.0714i$, ${}^3D_1 = -0.0290i$	8.75	4.1
	$B_s(1P_1')\eta$	${}^3S_1 = 0.00576i$, ${}^3D_1 = 0.0183i$	0.533	0.2
	$B_s(1^3P_2)\eta$	${}^5D_1 = -0.0296i$	1.16	0.5
	Total		213.7	100
$B_s(2D_2)$	BK^*	${}^3P_2 = -0.00225$, ${}^3F_2 = 0.0153$	1.07	0.9
6526	B^*K	${}^3P_2 = -0.000329$, ${}^3F_2 = 0.0787$	33.1	28.5
	B^*K^*	${}^3P_2 = -0.0228$, ${}^3F_2 = -0.0677$, ${}^5P_2 = 0.0142$, ${}^5F_2 = 0.0648$	36.6	31.6
	$B(2^3S_1)K$	${}^3P_2 = 7.61 \times 10^{-5}$, ${}^3F_2 = -0.0285$	0.844	0.7
	$B(1^3P_0)K$	${}^1D_2 = -0.0401i$	3.69	3.2
	$B(1P_1)K$	${}^3D_2 = -0.0585i$	7.32	6.3
	$B(1P_1')K$	${}^3D_2 = -0.0374i$	2.93	2.5
	$B(1^3P_2)K$	${}^5S_2 = 0.00108i$, ${}^5D_2 = -0.0427i$, ${}^5G_2 = -0.0457i$	7.83	6.8
	$B_s\phi$	${}^3P_2 = 0.0592$, ${}^3F_2 = 0.00304$	9.14	7.9
	$B_s^*\eta$	${}^3P_2 = 0.000407$, ${}^3F_2 = -0.0394$	7.07	6.1
	$B_s^*\eta'$	${}^3P_2 = -0.000566$, ${}^3F_2 = 0.0129$	0.418	0.4
	$B_s^*\phi$	${}^3P_2 = -0.0444$, ${}^3F_2 = -0.00614$, ${}^5P_2 = 0.0262$, ${}^5F_2 = 0.00585$	4.81	4.2
	$B_s(1^3P_0)\eta$	${}^1D_2 = 0.0151i$	0.354	0.3
	$B_s(1P_1)\eta$	${}^3D_2 = 0.0192i$	0.498	0.4
	$B_s(1P_1')\eta$	${}^3D_2 = 0.00984i$	0.128	0.1
	$B_s(1^3P_2)\eta$	${}^5S_2 = -0.000965i$, ${}^5D_2 = 0.0116i$, ${}^5G_2 = 0.00390i$	0.181	0.2
	Total		116.0	100

TABLE XXXIII. Partial widths and branching ratios for strong decays of the $2D$ B_s mesons. See the caption to Table XXIII for further explanations.

Initial state	Final state	$\mathcal{M}$	Width [MeV]	BR [%]
$B_s(2D_2')$	BK^*	${}^3P_2 = -0.00218$, ${}^3F_2 = -0.0806$	30.7	13.8
6553	B^*K	${}^3P_2 = 0.0838$, ${}^3F_2 = 0.000655$	39.2	17.6
	B^*K^*	${}^3P_2 = 0.00911$, ${}^3F_2 = 0.0590$, ${}^5P_2 = 0.00895$, ${}^5F_2 = 0.0835$	43.9	19.7
	$B(2^3S_1)K$	${}^3P_2 = 0.163$, ${}^3F_2 = 0.000346$	32.6	14.6
	$B(1^3P_0)K$	${}^1D_2 = 0.0294i$	2.16	1.0
	$B(1P_1)K$	${}^3D_2 = -0.0693i$	11.2	5.0
	$B(1P_1')K$	${}^3D_2 = -0.0409i$	3.83	1.7
	$B(1^3P_2)K$	${}^5S_2 = -0.0247i$, ${}^5D_2 = 0.121i$, ${}^5G_2 = 0.000351i$	33.4	15.0
	$B_s\phi$	${}^3P_2 = 0.0119$, ${}^3F_2 = -0.0201$	1.61	0.7
	$B_s^*\eta'$	${}^3P_2 = -0.0457$, ${}^3F_2 = -2.25 \times 10^{-5}$	5.91	2.6
	$B_s^*\phi$	${}^3P_2 = 0.0387$, ${}^3F_2 = 0.00859$, ${}^5P_2 = 0.0337$, ${}^5F_2 = 0.0121$	6.26	2.8
	$B_s(1^3P_0)\eta$	${}^1D_2 = -0.0116i$	0.236	0.1
	$B_s(1P_1)\eta$	${}^3D_2 = 0.0251i$	0.977	0.4
	$B_s(1^3P_2)\eta$	${}^5S_2 = -0.0771i$, ${}^5D_2 = -0.0373i$, ${}^5G_2 = -3.67 \times 10^{-5}i$	10.3	4.6
	Total		222.6	100
$B_s(2^3D_3)$	BK	${}^1F_3 = -0.0339$	6.82	6.4
6535	BK^*	${}^3F_3 = -0.0582$	15.4	14.4
	B^*K	${}^3F_3 = 0.0523$	14.8	13.8
	B^*K^*	${}^1F_3 = -0.0300$, ${}^5P_3 = 0.0235$, ${}^5F_3 = 0.0657$	22.7	21.2
	$B(2^1S_0)K$	${}^1F_3 = 0.0294$	1.13	1.1
	$B(2^3S_1)K$	${}^3F_3 = -0.0252$	0.702	0.6
	$B(1P_1)K$	${}^3D_3 = 0.0321i$, ${}^3G_3 = 0.0403i$	5.87	5.5
	$B(1P_1')K$	${}^3D_3 = -0.0530i$, ${}^3G_3 = 0.00252i$	6.08	5.7
	$B(1^3P_2)K$	${}^5D_3 = -0.0727i$, ${}^5G_3 = -0.0298i$	12.7	11.9
	$B_s\eta$	${}^1F_3 = 0.0219$	2.45	2.3
	$B_s\eta'$	${}^1F_3 = -0.0120$	0.467	0.4
	$B_s\phi$	${}^3F_3 = -0.0127$	0.440	0.4
	$B_s^*\eta$	${}^3F_3 = -0.0282$	3.68	3.4
	$B_s^*\eta'$	${}^3F_3 = 0.0105$	0.285	0.3
	$B_s^*\phi$	${}^1F_3 = -0.00330$, ${}^5P_3 = 0.0796$, ${}^5F_3 = 0.00724$	12.2	11.4
	$B_s(1P_1)\eta$	${}^3D_3 = -0.00758i$, ${}^3G_3 = -0.00448i$	0.110	0.1
	$B_s(1P_1')\eta$	${}^3D_3 = 0.0201i$, ${}^3G_3 = 0.000380i$	0.561	0.5
	$B_s(1^3P_2)\eta$	${}^5D_3 = 0.0210i$, ${}^5G_3 = 0.00280i$	0.572	0.5
	Total		107.1	100

TABLE XXXIV. Partial widths and branching ratios for strong and electromagnetic decays of the $1F$ B_s mesons. See the caption to Table XXIII for further explanations.

Initial state	Final state	M_f [MeV]	$\mathcal{M}$	Width [MeV]	BR [%]
$B_s(1^3F_2)$	$B_s(1^3D_1)\gamma$	6182	$\langle 1^3D_1\|r\|1^3F_2\rangle = 3.711$	0.101	0.039
6454	$B_s(1D_2)\gamma$	6169	$\langle 1^3D_2\|r\|1^3F_2\rangle = 3.835$	0.00946	0.0037
	$B_s(1D_2')\gamma$	6196	$\langle 1^3D_2\|r\|1^3F_2\rangle = 3.835$	0.0100	0.0039
	BK		$^1D_2 = 0.107i$	59.9	23.4
	BK^*		$^3D_2 = -0.0897i$	29.8	11.6
	B^*K		$^3D_2 = 0.0951i$	42.7	16.7
	B^*K^*		$^1D_2 = 0.0591i$, $^5D_2 = -0.0447i$, $^5G_2 = -0.0370i$	21.1	8.2
	$B(2^1S_0)K$		$^1D_2 = -0.0204i$	0.297	0.1
	$B(1P_1)K$		$^3P_2 = 0.212$, $^3F_2 = 0.0243$	73.9	28.8
	$B(1P_1')K$		$^3P_2 = 0.0167$, $^3F_2 = -0.00500$	0.481	0.2
	$B(1^3P_2)K$		$^5P_2 = 0.0739$, $^5F_2 = 0.0269$	9.21	3.6
	$B_s\eta$		$^1D_2 = -0.0439i$	8.49	3.3
	$B_s\eta'$		$^1D_2 = 0.0215i$	1.05	0.4
	$B_s^*\eta$		$^3D_2 = -0.0374i$	5.51	2.2
	$B_s(1P_1)\eta$		$^3P_2 = -0.0640$, $^3F_2 = -0.00144$	3.12	1.2
	Total			256.3	100
$B_s(1F_3)$	$B_s(1D_2)\gamma$	6169	$\langle 1^3D_2\|r\|1^3F_3\rangle = 3.839$, $\langle 1^1D_2\|r\|1^1F_3\rangle = 3.878$	0.105	0.076
6425	$B_s(1^3D_3)\gamma$	6179	$\langle 1^3D_3\|r\|1^3F_3\rangle = 3.992$	0.00503	0.0036
	BK^*		$^3D_3 = -0.137i$, $^3G_3 = -0.00443i$	64.1	46.3
	B^*K		$^3D_3 = 0.000570i$, $^3G_3 = -0.0930i$	38.8	28.0
	B^*K^*		$^3D_3 = 0.0869i$, $^3G_3 = 0.0156i$, $^5D_3 = -0.0616i$, $^5G_3 = -0.0151i$	32.8	23.7
	$B(1P_1)K$		$^3F_3 = -0.0172$	0.422	0.3
	$B(1^3P_2)K$		$^5P_3 = 7.11 \times 10^{-5}$, $^5F_3 = -0.0119$, $^5H_3 = -0.00248$	0.192	0.1
	$B_s^*\eta$		$^3D_3 = -0.000122i$, $^3G_3 = 0.0217i$	1.74	1.3
	Total			138.4	100
$B_s(1F_3')$	$B_s(1D_2)\gamma$	6169	$\langle 1^3D_2\|r\|1^3F_3\rangle = 3.839$, $\langle 1^1D_2\|r\|1^1F_3\rangle = 3.878$	0.000446	0.00016
6462	$B_s(1D_2')\gamma$	6196	$\langle 1^3D_2\|r\|1^3F_3\rangle = 3.839$, $\langle 1^1D_2\|r\|1^1F_3\rangle = 3.878$	0.114	0.042
	$B_s(1^3D_3)\gamma$	6179	$\langle 1^3D_3\|r\|1^3F_3\rangle = 3.992$	0.00989	0.0036
	BK^*		$^3D_3 = -0.0201i$, $^3G_3 = 0.0400i$	7.58	2.8
	B^*K		$^3D_3 = 0.150i$, $^3G_3 = 0.000813i$	108	39.4
	B^*K^*		$^3D_3 = -0.0851i$, $^3G_3 = -0.0198i$, $^5D_3 = -0.0791i$, $^5G_3 = -0.0250i$	46.1	16.8
	$B(1P_1)K$		$^3F_3 = -0.0247$	1.03	0.4
	$B(1^3P_2)K$		$^5P_3 = 0.243$, $^5F_3 = 0.0321$, $^5H_3 = 6.03 \times 10^{-5}$	92.9	33.9
	$B_s^*\eta$		$^3D_3 = -0.0606i$, $^3G_3 = -0.000211i$	14.7	5.4
	$B_s^*\eta'$		$^3D_3 = 0.0183i$, $^3G_3 = 7.98 \times 10^{-6}i$	0.538	0.2
	$B_s(1^3P_2)\eta$		$^5P_3 = -0.0679$, $^5F_3 = -0.00154$	3.04	1.1
	Total			274	100
$B_s(1^3F_4)$	$B_s(1^3D_3)\gamma$	6179	$\langle 1^3D_3\|r\|1^3F_4\rangle = 4.002$	0.113	0.082
6432	BK		$^1G_4 = 0.0702i$	24.8	17.9
	BK^*		$^3G_4 = 0.0252i$	2.20	1.6
	B^*K		$^3G_4 = -0.0729i$	24.1	17.4
	B^*K^*		$^1G_4 = 0.00834i$, $^5D_4 = -0.171i$, $^5G_4 = -0.0165i$	84.2	60.8
	$B(1P_1)K$		$^3F_4 = 0.0110$, $^3H_4 = 0.00306$	0.193	0.1
	$B(1P_1')K$		$^3F_4 = -0.00990$, $^3H_4 = 0.000183$	0.140	0.1
	$B(1^3P_2)K$		$^5F_4 = -0.0205$, $^5H_4 = -0.00173$	0.564	0.4
	$B_s\eta$		$^1G_4 = -0.0173i$	1.25	0.9
	$B_s^*\eta$		$^3G_4 = 0.0172i$	1.11	0.8
	Total			138.6	100

TABLE XXXV. Partial widths and branching ratios for strong decays of the $1G$ B_s mesons. In this table, we do not show strong decay modes which have BR $< 0.5\%$, although they are included in calculating the total width. See the caption to Table XXIII for further explanations.

Initial state	Final state	$\mathcal{M}$	Width [MeV]	BR [%]
$B_s(1^3G_3)$	BK	${}^1F_3 = -0.0662$	32.2	11.9
6685	BK^*	${}^3F_3 = 0.0656$	26.3	9.7
	B^*K	${}^3F_3 = -0.0630$	27.0	10.0
	B^*K^*	${}^1F_3 = -0.0450$, ${}^5F_3 = 0.0410$, ${}^5H_3 = 0.0666$	44.9	16.6
	$B(2^1S_0)K$	${}^1F_3 = 0.0446$	4.76	1.8
	$B(2^3S_1)K$	${}^3F_3 = 0.0351$	2.67	1.0
	$B(1P_1)K$	${}^3D_3 = 0.130i$, ${}^3G_3 = 0.0312i$	60.4	22.4
	$B(1^3P_2)K$	${}^5D_3 = 0.0570i$, ${}^5G_3 = 0.0409i$	15.8	5.8
	$B(1D_2)K$	${}^5P_3 = 0.175$, ${}^5F_3 = 0.0165$, ${}^5H_3 = 0.000413$	31.7	11.7
	$B(1^3D_3)K$	${}^7P_3 = 0.0403$, ${}^7F_3 = 0.00952$, ${}^7H_3 = 0.000533$	1.63	0.6
	$B_s\eta$	${}^1F_3 = 0.0254$	4.18	1.6
	$B_s\eta'$	${}^1F_3 = -0.0197$	1.91	0.7
	$B_s\phi$	${}^3F_3 = 0.0208$	1.96	0.7
	$B_s^*\eta$	${}^3F_3 = 0.0233$	3.26	1.2
	$B_s^*\phi$	${}^1F_3 = -0.0122$, ${}^5F_3 = 0.0112$, ${}^5H_3 = 0.00733$	1.28	0.5
	$B_s(1P_1)\eta$	${}^3D_3 = -0.0489i$, ${}^3G_3 = -0.00546i$	6.22	2.3
	Total		269.7	100
$B_s(1G_4)$	BK^*	${}^3F_4 = 0.0988$, ${}^3H_4 = 0.00519$	56.2	33.5
6650	B^*K	${}^3F_4 = -0.000169$, ${}^3H_4 = 0.0863$	48.2	28.7
	B^*K^*	${}^3F_4 = -0.0709$, ${}^3H_4 = -0.0307$, ${}^5F_4 = 0.0549$, ${}^5H_4 = 0.0299$	50.9	30.3
	$B(1P_1)K$	${}^3G_4 = -0.0263i$	2.14	1.3
	$B(1^3P_2)K$	${}^5D_4 = -9.42 \times 10^{-5}i$, ${}^5G_4 = -0.0225i$, ${}^5I_4 = -0.0122i$	1.92	1.1
	$B_s\phi$	${}^3F_4 = 0.0282$, ${}^3H_4 = 0.000613$	3.28	2.0
	$B_s^*\eta$	${}^3F_4 = 4.53 \times 10^{-6}$, ${}^3H_4 = -0.0199$	2.24	1.3
	$B_s^*\phi$	${}^3F_4 = -0.0166$, ${}^3H_4 = -0.00266$, ${}^5F_4 = 0.0129$, ${}^5H_4 = 0.00260$	1.58	0.9
	Total		168.2	100
$B_s(1G_4')$	BK^*	${}^3F_4 = 0.0111$, ${}^3H_4 = -0.0539$	18.7	6.3
6690	B^*K	${}^3F_4 = -0.0948$, ${}^3H_4 = -0.000248$	61.5	20.8
	B^*K^*	${}^3F_4 = 0.0658$, ${}^3H_4 = 0.0333$, ${}^5F_4 = 0.0635$, ${}^5H_4 = 0.0405$	61.8	20.9
	$B(2^3S_1)K$	${}^3F_4 = 0.0580$, ${}^3H_4 = 9.80 \times 10^{-5}$	7.44	2.5
	$B(1P_1)K$	${}^3G_4 = -0.0319i$	3.46	1.2
	$B(1^3P_2)K$	${}^5D_4 = 0.153i$, ${}^5G_4 = 0.0426i$, ${}^5I_4 = 0.000107i$	81.4	27.5
	$B(1^3D_3)K$	${}^7P_4 = 0.195$, ${}^7F_4 = 0.0185$, ${}^7H_4 = 0.000552$	37.6	12.7
	$B_s^*\eta$	${}^3F_4 = 0.0360$, ${}^3H_4 = 7.45 \times 10^{-5}$	7.82	2.6
	$B_s^*\eta'$	${}^3F_4 = -0.0254$, ${}^3H_4 = -2.49 \times 10^{-5}$	2.84	1.0
	$B_s^*\phi$	${}^3F_4 = 0.0186$, ${}^3H_4 = 0.00381$, ${}^5F_4 = 0.0179$, ${}^5H_4 = 0.00462$	2.77	0.9
	$B_s(1^3P_2)\eta$	${}^5D_4 = -0.0573i$, ${}^5G_4 = -0.00796i$, ${}^5I_4 = -1.11 \times 10^{-5}i$	8.25	2.8
	Total		295.5	100
$B_s(1^3G_5)$	BK	${}^1H_5 = -0.0615$	26.6	14.9
6654	BK^*	${}^3H_5 = -0.0356$	7.32	4.1
	B^*K	${}^3H_5 = 0.0655$	27.9	15.7
	B^*K^*	${}^1H_5 = -0.0160$, ${}^5F_5 = 0.137$, ${}^5H_5 = 0.0297$	103	57.9
	$B(1P_1)K$	${}^3G_5 = 0.0180i$, ${}^3I_5 = 0.0113i$	1.40	0.8
	$B(1P_1')K$	${}^3G_5 = -0.0200i$, ${}^3I_5 = 0.000685i$	1.23	0.7
	$B(1^3P_2)K$	${}^5G_5 = -0.0345i$, ${}^5I_5 = -0.00756i$	3.68	2.1
	$B_s\eta$	${}^1H_5 = 0.0146$	1.32	0.7
	$B_s^*\eta$	${}^3H_5 = -0.0153$	1.33	0.7
	$B_s^*\phi$	${}^1H_5 = -0.00144$, ${}^5F_5 = 0.0331$, ${}^5H_5 = 0.00267$	3.90	2.2
	Total		178	100

TABLE XXXVI. Summary of excited bottom mesons. Unless otherwise stated we quote values from the Particle Data Group [46].

State	Observed decays	Mass [MeV]	Width [MeV]	References
$B_1(5721)^+$	$B^{*0}\pi^+$	$5726.8^{+3.2}_{-4.0}$	$49^{+12+2}_{-10-1.3}$	
		$5725.1 \pm 1.8 \pm 3.1 \pm 0.17 \pm 0.4$	$29.1 \pm 3.6 \pm 4.3$	LHCb [4]
$B_1(5721)^0$	$B^{*+}\pi^-$	5724.9 ± 2.4	$23 \pm 3 \pm 4$	
		$5727.7 \pm 0.7 \pm 1.4 \pm 0.17 \pm 0.4$	$30.1 \pm 1.5 \pm 3.5$	LHCb [4]
$B_2^*(5747)^+$	$B^0\pi^+$	$5736.9^{+1.3}_{-1.6}$	11^{+4+3}_{-3-4}	
		$5737.20 \pm 0.72 \pm 0.40 \pm 0.17$	$23.6 \pm 2.0 \pm 2.1$	LHCb [4]
			$\Gamma(\to B^{*0}\pi^+)/\Gamma(\to B^0\pi^+) = 1.0 \pm 0.5 \pm 0.8$	LHCb [4]
$B_2^*(5747)^0$	$B^+\pi^-$, $B^{*+}\pi^-$	5739 ± 5	22^{+3+4}_{-2-5}	
			$\Gamma(\to B^{*+}\pi^-)/\Gamma(\to B^+\pi^-) = 1.10 \pm 0.42 \pm 0.31$	
		$5739.44 \pm 0.37 \pm 0.33 \pm 0.17$	$24.5 \pm 1.0 \pm 1.5$	LHCb [4]
		$5739.44 \pm 0.37 \pm 0.33 \pm 0.17$	$24.5 \pm 1.0 \pm 1.5$	LHCb [4]
			$\Gamma(\to B^{*+}\pi^-)/\Gamma(\to B^+\pi^-) = 0.71 \pm 0.14 \pm 0.30$	LHCb [4]
$B(5970)^+$	$B^0\pi^+$	5961 ± 13	$60^{+30}_{-20} \pm 40$	
$B(5970)^0$	$B^+\pi^-$	5977 ± 13	$70^{+30}_{-20} \pm 30$	
$B_{s1}(5830)^0$	$B^{*+}K^-$	5828.78 ± 0.35	$0.5 \pm 0.3 \pm 0.3$	
$B_{s2}^*(5830)^0$	B^+K^-	5839.83 ± 0.19	1.47 ± 0.33	
			$\Gamma(\to B^{*+}K^-)/\Gamma(\to B^+K^-) = 0.093 \pm 0.013 \pm 0.012$	

VIII. SUMMARY

The primary purpose of this paper is to calculate the properties of excited B and B_s mesons as a guide to help identify newly observed states. The masses were calculated using the relativized quark model of Godfrey and Isgur and an alternative relativistic quark model. Radiative transition widths were calculated using a nonrelativistic formalism and wave functions from the respective models. Strong decay widths were calculated with the $^3P_0$ quark creation model coupled with harmonic oscillator wave functions that were tuned to reproduce the rms radius of the relevant hadrons.

Our current experimental knowledge of bottom mesons is rather sparse, having only clearly identified the two narrow members of the B and B_s $1P$ multiplets. Two other excited states have also been observed and identified with the $B(2S)$ states but they have not been independently confirmed by a second experiment.

In the near future the LHCb experiment offers the possibility of significantly increasing our knowledge of excited bottom states. Numerous B and B_s states with moderate widths and with significant branching fractions to simple final states (such as $B\pi$, $B^*\pi$, BK, and B^*K) are expected. However, the spectrum consists of many overlapping states; thus measuring the spins of putative signals will be vital for the success of any B spectroscopy program. With the high statistics expected in future LHC runs we are optimistic that this can be achieved and that our knowledge of the bottom meson spectrum will be significantly expanded.

ACKNOWLEDGMENTS

The authors gratefully acknowledge Ted Barnes who was involved in an early iteration of this work. This research was supported in part by the Natural Sciences and Engineering Research Council of Canada under Grant No. 121209-2009 SAPIN.

[1] S. Godfrey and S. L. Olsen, The exotic XYZ charmonium-like mesons, Annu. Rev. Nucl. Part. Sci. **58**, 51 (2008); E. S. Swanson, The new heavy mesons: A status report, Phys. Rep. **429**, 243 (2006).

[2] E. Eichten, S. Godfrey, H. Mahlke, and J. L. Rosner, Quarkonia and their transitions, Rev. Mod. Phys. **80**, 1161 (2008).

[3] S. Godfrey, Topics in hadron spectroscopy in 2009, arXiv:0910.3409.

[4] R. Aaij *et al.* (LHCb Collaboration), Precise measurements of the properties of the $B_1(5721)^{0,+}$ and $B_2^*(5747)^{0,+}$ states and observation of $B^{+,0}\pi^{-,+}$ mass structures, J. High Energy Phys. 04 (2015) 024.

[5] C. B. Lang, D. Mohler, S. Prelovsek, and R. M. Woloshyn, Predicting positive parity B_s mesons from lattice QCD, Phys. Lett. B **750**, 17 (2015).

[6] S. Godfrey and N. Isgur, Mesons in a relativized quark model with chromodynamics, Phys. Rev. D **32**, 189 (1985).

[7] S. Godfrey and R. Kokoski, Properties of p wave mesons with one heavy quark, Phys. Rev. D **43**, 1679 (1991).

[8] S. Godfrey, Spectroscopy of B_c mesons in the relativized quark model, Phys. Rev. D **70**, 054017 (2004).

[9] S. Godfrey, Properties of the charmed P-wave mesons, Phys. Rev. D **72**, 054029 (2005).

[10] For more information on this point see O. Lakhina and E. S. Swanson, Dynamic properties of charmonium, Phys. Rev. D **74**, 014012 (2006).

[11] O. Lakhina and E. S. Swanson, A canonical $D_s(2317)$?, Phys. Lett. B **650**, 159 (2007).

[12] E. S. Swanson (work in progress).

[13] This is discussed more fully in Appendix A of T. Barnes, N. Black, and P. R. Page, Strong decays of strange quarkonia, Phys. Rev. D **68**, 054014 (2003).

[14] E. J. Eichten and C. Quigg, Mesons with beauty and charm: Spectroscopy, Phys. Rev. D **49**, 5845 (1994).

[15] N. Brambilla, A. Pineda, J. Soto, and A. Vairo, Effective-field theories for quarkonium, Rev. Mod. Phys. **77**, 1423 (2005).

[16] This form for the spin-dependent interaction was obtained in the Wilson loop approach by Eichten and Feinberg [E. Eichten and F. Feinberg, Spin-dependent forces in quantum chromodynamics, Phys. Rev. D **23**, 2724 (1981)], who extended the analysis by Brown and Weisberger [L. S. Brown and W. I. Weisberger, Remarks on the static potential in quantum chromodynamics, Phys. Rev. D **20**, 3239 (1979)].Subsequently, Gupta and Radford [S. N. Gupta and S. F. Radford, Quark-quark and quark-antiquark potentials, Phys. Rev. D **24**, 2309 (1981); S. N. Gupta, S. F. Radford, and W. W. Repko, Quantum chromodynamic potential model for light and heavy quarkonia, Phys. Rev. D **28**, 1716 (1983)] performed a one-loop computation of the heavy quark interaction and showed that a fifth interaction, V_5 is present in the case of unequal quark masses. [See also J. T. Pantaleone, S. H. H. Tye, and Y. J. Ng, Spin splittings in heavy quarkonia, Phys. Rev. D **33**, 777 (1986)].

[17] Y. Koma and M. Koma, Spin-dependent potentials from lattice QCD, Nucl. Phys. **B769**, 79 (2007).

[18] For a review of the relationship of QCD to vector and scalar confinement see A. P. Szczepaniak and E. S. Swanson, On the Dirac structure of confinement, Phys. Rev. D **55**, 3987 (1997).

[19] M. Di Pierro and E. Eichten, Excited heavy-light systems and hadronic transitions, Phys. Rev. D **64**, 114004 (2001).

[20] A. Manohar and H. Georgi, Chiral quarks and the nonrelativistic quark model, Nucl. Phys. **B234**, 189 (1984); J. L. Goity and W. Roberts, Relativistic chiral quark model for pseudoscalar emission from heavy mesons, Phys. Rev. D **60**, 034001 (1999).

[21] F. E. Close and E. S. Swanson, Dynamics and decay of heavy-light hadrons, Phys. Rev. D **72**, 094004 (2005).

[22] T. Matsuki, T. Morii, and K. Sudoh, New heavy-light mesons $Q\bar{q}$, Prog. Theor. Phys. **117**, 1077 (2007).

[23] D. Ebert, R. N. Faustov, and V. O. Galkin, Heavy-light meson spectroscopy and Regge trajectories in the relativistic quark model, Eur. Phys. J. C **66**, 197 (2010).

[24] N. Devlani and A. K. Rai, Spectroscopy and decay properties of B and B_s mesons, Eur. Phys. J. A **48**, 104 (2012).

[25] L. Y. Xiao and X. H. Zhong, Strong decays of higher excited heavy-light mesons in a chiral quark model, Phys. Rev. D **90**, 074029 (2014).

[26] Y. Sun, Q. T. Song, D. Y. Chen, X. Liu, and S. L. Zhu, Higher bottom and bottom-strange mesons, Phys. Rev. D **89**, 054026 (2014).

[27] J. Ferretti and E. Santopinto, Open-flavor strong decays of open-charm and open-bottom mesons in the $^3P_0$ pair-creation model, arXiv:1506.04415.

[28] J. B. Liu and M. Z. Yang, Spectrum of higher excitations of B and D mesons in the relativistic potential model, Phys. Rev. D **91**, 094004 (2015).

[29] J. B. Liu and C. D. Lu, Spectra of heavy-light mesons in a relativistic model, arXiv:1605.05550.

[30] Q. F. Lü, T. T. Pan, Y. Y. Wang, E. Wang, and D. M. Li, Excited bottom and bottom-strange mesons in the quark model, arXiv:1607.02812.

[31] E. S. Ackleh, T. Barnes, and E. S. Swanson, On the mechanism of open-flavor strong decays, Phys. Rev. D **54**, 6811 (1996).

[32] See, for example, W. Kwong and J. L. Rosner, D-wave quarkonium levels of the Υ family, Phys. Rev. D **38**, 279 (1988).

[33] A. J. Siegert, Note on the interaction between nuclei and electromagnetic radiation, Phys. Rev. **52**, 787 (1937).

[34] R. McClary and N. Byers, Relativistic effects in heavy quarkonium spectroscopy, Phys. Rev. D **28**, 1692 (1983).

[35] P. Moxhay and J. L. Rosner, Relativistic corrections in quarkonium, Phys. Rev. D **28**, 1132 (1983).

[36] J. D. Jackson, Lecture on the new particles, in *Proceedings of the Summer Institute on Particle Physics, 1976*, edited by M. C. Zipf, Stanford Linear Accelerator Center Report No. SLAC-198, 1977, p. 147.

[37] V. A. Novikov, L. B. Okun, M. A. Shifman, A. I. Vainshtein, M. B. Voloshin, and V. I. Zakharov, Charmonium and gluons, Phys. Rep. **41**, 1 (1978).

[38] Relativistic effects in M1 transitions are discussed in the following: J. S. Kang and J. Sucher, Radiative M1 transitions of the narrow resonances, Phys. Rev. D **18**, 2698 (1978); H. Grotch and K. J. Sebastian, Magnetic dipole transitions of narrow resonances, Phys. Rev. D **25**, 2944 (1982); V. Zambetakis and N. Byers, Magnetic dipole transitions in quarkonia, Phys. Rev. D **28**, 2908 (1983); H. Grotch, D. A. Owen, and K. J. Sebastian, Relativistic corrections to radiative transitions and spectra of quarkonia, Phys. Rev. D **30**, 1924 (1984); X. Zhang, K. J. Sebastian, and H. Grotch, M1 decay rates of heavy quarkonia with a nonsingular potential, Phys. Rev. D **44**, 1606 (1991).

[39] D. Ebert, R. N. Faustov, and V. O. Galkin, Properties of heavy quarkonia and B_c mesons in the relativistic quark model, Phys. Rev. D **67**, 014027 (2003).

[40] L. Micu, Decay rates of meson resonances in a quark model, Nucl. Phys. **B10**, 521 (1969).

[41] A. Le Yaouanc, L. Oliver, O. Pene, and J. C. Raynal, Naive quark pair creation model of strong interaction vertices, Phys. Rev. D **8**, 2223 (1973).

[42] H. G. Blundell and S. Godfrey, The Xi (2220) revisited: Strong decays of the 1^3F_2 and 1^3F_4 $s\bar{s}$ mesons, Phys. Rev. D **53**, 3700 (1996).

[43] T. Barnes, S. Godfrey, and E. S. Swanson, Higher charmonia, Phys. Rev. D **72**, 054026 (2005).

[44] P. Geiger and E. S. Swanson, Distinguishing among strong decay models, Phys. Rev. D **50**, 6855 (1994).

[45] S. Godfrey and K. Moats, Bottomonium mesons and strategies for their observation, Phys. Rev. D **92**, 054034 (2015).

[46] K. A. Olive *et al.* (Particle Data Group Collaboration), Review of particle physics (RPP), Chin. Phys. C **38**, 090001 (2014).

[47] H. G. Blundell, Meson properties in the quark model: A look at some outstanding problems, arXiv:hep-ph/9608473.

[48] S. Godfrey and K. Moats, $D_{sJ}^{*}(2860)$ mesons as excited D-wave $c\bar{s}$ states, Phys. Rev. D **90**, 117501 (2014); **92**, 119903(E) (2015).

[49] For a recent overview of this topic see, for example, S. Godfrey and K. Moats, Properties of excited charm and charm-strange mesons, Phys. Rev. D **93**, 034035 (2016).

[50] See Supplemental Material at http://link.aps.org/supplemental/10.1103/PhysRevD.94.054025 for more complete tables of B and B_s meson decay modes.